

# Mid-Latitude calcareous nannofossil biostratigraphy and biochronology across the middle to late Eocene transition

Eliana Fornaciari<sup>1</sup>, Claudia Agnini<sup>1,2</sup>, Rita Catanzariti<sup>3</sup>, Domenico Rio<sup>1</sup>,  
Eleonora M. Bolla<sup>4</sup> and Elisabetta Valvasoni<sup>1</sup>

<sup>1</sup>Dipartimento di Geoscienze, Università di Padova, Via Giotto, Gradenigo, 6, I-35131 Padova, Italy

<sup>2</sup>Istituto di Geoscienze e Georisorse, CNR-Padova c/o Dipartimento di Geoscienze,  
Università di Padova, Via Gradenigo, 6, I-35131 Padova, Italy

<sup>3</sup>Istituto di Geoscienze e Georisorse, CNR-Pisa, c/o Dipartimento di Scienze della Terra -  
Università di Pisa - Via S. Maria, 53 - I-56126 Pisa, Italy

<sup>4</sup>ENI E&P Division - Sedimentology, Petrography & Stratigraphy Dpt. -  
Via Emilia, 1 - I-20097 S. Donato Milanese (MI), Italy  
email: eliana.fornaciari@unipd.it

---

**ABSTRACT:** Calcareous nannofossil biostratigraphic studies are presented from 11 sedimentary sections, nine located in the Mediterranean area and one each from the middle latitude North and South Atlantic, respectively. The distribution patterns of middle to late Eocene calcareous nannofossils are studied by means of quantitative and semiquantitative methods. Our main goal was to test the biostratigraphic reproducibility of bioevents used in two classical standard biozonations, and to introduce new biostratigraphically useful biohorizons, resulting in a series of new middle latitude biostratigraphic events. The new zonal scheme substantially improves the available biochronologic resolution, doubling the current partitioning based on the classical standard zonations. This study extends the terminal Eocene and Oligocene calcareous nannofossil zonal scheme proposed for the Mediterranean area (Catanzariti et al. 1997), into the middle Eocene. New age estimates are provided, which highlight the need to revise the present middle-late Eocene calcareous nannofossil biochronology. Two new species are described: *Cribozentrum erbae* sp. nov. and *Cribozentrum isabellae* sp. nov.

---

## INTRODUCTION

The Cenozoic climate evolution was characterized by the transition between Greenhouse and Icehouse conditions. The Early Eocene Climatic Optimum (EECO), when Earth's temperatures reached the maximum values of the last 65 Myr, was followed by a long-term cooling trend that eventually led to the permanent establishment of the Antarctic ice sheet at the Eocene/Oligocene boundary (ca. 33.9 Ma; Zachos et al. 2001).

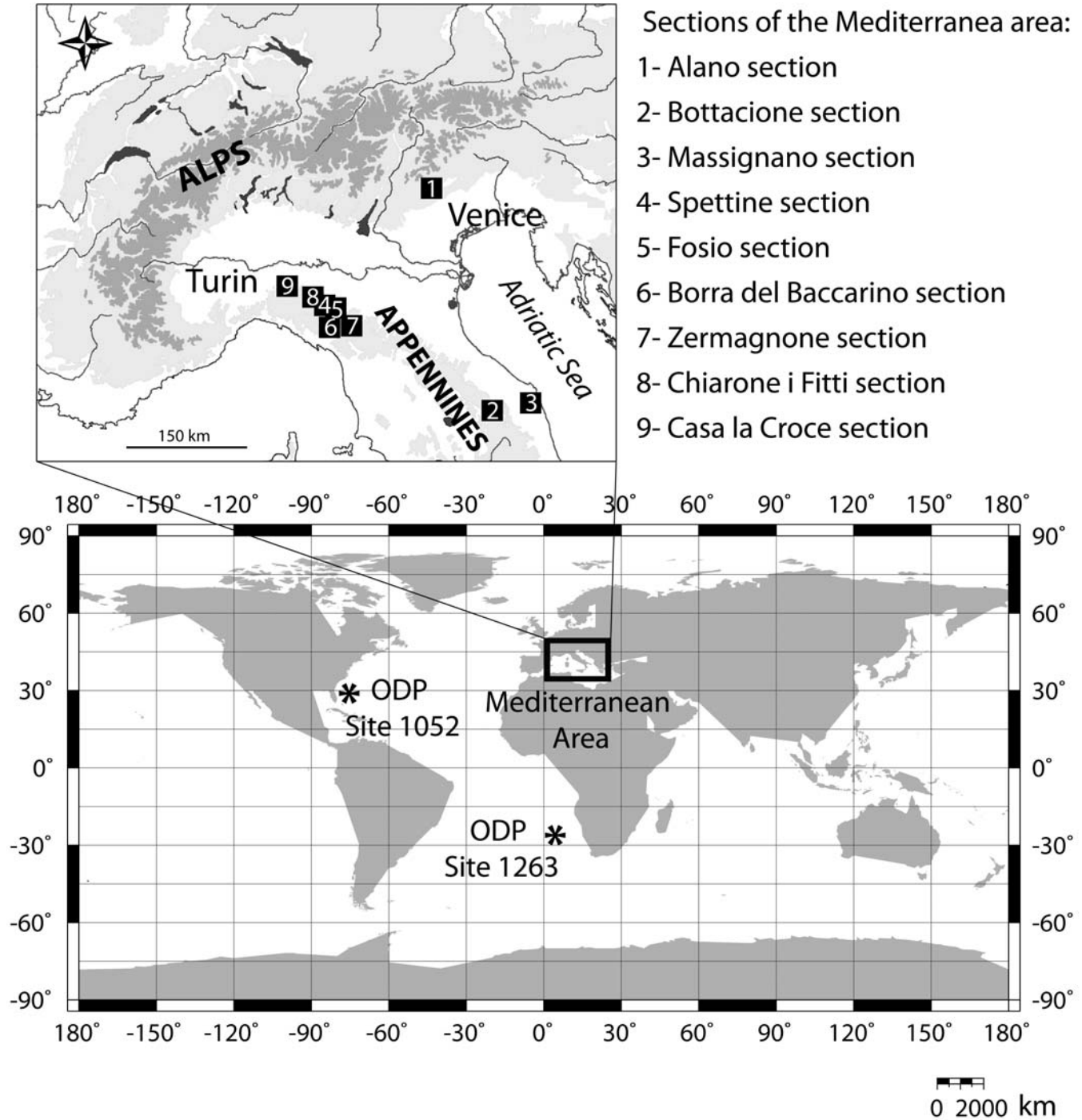
The long-term cooling transition has been considered to be gradual and monotonic, but recent studies suggest a more complex evolution, which includes short- and long-term reversals in the overall climatic trend (Bohaty and Zachos 2003; Sexton et al. 2006; Edgar et al. 2007). The deterioration of climate during the middle to late Eocene resulted in latitudinal gradients and enhanced seasonality, and has been proposed as a likely trigger mechanism for explaining the enhanced rate of extinctions observed during this time among calcareous plankton assemblages (Aubry 1992; 1998; Wade 2004; Aubry and Bord 2009). Although there is a great potential interest of the middle to late Eocene interval, it still remains poorly known for at least two main reasons: 1) there are few expanded and well-preserved sections available and 2) there are even fewer high resolution studies published from this time interval.

The focus of this study is on calcareous nannoplankton, photosynthetic plants that make up the base of the food chain, and play a crucial role in marine biogeochemical cycles. These algae have great abundance (millions of individuals per gram calcareous bearing sediment), wide biogeographical distribution

(tropics to polar regions) and high evolutionary rates in the fossil record. Therefore, they are used to produce global biostratigraphic and biochronologic frameworks (Martini 1971; Okada and Bukry 1980; Berggren et al. 1995) and to provide reliable paleoenvironmental reconstructions of both Mesozoic and Cenozoic (Erba 2006).

Here, we present calcareous nannofossil data from 11 sections/sites, nine of which are on-land sections located in the Mediterranean area. The remaining two are Ocean Drilling Program (ODP) sites from the Atlantic Ocean (text-fig. 1). In the Mediterranean area, the Alano section, crops out in the Southern Alps of northeastern Italy, whereas the other eight sections are located in the Northern Apennines. The two ODP sites were recovered during Legs 171b and 208 (N and S Atlantic; Norris et al. 1998; Zachos et al. 2004).

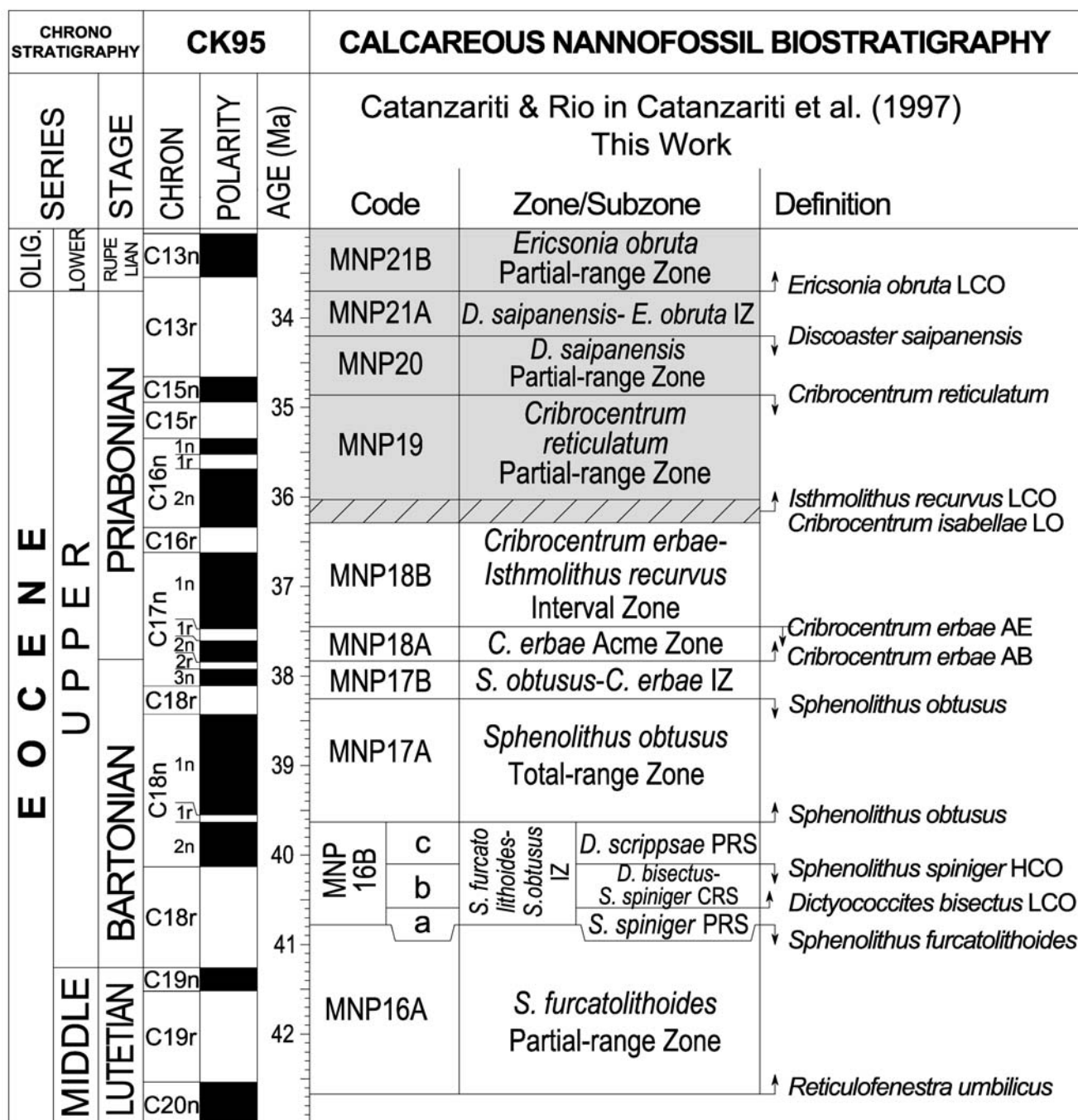
Our goal here is to provide a reliable and improved biostratigraphic/biochronologic framework for the Mediterranean and Atlantic regions during the middle to late Eocene because they are able to provide: 1) a first order calibration of key index taxa to the geomagnetic polarity time scale (GPTS; Cande and Kent 1995; CK95), both at Alano and ODP Site 1052. The obtained age estimates highlight some discrepancies relative to the reference biochronology proposed by Berggren et al. (1995), suggesting that revisions are needed, 2) new potential biohorizons not yet utilized in the standard zonations and 3) a platform for a discussion about distribution patterns, calibration to the GPTS, and ranking and spacing of standard and new biohorizons. The outcome is used to evaluate the re-



TEXT-FIGURE 1  
Location map showing the position of investigated sections in the Atlantic and Mediterranean.

liability of all calcareous nanofossil biohorizons in the studied sections. In addition biostratigraphic results acquired during this study thus have been used to extend the Mediterranean Nannoplankton Paleogene (MNP) calcareous nanofossil zonation of Catanzariti et al. (1997) into the middle Eocene

(text-fig. 2a). In the Mediterranean area, the middle to late Eocene transition was a crucial period in terms of geodynamics and paleogeographic evolution, because of the continued northwards migration of the African plate related to the opening of the Liguro-Provençal Basin leading up to the construction of the



TEXT-FIGURE 2a

New middle Eocene – Early Oligocene zonation. Calcareous nannofossil events are plotted against chronostratigraphy and GPTS of Cande and Kent (1995). MNP = Mediterranean Nannoplankton Paleogene (Catanzariti et al. 1997); IZ= Interval Zone; PRS= Partial-range Subzone; CRS= Concurrent-range Subzone. Grey shaded area: Catanzariti and Rio in Catanzariti et al. (1997).

Alpi-Appennine orogenic system (Doglioni et al. 1997). Because of this complex scenario, the MNP biostratigraphic scheme was originally proposed solely for the Mediterranean area, however, data collected from the northern and southern Atlantic areas are consistent with those of the Mediterranean region, suggesting a possible supraregional value, at least for mid-latitude sediments of middle through late Eocene age.

#### BIOSTRATIGRAPHY, BIOCHRONOLOGY AND TIME SCALE

The geologic time scale of the Paleogene System is in a state of flux (Berggren and Pearson 2005; Hilgen 2008), essentially because the existing age models are not yet well established, being based on limited biostratigraphic and biochronologic datasets. In the middle to late Eocene interval, the calcareous nannofossil

STANDARD ZONATIONS		BIOHORIZON		MEDITERRANEAN ZONATIONS									
Martini, 1971		Okada and Bukry, 1980		Perch-Nielsen, 1985		Roth et al., 1971		Proto Decima et al., 1975		Nocchi et al., 1988		Catanzariti & Rio, in Catanzariti et al., 1997	
Zone	Definition	Zone/Subzone	Definition	Backman, 1987		Zone/Subzone	Definition	Zone	Definition	Zone	Definition	Zone/Subzone	Definition
NP21	<i>E.formosa</i>	CP16b	<i>E.formosa</i>	▼ <i>E.formosa</i>	▼ <i>E.formosa</i>		<i>E.formosa</i>	Not considered		CP16b	<i>E.formosa</i>	MNP21B	<i>E.formosa</i>
			<i>C.subdistichus</i>	▲ <i>E.obruta</i> LCO	▲ <i>E.obruta</i> LCO		<i>E.subdisticha</i>				<i>E.obruta</i> acme		<i>E.obruta</i> acme
				▼ <i>C.protoannula</i>	▼ <i>C.protoannula</i>					CP16a	<i>D.barbadiensis</i>	MNP21A	<i>D.saipanensis</i>
	<i>D.saipanensis</i>	CP16a	<i>D.barbadiensis</i>	▼ <i>D.saipanensis</i>	▼ <i>D.saipanensis</i>		<i>D.barbadiensis</i>	<i>D.barbadiensis</i>			<i>D.saipanensis</i>		<i>D.saipanensis</i>
NP20	<i>C.oamaruensis</i>		<i>D.saipanensis</i>	▼ <i>D.saipanensis</i>	▼ <i>D.saipanensis</i>		S. <i>pseudoradians</i>	S. <i>pseudoradians</i>			<i>D.barbadiensis</i>		<i>C.reticulatum</i>
				▼ <i>C.reticulatum</i>	▼ <i>C.reticulatum</i>						<i>D.saipanensis</i>		<i>C.reticulatum</i>
NP19	<i>I.recurvus</i>	CP15b	<i>I.recurvus</i>	▲ <i>I.recurvus</i>	▲ <i>I.recurvus</i>		<i>I.recurvus</i>	<i>I.recurvus</i>		CP15b	<i>I.recurvus</i>	MNP19	<i>I.recurvus</i> LCO
													<i>C.isabellae</i> LO
NP18	<i>C.oamaruensis</i>	CP15a	<i>C.grandis</i>				Ch. <i>oamaruensis</i>	Ch. <i>oamaruensis</i>		CP15a	<i>C.grandis</i>	MNP18B	<i>C.erbeae</i> AE
													<i>C.erbeae</i> AB
NP17		CP14b					<i>D.saipanensis</i>					MNP17B	<i>S.obtusus</i>
													<i>S.obtusus</i>
NP16	<i>C.solitus</i>	CP14a	<i>D.bifax</i>	▲ <i>D.bisectus</i>	▲ <i>D.bisectus</i>		<i>D.mirus</i>	<i>C.solitus</i>				MNP16Bc	<i>S.spiniger</i> HCO
	<i>R.gladus</i>		<i>C.solitus</i>	▼ <i>S.furcatolithoides</i>	▼ <i>S.furcatolithoides</i>			<i>T.inversus</i>				MNP16Bb	<i>D.bisectus</i> LCO
				▼ <i>Nannotetrina</i> spp.	▼ <i>Nannotetrina</i> spp.							MNP16Ba	<i>S.furcatolithoides</i>
			<i>R.umbilicus</i>	▲ <i>R.umbilicus</i> >14 μm	▲ <i>R.umbilicus</i> >14 μm		<i>L.minutus</i>						
			<i>D.bifax</i>										
			<i>C.gigas</i>										
NP15		CP13c		▲ <i>S.furcatolithoides</i>	▲ <i>S.furcatolithoides</i>		<i>S.radians</i>	<i>R.umbilicus</i>			<i>R.umbilicus</i> >12.5 μm		
								<i>D.tanii nodifer</i>					
			<i>C.gigas</i>				<i>C.alatus</i>	<i>D.barbadiensis</i>		CP13	<i>Nannotetrina</i> spp.		Not considered
	<i>C.alatus</i>	CP13a	<i>N.quadrata</i>	▲ <i>Nannotetrina</i> spp.	▲ <i>Nannotetrina</i> spp.			<i>N.fulgens</i>					

TEXT-FIGURE 2b

Middle Eocene – Early Oligocene calcareous nannofossil events and zonations proposed for the Mediterranean area are compared with the standard zonations of Martini (1971) and Okada and Bukry (1980). MNP = Mediterranean Nannoplankton Paleogene (Catanzariti et al. 1997). Grey shaded area: Catanzariti and Rio in Catanzariti et al. (1997).

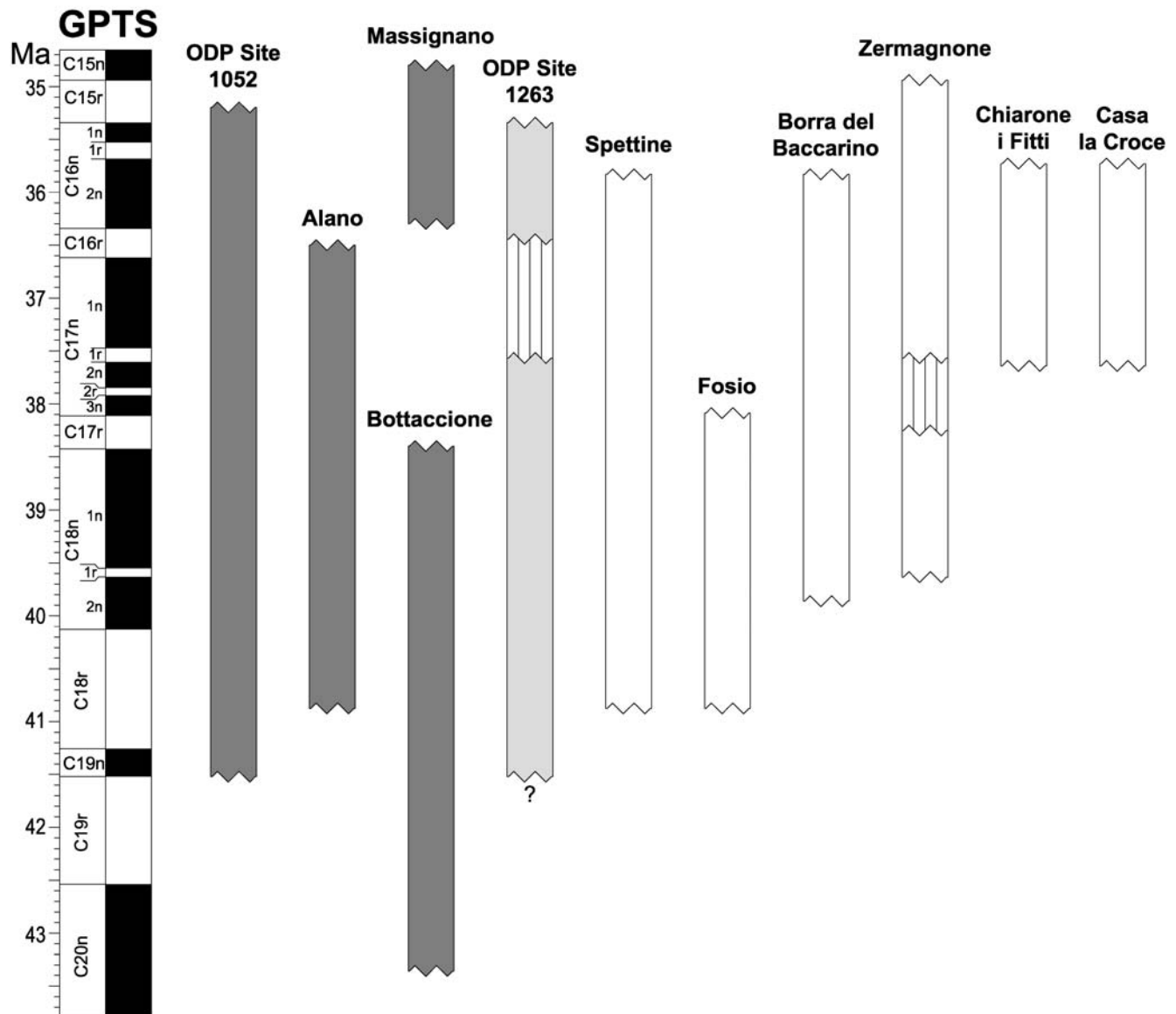
standard zonations of Martini (1971) and Okada and Bukry (1980), represent a fundamental biostratigraphic tool, but are somewhat problematic because the markers adopted in both zonal schemes are based on index species that are latitudinally restricted, facies dependent, and/or poorly defined. Not surprisingly, the calibration of these standard calcareous nannofossil biohorizons, as well as planktic foraminiferal zonations, to the GPTS (CK95) remains controversial for Paleogene times. This problem is accentuated by the lack of good sections studied at high resolution and which have reliable magneto- and cyclostratigraphies (Berggren et al. 1995; Agnini et al., in press).

This study is based on calcareous nannofossils from middle through upper Eocene sections having well-understood magnetostratigraphies: ODP Site 1052, Massignano, Bottaccione and Alano (Ogg and Bardot 2001; Wade 2004; Jovane et al. 2007b, Agnini et al., in press; text-fig. 3), providing age estimates for biohorizons through direct correlation to the GPTS. Specifically, we constructed age-depth plots by means of magnetostratigraphic correlation to the GPTS of CK95, assuming constant sedimentation rates between magnetostratigraphic tie points. This assumption results in less precise biochronologic estimates espe-

cially in chrons, because magnetostratigraphy offers no control on sedimentation rate variations within individual polarity zones (Backman and Raffi 1997). As a result, age calibrations of biohorizons can have uncertainties on the order of one to a few hundred thousand of years. This lack of precision can only be overcome with cyclostratigraphy. In our dataset, an orbitally tuned cyclostratigraphy is available only for ODP Site 1052 (Pälike et al. 2001).

#### Middle to late Eocene calcareous nannofossil biostratigraphy

Currently used zonal schemes for the middle and late Eocene are the standard zonations of Martini (1971) and Okada and Bukry (1980) (text-fig. 2b). These zonations are by-and-large based on the pioneering work of Hay et al. (1967), Bramlette and Wilcoxon (1967), Roth (1970, 1973), Roth et al. (1971), and Bukry (1973, 1975). Since these two zonal schemes, regarded as an international standard for dating (Haq et al. 1987), generally offer a low capacity in resolving time, other authors (e.g., Beckmann et al. 1981; Perch-Nielsen 1985; Backman 1987) proposed a set of additional biohorizons, reported in text-figure 2b, in order to improve the time resolution available



TEXT-FIGURE 3

Position of the investigated sections relative to the Geomagnetic Polarity Time Scale (GPTS) of Cande and Kent (1995). Grey color: magnetostratigraphy available. Light grey color: magnetostratigraphy not reliable. White color: no magnetostratigraphy available. Hatchured: hiatus

for the middle-late Eocene. Clearly, standard zonations can not always be applicable in all types of environments, for example high latitude or marginal basin settings, so that some regional schemes have been established for such areas (e.g., Wei and Wise 1990; Wei and Thierstein 1991). In the Mediterranean area, several marker species used in standard zonations were often absent or rare and several biohorizons in the classical zonations are thus unreliable in this region (Roth et al. 1971; Proto Decima et al. 1975; Verhallen and Romein 1983; Monechi and Thierstein 1985; Nocchi et al. 1986; 1988; Coccioni et al. 1988; Parisi et al. 1988; Premoli Silva et al. 1988). The serious difficulty encountered in applying standard zonations in the

Mediterranean area was partially solved when Roth et al. (1971) and Proto Decima et al. (1975) established new regional schemes and Nocchi et al. (1988) emended some of the Okada and Bukry's (1980) zonal boundary definitions (text-fig. 2b). More recently, Catanzariti et al. (1997) proposed a late Eocene to Oligocene regional scheme for the Mediterranean, whose extension to the middle Eocene is the original aim of this work. Other biostratigraphic works on middle upper Eocene Mediterranean sections (Mancin and Cobianchi 2000; Luciani et al. 2002; Cascella and Dinarès-Turell 2009) provide additional information about the magnetobiostratigraphic framework available from this area.

## STUDY MATERIAL AND METHODS

### Study Material

Locations and stratigraphic characterization of the 11 sedimentary successions investigated in this study are presented in Table 1. The Alano section and ODP Site 1052 have published magnetostratigraphies (Ogg and Bardot 2001; Pälke et al. 2001; Agnini et al. in press). These are used as reference sections for the present work, and have been sampled at an average sampling density of 20–30 cm. This data set permits us to establish detailed distribution patterns and biochronologic datums of index calcareous nannofossil between about ca. 41.5 and 35.3 Ma.

In order to obtain age estimates for middle Eocene biohorizons recorded in the Chron C20n–C18n interval, we studied the classical Bottacione section (Umbria, Italy), whose magneto-biostratigraphy was largely used by Berggren et al. (1985; 1995) in the construction of their widely accepted marine Cenozoic timescales. The seventeen samples analyzed for this study are the same investigated by Monechi and Thierstein (1985).

With the aim to produce biochronological data of late Eocene biohorizons above Chron C17n, we have studied the abundance patterns of selected calcareous nannofossil species in the lower part of the Massignano section (Central Italy), where the GSSP of the Rupelian Stage and the Eocene-Oligocene boundary were established (Premoli Silva and Jenkins 1993). At Massignano, we analyzed the first 10m of the section, with a sample resolution of 10 cm in the critical interval. In order to expand our biostratigraphic data base and investigate the reproducibility of the distribution patterns observed in the key sections having magnetostratigraphy, we also studied six other sections from the Northern Apennines.

All the above successions are located in middle latitude areas in the Northern Hemisphere. We have therefore investigated the distribution patterns of the considered index species at ODP Site 1263, located in the mid-latitude South Atlantic (text-fig. 1). The magnetostratigraphic record at ODP Site 1263 (Zachos et al. 2004), however, can be only partially utilized for biochronological estimates.

### Methods

All samples were prepared from unprocessed material as smear slides and examined using a light microscope at 1250x magnification. After a preliminary qualitative analysis in order to evaluate the abundance and state of preservation of calcareous nannofossil assemblages, the following quantitative and semiquantitative counting methods were applied in order to quantify the presence or absence of index species:

- 1) Counting species versus total assemblage, taking into account at least 500 specimens (Thierstein et al. 1977);
- 2) Counting a prefixed number of taxonomically related forms, i.e., 50–100 sphenoliths (Rio et al. 1990)
- 3) Counting the number of specimens of rare but biostratigraphically useful species in an area of about 6–7 mm<sup>2</sup>, which is roughly equivalent to 3 vertical traverses (modified after Backman and Shackleton 1983).

## REMARKS ON TAXONOMY

A list of taxa considered in the present work can be found in Appendix A; for most of them we followed the taxonomy proposed by Perch Nilesen (1985) and Aubry (1984; 1988; 1989; 1990; 1999). In order to avoid any possible taxonomic ambiguity we provide microphotos of index species (Plates 1 and 2). In fact, a strong consistency in taxonomic criteria is a key factor in biostratigraphy and biochronology, especially when intermediate morphotypes in evolving lineages are involved. Therefore, a summary of the taxonomic concept adopted in this work for controversial index species is reported below.

### *Reticulofenestra*, *Cribozentrum* and *Dictyococcites*

In spite of the fact that several authors have suggested that specimens of the genus *Reticulofenestra* also include members from the genera *Cribozentrum* and *Dictyococcites* (e.g., Gallagher 1989; Young 1990), we decided, to follow Perch-Nielsen (1985), and to maintain these three genera as three separate taxonomic units at the genus level.

### *Cribozentrum*

Within this genus, we recognized three distinct species: *Cribozentrum reticulatum* s.s., *Cribozentrum erbae* sp. nov. and *Cribozentrum isabellae* sp. nov. A detailed description of these new species is available in the systematic Paleontology section.

### *Dictyococcites*

This genus has been subdivided into two species (*D. scrippsae* and *Dictyococcites bisectus*) and one group (*Dictyococcites* spp.), in which we lumped together all small to medium sized specimens of this genus having an elliptical outline, continuous extinction lines and lacking a well developed central plug. By contrast, we ascribe to *D. scrippsae* specimens smaller than 10 µm, with an elliptical to subcircular outline, continuous extinction lines and a well-developed central plug. In the literature, these morphotypes have been referred to as *D. hesslandii* (see Backman 1987). Finally, *D. bisectus* consists of specimens >10µm in size, with a well developed central plug, elliptical-subcircular outline and extinction lines nearly straight and disjunct.

### *Reticulofenestra*

The conventional taxonomy of the reticulofenestrids is notoriously problematic (Young 1990), because the species differentiation is mainly based on the sized of the central opening and width of the coccolith wall. These morphological and morphometric features are ambiguously defined and thus we followed the taxonomic criteria adopted in Backman and Hermelin (1986) to define *Reticulofenestra umbilicus* (Plate 1), which ascribe to this species all specimens >14 µm. All other species included in this genus, are lumped together as *Reticulofenestra* spp.

### *Chiasmolithus*

Although this genus provides several biohorizons in Martini's and Okada and Bukry's middle and late Eocene standard zonations, it often represents a minor component of the assemblages both at middle and high latitudes. During this study, we have quantified all specimens ascribable to this genus to species level, despite either the pervasive dissolution and/or overgrowth that sometime affects the assemblages or the presence of transitional morphotypes that make speciation difficult (e.g.,

TABLE 1  
Summary of stratigraphic sections studied in this work.

Section/Site	Thickness (m)	# of studied samples	Location	Geological setting and main Lithology	Stratigraphic information	Previous biostratigraphic studies	Magnetostratigraphy studies
ALANO	100,00	303	Veneto, NE Italy (Southern Alps)	Slope, hemipelagic sediments	Agnini et al., in press		Agnini et al., in press.
CASA LA CROCE	160,00	22	Piedmont, NW Italy (Northern Apennines)	Episutural basin, hemipelagic sediments	Marroni et al., in press		
CHIARONE I FITTI	75,00	56	Emilia, NW Italy (Northern Apennines)	Episutural basin, pelagic and hemipelagic sediments	Di Dio et al., 2005a	Catanzariti et al., 1997	
SPETTINE	135,00	78	Emilia, NW Italy (Northern Apennines)	Episutural basin, pelagic and hemipelagic sediments	Di Dio et al., 2005a	Catanzariti et al., 1997	
BORRA DEL BACCARINO	82,00	23	Emilia, NW Italy (Northern Apennines)	Episutural basin, pelagic and hemipelagic sediments	Vescovi, 2002	Catanzariti et al., 1997	
FOSIO	54,00	17	Emilia, NW Italy (Northern Apennines)	Episutural basin, pelagic and hemipelagic sediments	Di Dio et al., 2005b	Catanzariti et al., 1997; Mancin and Pirini, 2001	
ZERMAGNONE	88,00	44	Emilia, NW Italy (Northern Apennines)	Episutural basin, mainly outer shelf and slope pelagic and hemipelagic sediments	Cerrina Feroni et al., 2002	Catanzariti et al., 1997	
BOTTACCIONE	28,00	17	Umbria, Central Italy (Northern Apennines)	Foreland basin, pelagic limestone (Scaglia variegata)	Renz, 1936, 1951; Barnaba, 1958; Monechi and Thierstein 1985; Cresta et al., 1989	Premoli Silva et al., 1974; Napoleone et al., 1983; Monechi and Thierstein, 1985; Cresta et al., 1989	Napoleone et al., 1983
MASSIGNANO	10,00	43	Marche, Central Italy (Northern Apennines)	Foreland basin, pelagic limestone (Scaglia variegata)	Montanari et al., 1985; Coccioni et al., 1988	Coccioni et al., 1986, 1988	Bice and Montanari, 1988; Lowrie and Lanci 1994; Lanci et al., 1996; Jovane et al., 2004; 2006; 2007b; 2009
ODP SITE 1052	164,50	300	Blake Nose, western North Atlantic Ocean	Ramp of plateau; siliceous nannofossil ooze and nannofossil and foraminifer chalk	Norris, Kroon, Klaus et al., 1998	Norris, Kroon, Klaus et al., 1998	Ogg and Bardot, 2001
ODP SITE 1263	48,00	71	Walvis Ridge, eastern South Atlantic Ocean	Asismic ridge, nannofossil oozes and chalky nannofossil ooze with occasional layers of volcanic ash and stringers chert	Zachos, Kroon, Blum, et al., 2004	Zachos, Kroon, Blum, et al., 2004	Zachos, Kroon, Blum, et al., 2004

*Chiasmolithus solitus*/*C. expansus* intergrade; *Chiasmolithus expansus*/*C. oamaruensis* intergrade).

### Sphenolithus

The sphenoliths are a significant constituent of many Eocene nannofossils assemblages and several species provide important biohorizons. The taxonomic criteria we adopted in this study for *Sphenolithus furcatolithoides*, *Sphenolithus obtusus*, *Sphenolithus predistentus* and *Sphenolithus spiniger* are clarified as follows:

-*Sphenolithus furcatolithoides* includes also specimens with two long apical spines that do not diverging distally, for example, see *Sphenolithus* sp. 1 illustrated in Perch-Nielsen (1977; Plate 49, figs. 42-44);

-*Sphenolithus obtusus* also includes morphotypes lacking a median suture in the apical spine at 0° to crossed nicols. These forms are thought to represent an early morphotype of this species;

-*Sphenolithus predistentus* includes specimens with an extinction line between the proximal cycles and apical spine, which is straight, or tends to extend slightly upward at 45° to the polarizers. These morphotypes were observed in middle Eocene sediments, but strongly resemble the Oligocenic *Sphenolithus predistentus-distentus* group *sensu* Huang (1977);

-Following the strict taxonomic concept of Bukry (1971), *Sphenolithus spiniger* does not include, specimens with an outline similar to *S. spiniger* but without spine or with a short spine but a triangular outline.

### RESULTS

The investigated Tethyan and Atlantic sediments contain common to abundant calcareous nannofossils, which display, except for the poorly preserved Bottaccione section, moderate to good preservation. Assemblages in all sections are largely dominated by placoliths belonging to *Reticulofenestra*, *Criboecentrum* and *Dictyococcites*. Sphenoliths are also well represented and provide first order biostratigraphic information. *Discoaster* and *Chiasmolithus*, which provide the basis for the biohorizons of the standard zonations of Martini (1971), and Okada and Bukry (1980), are often rare or missing. Furthermore, identification of *Chiasmolithus* and *Discoaster* specimens to the species level may be difficult when preservation is poor due to pervasive etching and overgrowth. *Isthmolithus recurvus* is generally rare and thus represents a negligible component of the total assemblage.

The distribution patterns of 14 biostratigraphically important late middle to late Eocene calcareous nannofossil taxa are presented in text-figures 4-14. These distribution patterns are established by means of different counting methods and allow the definition of the following types of biohorizons: Lowest Occurrence (LO), Lowest Common Occurrence (LCO), Temporary High Occurrence (THO), Highest Common Occurrence (HCO), Highest Occurrence (HO), Acme Beginning (AB) and Acme Ending (AE). For a detailed definition of different types of biohorizons see Raffi et al. (2006) except for THO, an informal term here adopted to describe the Temporary High Occurrence (THO) observed of *Sphenolithus predistentus*. This biohorizon is defined as the layer where *S. predistentus* temporally disappears during the middle Eocene. The reliability of biohorizons has been a topic of much discussion (i.e., Gradstein et al. 1985;

TABLE 2

Age estimations of calcareous nannofossil biohorizons based on the GPTS of Cande and Kent (1995). We also provide biochronologic estimations based on revised Time Scale of Pälike et al. (2001). At ODP Site 1263, we use tie points after Bohaty et al. 2009 for biochronologic estimates. The relative position of biohorizons within magnetochrons follows the system of Hallam et al. (1985) and the recommendation of Cande and Kent (1992) to use an inverted stratigraphic placement relative to the present. Thickness, position to Chron top and age for Massignano section are reported in italic.

Biohorizon	Alano			ODP Site 1052				Massignano and Bottaccione			Site 1263					
	Thickness (m)	Position to chron top	Age (Ma) CK95	Depth (rmcd)	Position to chron top	Age (Ma) CK95	Age (Ma) Pälike et al. (2001)	Thickness (m)	Position to chron top	Age (Ma) CK95	Thickness (m)	Age (Ma) CK95	Age (Ma) Bohaty et al. (2009)			
<i>C. reticulatum</i> HO?								9,75	<i>C15n</i>	<i>0,73</i>	<i>34,863 ±0,040</i>					
<i>C. isabellae</i> HO?								9,75	<i>C15n</i>	<i>0,73</i>	<i>34,863 ±0,040</i>					
<i>S. predistentus</i> RE								1,7	<i>C16n.2n</i>	<i>/</i>	<i>36,090 ±0,016</i>					
<i>C. isabellae</i> LO				36,64	<i>C16n.2n</i>	0,684	36,134 ±0,013	0,5	<i>C16n.2n</i>	<i>/</i>	<i>36,288 ±0,016</i>					
<i>I. recurvus</i> LCO				55,89	<i>C17n.1n</i>	0,198	36,787 ±0,009	2,05	<i>C16n.2n</i>	<i>/</i>	<i>36,032 ±0,008</i>					
<i>I. recurvus</i> spike end	79,91	<i>C17n.1n</i>	0,784	37,288 ±0,003	72,42	<i>C17n.1n</i>	0,795	37,298 ±0,009								
<i>I. recurvus</i> spike beginning	78,11	<i>C17n.1n</i>	0,853	37,347 ±0,003	81,29	<i>C17n.1r</i>	0,885	37,589 ±0,005								
<i>C. erbae</i> AE	75,01	<i>C17n.1n</i>	0,972	37,449 ±0,019	76,27	<i>C17n.1n</i>	0,934	37,417 ±0,008								
<i>C. grandis</i> HO	66,47	<i>C17n.2n</i>	0,492	37,724 ±0,003	84,71	<i>C17n.2n</i>	0,453	37,714 ±0,011								
<i>C. erbae</i> AB	62,96	<i>C17n.2n</i>	0,939	37,833 ±0,019	87,63	<i>C17n.2n</i>	0,891	37,821 ±0,005								
<i>C. oamaruensis</i> LRO	62,85	<i>C17n.2n</i>	0,953	37,837 ±0,003	86,50	<i>C17n.2n</i>	0,722	37,780 ±0,011								
<i>S. predistentus</i> THO	50,85	<i>C17r</i>	0,261	38,195 ±0,031	130,28	<i>C18n.2n</i>	0,068	39,665 ±0,019	25	<i>C18n</i>	0,490	39,260 ±0,178				
<i>S. obtusius</i> HO	49,59	<i>C17r</i>	0,448	38,253 ±0,028	108,12	<i>C18n.1n</i>	0,021	38,449 ±0,017	28,50	<i>C18n</i>	0,125	38,639 ±0,089				
<i>C. solitus</i> HO	44,73	<i>C18n.1n</i>	0,057	38,490 ±0,037	106,76	<i>C17r</i>	0,910	38,398 ±0,009								
<i>C. grandis</i> HCO	36,18	<i>C18n.1n</i>	0,484	38,971 ±0,033	110,62	<i>C18n.1n</i>	0,143	38,587 ±0,016	17	<i>C18r</i>	0,284	40,814 ±0,221				
<i>C. solitus</i> HCO	27,900	<i>C18n.1n</i>	0,898	39,437 ±0,033	155,29	<i>C18r</i>	<i>/</i>	40,926 ±0,015	<i>/</i>			146,6	41,067	41,1435		
<i>S. obtusius</i> LO	22,65	<i>C18n.2n</i>	0,005	39,633 ±0,009	139,44	<i>C18n.2n</i>	0,994	40,127 ±0,008	23,00	<i>C18n</i>	0,698	39,615 ±0,177	132,32	39,215	39,2236	
<i>H. spiniger</i> HO	22,65	<i>C18n.2n</i>	0,005	39,633 ±0,028	138,84	<i>C18n.2n</i>	0,934	40,097 ±0,008	39,804			132,32	39,215	39,2236		
<i>H. spiniger</i> HCO	17,55	<i>C18n.2n</i>	0,940	40,100 ±0,009	142,19	<i>C18r</i>	<i>/</i>	40,266 ±0,040	>39,902	19,00	<i>C18r</i>	0,101	40,373 ±0,221	135,39	39,695	39,6642
<i>D. bisectus</i> LCO	9,5	<i>C18r</i>	<i>/</i>	40,590 ±0,005	143,94	<i>C18r</i>	<i>/</i>	40,354 ±0,008	<i>/</i>	19,00	<i>C18r</i>	0,101	40,373 ±0,221	140,24	40,316	40,2939
<i>D. scrippsae</i> LCO	9,3	<i>C18r</i>	<i>/</i>	40,601 ±0,006	143,94	<i>C18r</i>	<i>/</i>	40,354 ±0,008	<i>/</i>	19,00	<i>C18r</i>	0,101	40,373 ±0,221	140,24	40,316	40,2939
<i>S. predistentus</i> LO	6,3	<i>C18r</i>	<i>/</i>	40,780 ±0,018	143,94	<i>C18r</i>	<i>/</i>	40,354 ±0,008	<i>/</i>	21,00	<i>C18n</i>	0,906	39,970 ±0,178	140,99	40,398	40,3873
<i>S. furcatolithoides</i> HO	6,3	<i>C18r</i>	<i>/</i>	40,780 ±0,018	144,54	<i>C18r</i>	<i>/</i>	40,384 ±0,008	<i>/</i>	17,00	<i>C18r</i>	0,284	40,814 ±0,221	141,895	40,527	40,5327
<i>C. reticulatum</i> LCO	0,6	<i>C18r</i>	<i>/</i>	41,119 ±0,036	157,69	<i>C18r/C19n</i>	<i>/</i>	<i>/</i>	<i>/</i>							
<i>R. umbilicus</i> LCO				161,59	upper <i>C19n</i>	<i>/</i>	<i>/</i>	<i>/</i>	<i>/</i>							
<i>R. umbilicus</i> LO								8,25	<i>C20n</i>	0,11	42,673 ±0,108					

Bralower et al. 1989; Hills and Thierstein 1989; Rio et al. 1990; Raffi 1999) and it is now widely accepted that an evaluation on the reliability of the bioevents should be essentially based on the degree of synchrony of biohorizons (e.g., Thierstein et al. 1977; Backman and Shackleton 1983; Raffi et al. 1993).

A synchronous biohorizon is thus considered to be biostratigraphically reliable (e.g., Raffi et al. 1993), but some biohorizons which are diachronous to different degrees even over short distances may still be useful. Their stratigraphic utility is due to the fact that they are non-repetitive events, which are needed in order to identify synchronous but repetitive signals such as magnetic reversals or cyclostratigraphic properties, (e.g., rhythmic changes in oxygen isotopes or lithology). Thus, an event is considered as reliable when it is easily reproducible among different researchers, and when it keeps the same ranking and relative spacing in different geologic sections (Gradstein et al. 1985; Fornaciari and Rio 1996; Catanzariti et al. 1997).

**Standard zonation calcareous nannofossil biohorizons**

Below follows comments on standard (Martini 1971; Okada and Bukry 1980) and additional/alternative biohorizons in stratigraphic order. Their positions, calibrations and biostratigraphic use are reported in Tables 2 and 3. (see also Table A, Supplementary Data).

*The LO and LCO of Reticulofenestra umbilicus*

The LO of *R. umbilicus* defines the base of Zone CP14 of Okada and Bukry (1980). Following the biometric definition proposed by Backman and Hermelin (1986) for this taxon, Wei and Wise (1989) demonstrated a consistent position of the LO of *R. umbilicus* at the Chron C20n/C19r transition from low to middle latitude settings. Wei and Wise (1992) noted that the initial range of *R. umbilicus* is somewhat sporadic. They there-

fore proposed to use the lowest common occurrence rather than its absolute LO. In our material, the initial range of *R. umbilicus* has been documented only at the Bottaccione section, where it occurs at the topmost part of Chron C20n, which is in fairly good agreement with the finding of Wei and Wise (1989). Unfortunately, our data base from ODP Site 1052 is not large enough for discussing the reliability of the LCO of *R. umbilicus* that was apparently observed roughly in correspondence to the top of Chron C19n (text-fig. 5).

*The HCO and HO of Chiasmolithus solitus*

The HO of *C. solitus* is the primary criterion for defining the NP16/NP17 and CP14a/CP14b boundary (Martini 1971; Okada and Bukry 1980). The index species is rare or absent in low latitude sediments, difficult to recognize in poorly preserved material and strongly diachronous at different latitudes (e.g., Perch-Nielsen 1985; Wei and Wise 1989; Aubry 1992; Berggren et al. 1995; Marino and Flores 2002a; b; Villa et al. 2008). The HO of *C. solitus* occurred in Chron C18r at low southern latitudes (Wei and Wise 1989; 1990; 1992; Okada 1990), whereas it was recorded at the Chron C18n.1n/C17r transition or within Chron C17r at southern middle to high latitudes as discussed by Villa et al. (2008). Previous works reported an uneven distribution of *C. solitus* in the Mediterranean region (Monechi and Thierstein 1985; Nocchi et al. 1988). This is in agreement with our findings, where *C. solitus* is virtually absent in all Italian sections, except for Alano, where it is very rare. We have monitored the final distribution pattern of *C. solitus* at Alano and ODP Sites 1052 and 1263 using different counting methods (text-figs. 5, 14). When counting 500 specimens, the species is recorded with good continuity, albeit in low frequencies (less than 1-2%), up to levels we have tentatively labeled as the HCO (text-figs. 4, 5, 14). At Alano, the HCO of *C. solitus* is associated with the lower part of Chron C18n.1n, whereas at ODP Site 1052 it occurs in the lower part of Chron C18r



TABLE 3

Summary of biostratigraphic use, reliability and biochronology of the main calcareous nannofossil biohorizons considered in this study. Biohorizons used in standard zonations are reported in bold.

	Biohorizon	"Morphology" of the event	Reliability ranking	Biochronology This work		Biochronology	Remarks
				Central Tethys Age (Ma)	Western Atlantic Age (Ma)	BKSA95 Age (Ma)	
16	<i>I. recurvus</i> LCO	Fairly neat	Fairly reliable for regional correlation in central Tethys	36.032 $\pm$ 0.01	36.79 $\pm$ 0.01	--	
15	<i>C. isabellae</i> LO	Although in low abundances is continuously present; fairly neat	Enough good although the marker is generally few	36.29 $\pm$ 0.01	36.13 $\pm$ 0,01	--	
14	<i>I. recurvus</i> LO	Neat, but detectable only in high-resolution study	Usefully for detailed correlation in high-resolution study	37.35 $\pm$ 0.01	37.59 $\pm$ 0.01	36.0	Detected in the lower part of C17n.1n at Site 523 but considered as down hole contamination (1)
13	<i>C. erbae</i> AE	Fairly neat	Excellent	37.45 $\pm$ 0.02	37.42 $\pm$ 0.01	--	
12	<i>C. grandis</i> HO	Exceedingly rare and sporadic	Poor. It should be used with caution	37.72 $\pm$ 0.01	37.71 $\pm$ 0.01	37.1	Biogeographically controlled (2, 3,)
11	<i>C. erbae</i> AB	Neat	Excellent.	37.83 $\pm$ 0.02	37.82 $\pm$ 0.01	--	
10	<i>C. oamaruensis</i> LRO	Exceedingly rare and sporadic	poorly reliable	37.84 $\pm$ 0.034	37.78 $\pm$ 0.01	37	Recorded at 38.78 Ma in high latitude southern Ocean (6). In North Apennines sections the marker is present as spike within the range of <i>S. obtusus</i> .
9	<i>S. obtusus</i> HO	Neat	Good	38.25 $\pm$ 0.034	38.45 $\pm$ 0.02	--	
8	<i>C. solitus</i> HO	Missing in most sections and, when present, rare and discontinuous	Not reliable	38.49 $\pm$ 0.04	38.40 $\pm$ 0.01	40.4	Recorded at 38.03 Ma in high latitude southern Ocean (6)
7	<i>S. obtusus</i> LO	Neat	Moderately good, slightly diachronous	39.63 $\pm$ 0.01	40.13 $\pm$ 0.01	--	
6	<i>S. spiniger</i> HCO	Neat	Moderately good	40.10 $\pm$ 0.01	40.27 $\pm$ 0.04	--	
5	<i>D. bisectus</i> LCO	Neat	Good even if environmentally controlled	40.59 $\pm$ 0.01	40.35 $\pm$ 0.01	38,0	Site 1263 40.32 Ma
4	<i>D. scrippsae</i> LCO	Neat	Possibly good but not sufficiently tested and probably controlled by environment	40.60 $\pm$ 0.01	40.35 $\pm$ 0.01	--	At Site 1263 age estimated is 40.32 Ma, apparently in agreement with (1) who refers to this species as <i>D. hesslandii</i>
3	<i>S. furcatolithoides</i> HO	Neat	good. Probably worldwide correlable	40.78 $\pm$ 0.02	40.38 $\pm$ 0.01	--	The age evaluation at Alano is to be considered with caution because it is based on extrapolation of sedimentation rate throughout a long interval, most probably the best evaluation is that of Site 1052. At the Contessa Highway section (Umbria) the estimated age by (5) is ca. 40.6 Ma
2	<i>C. reticulatum</i> LCO	Documented at Alano and Site 1052; Apparently neat	Scattered in the initial range, possibly good as LCO, but not sufficiently tested	41.12 $\pm$ 0.04	--	42.00	(4) estimate the LO of <i>C. reticulatum</i> .
1	<i>R. umbilicus</i> LO	Documented only at Bottacione; To be further tested	Scattered in the initial range, possibly good as LCO, but not sufficiently tested	42.67 $\pm$ 0.11	--	43.7	Recorded as LCO at ca 42.3 Ma in the Contessa Highway section (5)

1) Backman (1987); 2) Wei and Wise (1990a); 3) Wei and Thierstein, (1991); 4) Berggren et al. (1995); 5) Jovane et al. (2007a); 6) Villa et al. (2008).  
\* Alano  
\* Umbria-Marche

(text-figs. 4, 5), suggesting a distinct diachrony between these two areas. At ODP Site 1263 (text-fig. 14), the event is recorded in a negative interval that can be interpreted as the lower part of Chron C18r, i.e., in a position that agrees with that observed at ODP Site 1052, and some previous calibrations (Poore et al. 1984; Wei and Wise 1989; 1990).

Above its HCO, *C. solitus* is recorded only sporadically when counting 500 nannofossil specimens. In order to better assess the patterns of its final distribution at ODP Site 1052, we counted *C. solitus* in an area of about 6–7 mm<sup>2</sup> (text-fig. 5). This, however, is a very time-consuming analysis that is difficult to accomplish in routine biostratigraphic work. Within this extended counting, the species is present with good continuity at both locations up to its very final exit (the HO). The HO of *C. solitus* occurs at the top of Chron C18n at Alano and at the transition between C18n and C17r at ODP Site 1052 (text-figs. 4, 5; Table 2). After interpolation between nearest reversal boundaries, age estimates of 38.49 Ma (Alano) and 38.40 Ma (Site 1052) were obtained. Surprisingly, these findings are in good agreement with previous estimated ages from southern mid-high latitudes (Villa et al. 2008), suggesting synchronous extinction of *C. solitus* over large distances. However, both the HO and HCO of *C. solitus* are here considered poorly reproducible biohorizons, at least in middle latitude areas.

#### The HO of *Blackites gladius*

The total range of *B. gladius* is believed to be short (Varol 1998). Its HO was used in Martini's zonation (1971) to mark

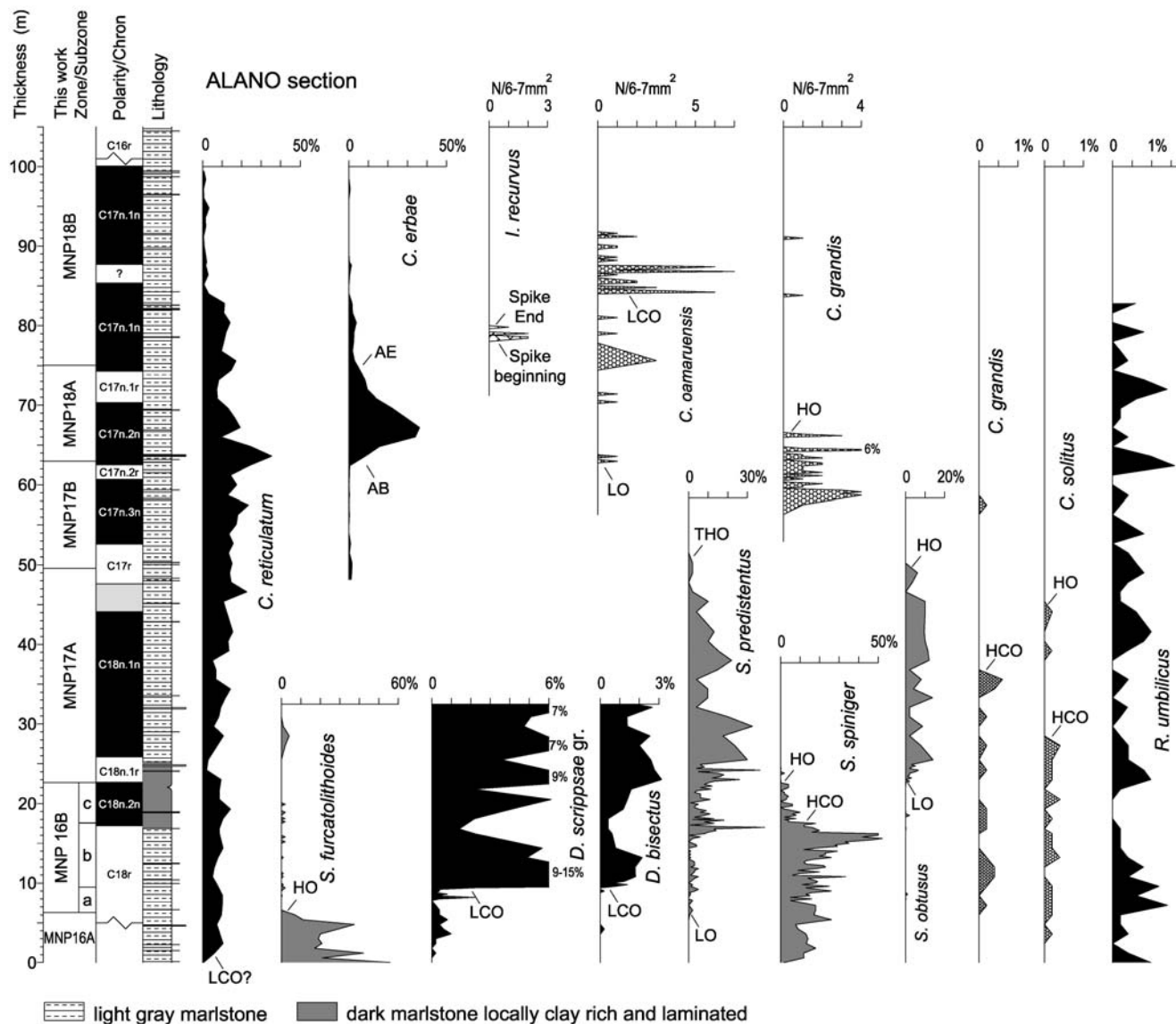
the base of Zone NP16. This biohorizon is rarely used because the species distribution is thought to be facies controlled (Martini and Müller 1986; Bukry et al. 1971), showing very low abundances in deep-sea sediments (e.g., Wei and Wise 1989). Berggren et al. (1995) tied the HO of *B. gladius* to uppermost part of Chron C19n. The virtual absence of this taxon in our study material, which probably is related to an ecological and/or stratigraphic exclusion (text-figs. 4, 5, 6, and 14), prevents reliable calibration of this biohorizon.

#### The HO of *Discoaster bifax*

The HO of *D. bifax* has been used as a secondary criterion to mark the base of Zone CP14b (Okada and Bukry 1980), but it is seldom if ever used because of its strictly biogeographically-controlled distribution. *Discoaster bifax* is found to be common in equatorial sediments (Bukry 1973; Okada 1990), but sporadic to absent at middle to high latitudes (Percival 1984; Proto Decima et al. 1975; Nocchi et al. 1988; Wei and Wise 1989; 1992; Wei and Thierstein 1991; Marino and Flores 2002a; b). Recently, Marino and Flores (2002a) correlated the HO of *D. bifax* to Chron C18r. We were unable to recognize specimens ascribable to *D. bifax*, and consequently its final presence in our material is not identified.

#### The LO and LCO of *Chiasmolithus oamaruensis*

The LO of *C. oamaruensis* defines the base of Zone NP18, and is used as a secondary criterion for defining the CP15 Zone (Martini 1971; Okada and Bukry 1980). This species is always a



TEXT-FIGURE 4

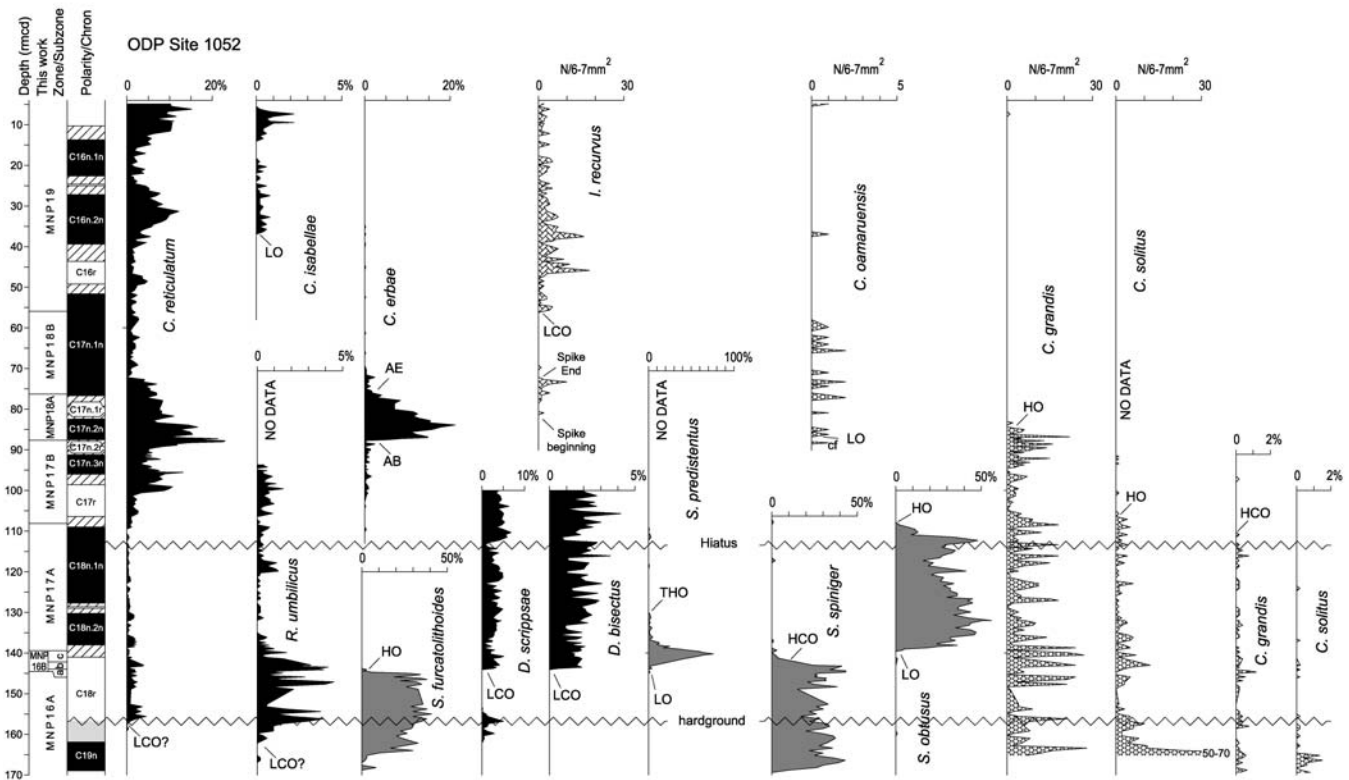
Alano section (Belluno province, Southern Alps, NE Italy). Abundance patterns of selected calcareous nanofossil species are plotted against the magnetostratigraphy and biostratigraphy. The lithologic column is also reported. The X-axis values represent the percentages relative to 500 specimens counted, except for sphenoliths (percentage relative to 50-100 sphenoliths) and when it is differently specified (N/6-7 mm<sup>2</sup>). Magnetostratigraphy after Agnini et al. (in press). THO= Temporary High Occurrence

rare component among nanofossil assemblages in low and middle latitude areas, where its LO is difficult to recognize (Wei and Wise 1989).

Villa et al. (2008) discussed the poor utility of the *C. oamaruensis* datum in Southern Ocean high latitudes. They observed, in agreement with previous data (e.g., Proto Decima et al. 1978; Marino and Flores 2002a; b), that the LO of *C. oamaruensis* is located below the HO of *C. solitus*, thus invalidating the NP18 Zone of Martini (1971). For this reason, Villa et al. (2008) employed the HCO of *C. solitus* and the LCO of *C. oamaruensis*, which, at least, maintains the ranking assumed in the standard zonations.

As a result, the calibrations available for the LO of *C. oamaruensis* are highly contradictory (Wei and Wise 1989; 1990; 1992; Aubry 1992; Wei et al. 1992; Marino and Flores 2002a; b; Villa et al. 2008) and diachrony between high and middle-low latitude areas have often been suggested (Wei and Thierstein 1991; Aubry 1992; Wei and Wise 1992; Marino and Flores 2002a; b; Villa et al. 2008; Table 3).

Here, the range of *C. oamaruensis* has been monitored in high resolution at the “master” sections of Alano and ODP Site1052. Lower resolution data have been collected from ODP Site1263 (Walvis Ridge) and in the Spettine, Fosio, Borra del Baccarino, Zermagnone and Casa la Croce sections (text-figs. 4, 5, 8-14).



TEXT-FIGURE 5

ODP Site 1052 (Leg 171B, Blake nose, NW Atlantic Ocean). Abundance patterns of selected calcareous nannofossil species are plotted against the magnetostratigraphy. The X-axis values represent the percentages relative to 500 specimens counted, except for sphenoliths (percentage relative to 50-100 sphenoliths) and when it is differently specified ( $N/6-7 \text{ mm}^2$ ). The 600 kyr hiatus at ca. 205 mcd is based on cyclostratigraphic data of Pälike et al. (2001). Magnetostratigraphy after Ogg and Bardot (2001) and Pälike et al. (2001).

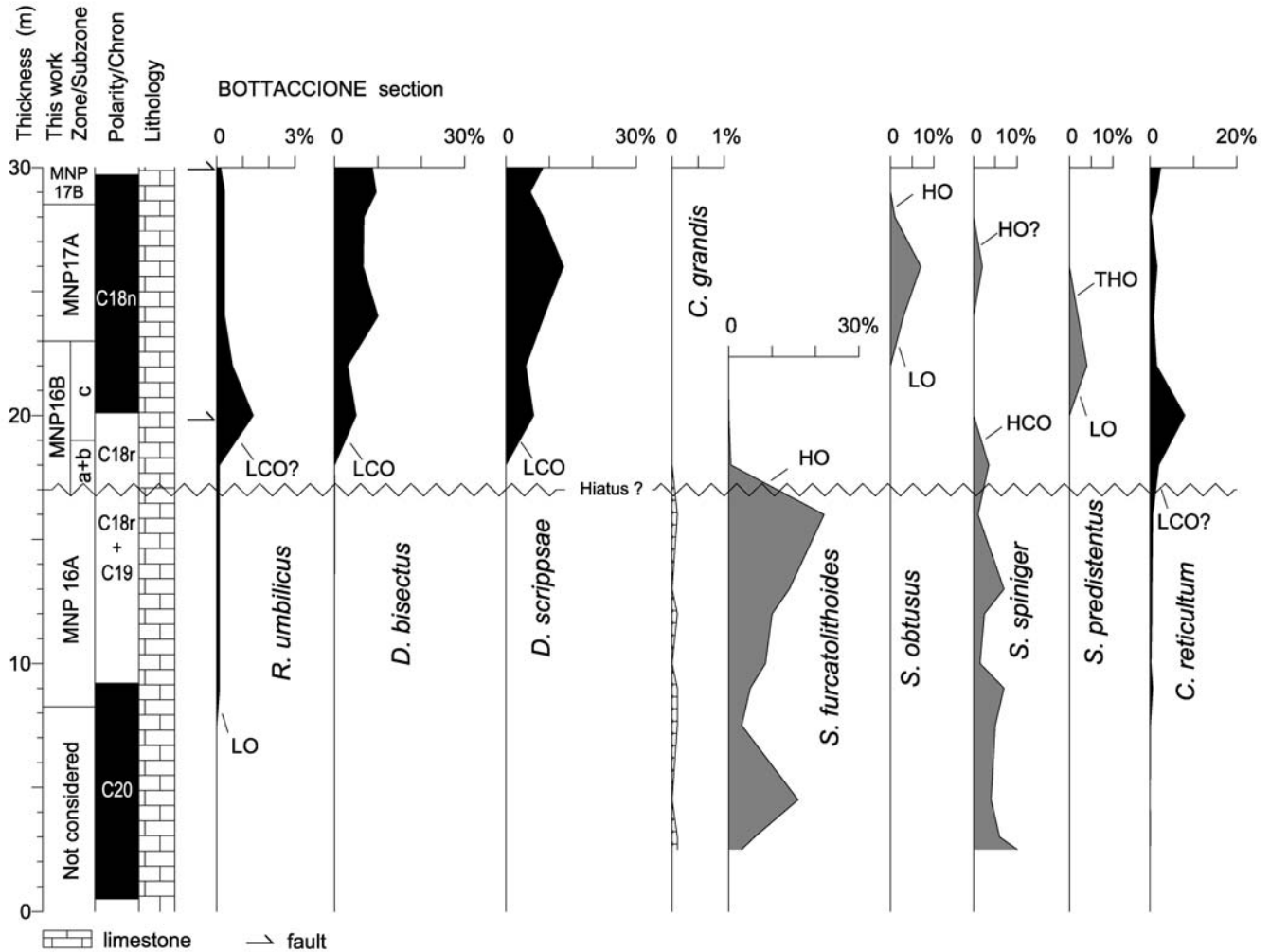
The species exhibits an exceedingly rare and sporadic occurrence and is virtually never recorded in the 500 specimens counted. At Alano, on the basis of data collected with extended areal counting, we have tentatively distinguished the LO from the LCO of *C. oamaruensis* (text-fig. 4). However, it should be noted that at ODP Site 1052 such distinction is not apparent (text-fig. 5), whereas the LO and LCO of the species are detectable in the Fosio and Borra del Baccarino sections (text-figs. 9, 10). Text-figure 15 clearly indicates the different relative positions of the LCO of *C. oamaruensis* with respect to other more reliable events. In addition, the LCO of the species observed in the two Apennines sections seems to correlate with the LO of *C. oamaruensis* at Alano (text-figs. 4, 9, 10, 15). We conclude that the LCO of *C. oamaruensis* is not a reliable event. However, we notice that, the LO of *C. oamaruensis* is consistently associated with the upper part of Chron C17n.2n at both Alano and ODP Site 1052, which is older than the previous calibration of Berggren et al. (1995) at the top of Chron C17n.1n (Table 3). However, LO datums from the Fosio and Borra del Baccarino sections are located in a still lower stratigraphic position. Although no magnetic stratigraphy is available in these sections, correlations shown in text-figure 15 suggests that the evolutionary appearance of *C. oamaruensis*, the First Appearance Datum (FAD), might be associated with Chron C18n.1n. This is in agreement with results reported by Villa et al. (2008) from the

high latitude Southern Ocean: upper Chron C18n.1n (38.80 Ma).

#### *The HCO and HO of Chiasmolithus grandis*

The HO of *Chiasmolithus grandis* defines the base of Zone CP15a (Okada and Bukry 1980). The species is common at low to middle latitudes, whereas it is found to be exceedingly rare or absent at the high latitudes (Wei and Wise 1990; 1992; Wei and Thierstein 1991). The relative position of the HO of *C. grandis* and LO of *C. oamaruensis*, the two alternative events used for recognizing the base of Zone CP 15a, are highly contradictory. As a matter of fact most authors report the HO of *C. grandis* just below the LO of *C. oamaruensis* (Wei and Wise 1989; Percival 1984; Berggren 1995; Marino and Flores 2002a,b), but others observed a reversed position between the two biohorizons (Proto Decima et al. 1975; 1978; Nocchi et al. 1988).

At Alano and ODP Site 1052, *C. grandis* is recorded in the 500 specimens counted, albeit in low frequencies, with good continuity allowing us to define its HCO (text-figs. 4 and 5). Above the HCO, the species is only sporadically observed. In order to better constrain the final occurrence of *C. grandis*, we did areal counts that record a different result (text-figs. 4 and 5). The species persists for a long interval above its HCO, allowing us to



TEXT-FIGURE 6  
Bottaccione section (Umbria Region, Northern Apennines, Central Italy). Abundance patterns of selected calcareous nannofossil species are plotted against the magnetostratigraphy and biostratigraphy. The lithologic column is also reported. The X-axis values represent the percentages relative to 500 specimens counted, except for sphenoliths (percentage relative to 50-100 sphenoliths). Magnetostratigraphy after Napoleone et al. (1983). THO= Temporary High Occurrence.

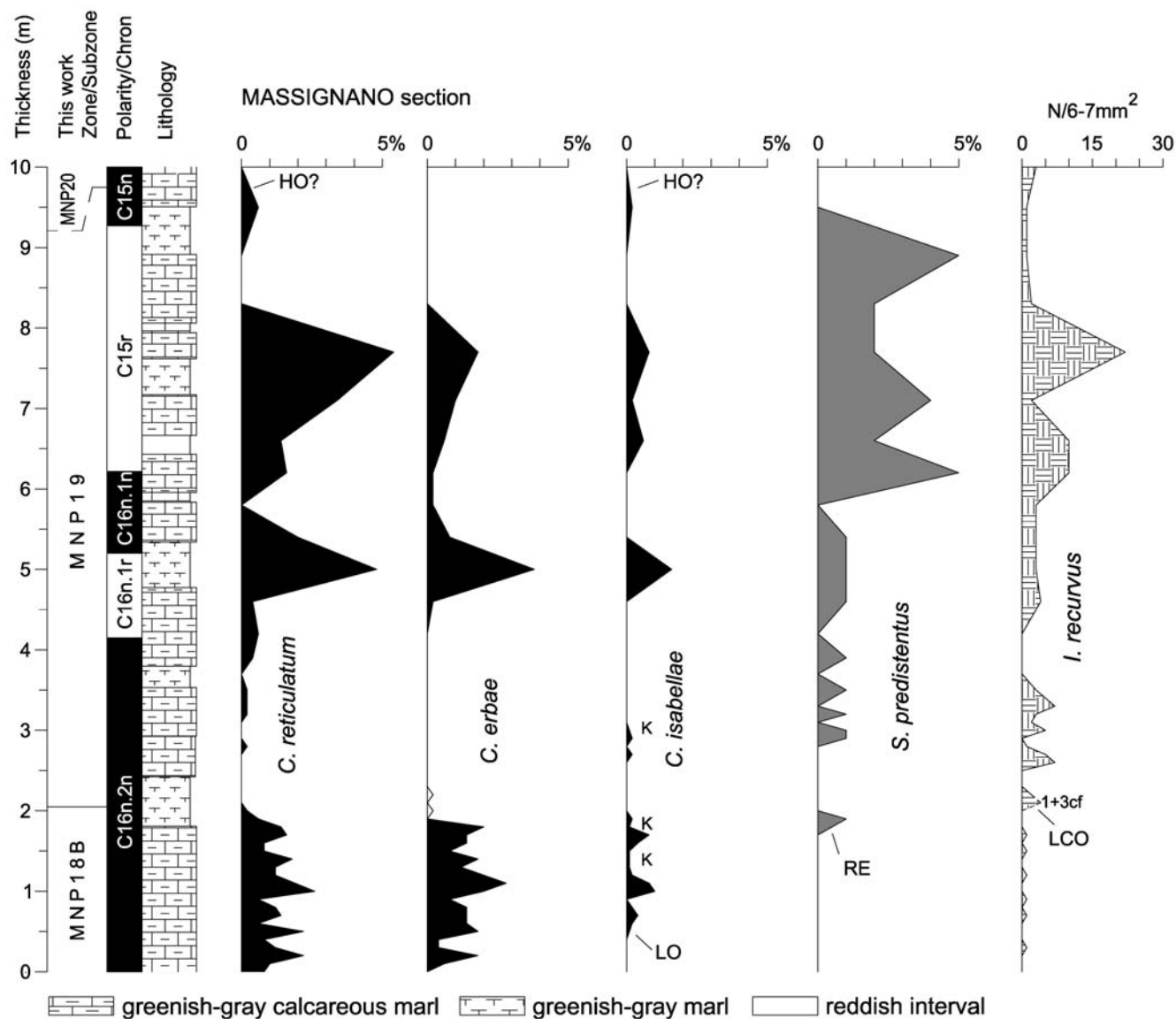
define the last occurrence of the species both at Alano and ODP Site 1052.

From the biochronologic point of view, the HCO is associated with Chron C18n.1n, while the HO is consistently correlated to the middle part of Chron C17n.2n (Tables 2 and 3). Based on data of Backman (1987) from DSDP Site 523, Berggren et al. (1995) positioned the final presence of *C. grandis* within Chron C17n.1n. By contrast, in the Mediterranean region, Monechi and Theirstein (1985) correlated the bioevent to the top of Chron C18n. Our results indicate that, based on data from ODP Site 1263, the HO of *C. grandis* occurs in an interval where the clustering of several normally well spaced events suggests the presence of a hiatus (text-fig. 14). In the Northern Apennines sections, the HO of the species, as shown in text-figure 15, surprisingly remains in the same stratigraphic position. In spite of the positive results that indicate a substantial correlability of the event on a supraregional base, we consider both the HCO and

HO of *C. grandis* as problematic biohorizons that should be used with caution for long distance correlation.

#### The spike and LCO of *Isthmolithus recurvus*

*Isthmolithus recurvus* provides two distinct events in the Mediterranean area, namely its first spike in abundance and the subsequent LCO. The evolutionary appearance of *I. recurvus* is widely used as an intra-Priabonian event defining the base of Zone the NP19 and the CP15b Subzone (Martini 1971; Okada and Bukry 1980). However, the reliability of the event has been debated because *I. recurvus* seems to be restricted to middle and high latitudes (e.g., Backman 1987; Wei and Wise 1989; Bukry 1975; 1978). Catanzariti et al. (1997) studied calcareous nannofossils in several sections in the Northern Apennines and observed a peculiar distribution of *I. recurvus*. After a short interval where it is present (the spike), the species disappeared to re-enter higher up in the sections, with continuous occurrences (the LCO). On the basis of these findings, they distin-



TEXT-FIGURE 7

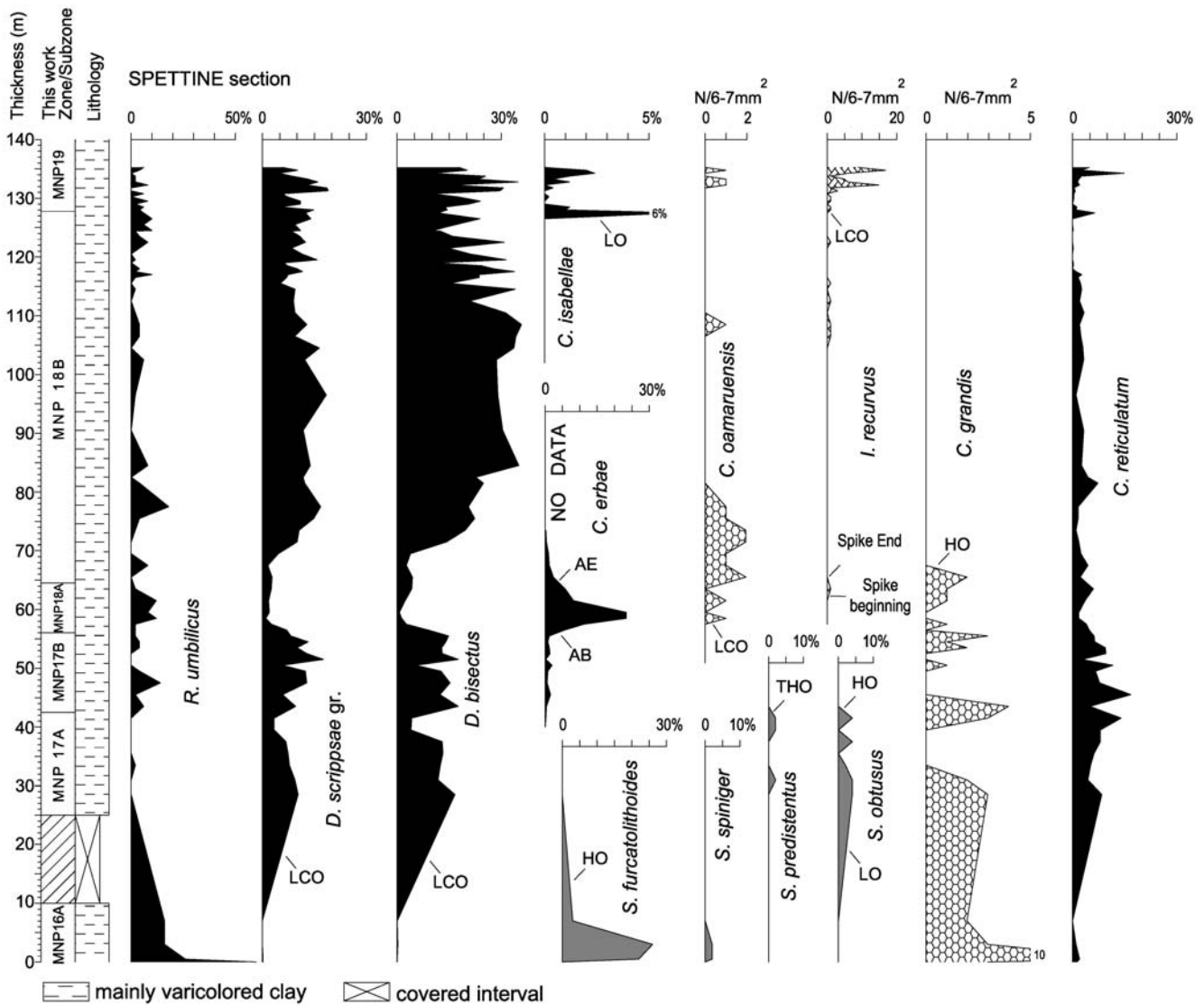
Massignano section (Marche Region, Northern Apennines, Central Italy). Abundance patterns of selected calcareous nannofossil species are plotted against the magnetostratigraphy and biostratigraphy. The lithologic column is also reported. The X-axis values represent the percentages relative to 500 specimens counted, except for sphenoliths (percentage relative to 50-100 sphenoliths) and when it is differently specified (N/6-7 mm<sup>2</sup>). Magnetostratigraphy after Jovane et al. (2007b). RE=re-entrance; K= extra-counting presence.

guished two datums, the LO (the beginning of the spike) and the LCO, the second of which was used for reliable regional correlation and as a definition of a regional zonal boundary.

This distribution pattern is confirmed in our high resolution data from ODP Site 1052 (text-fig. 5). A first short interval of occurrence, referred to as the spike, (text-fig. 5; Tables 2, 3) was observed from the base of Chron C17n.1r to the base of Chron C17n.1n. The beginning of the common and continuous distribution of the species (the LCO) correlated to the top of Chron C17n.1n (text-fig. 5). The spike of *I. recurvus* occurs also at Alano, albeit slightly later and for a shorter interval compared to ODP Site 1052 (text-fig. 15). The LCO of *I. recurvus*

was not observed at Alano up to the top of the section, that is the very base of Chron C16r.

At the Massignano section, the LCO of *I. recurvus* correlates with Chron C16n.2n (text-fig. 7). These findings suggest that the LCO datum of the index species is diachronous between the two areas (text-fig. 15). A distribution pattern of *I. recurvus*, similar to that observed at ODP Site 1052, has been documented by Backman (1987; in his text-fig.5) at DSDP Site 523 (Walvis Ridge), where this taxon shows an early and shorth occurrence (the spike) followed by an interval of absence and, finally, by the beginning of a continuous and common distribution. correlating with the top of Chron C17n.1n (LCO). Backman (1987)

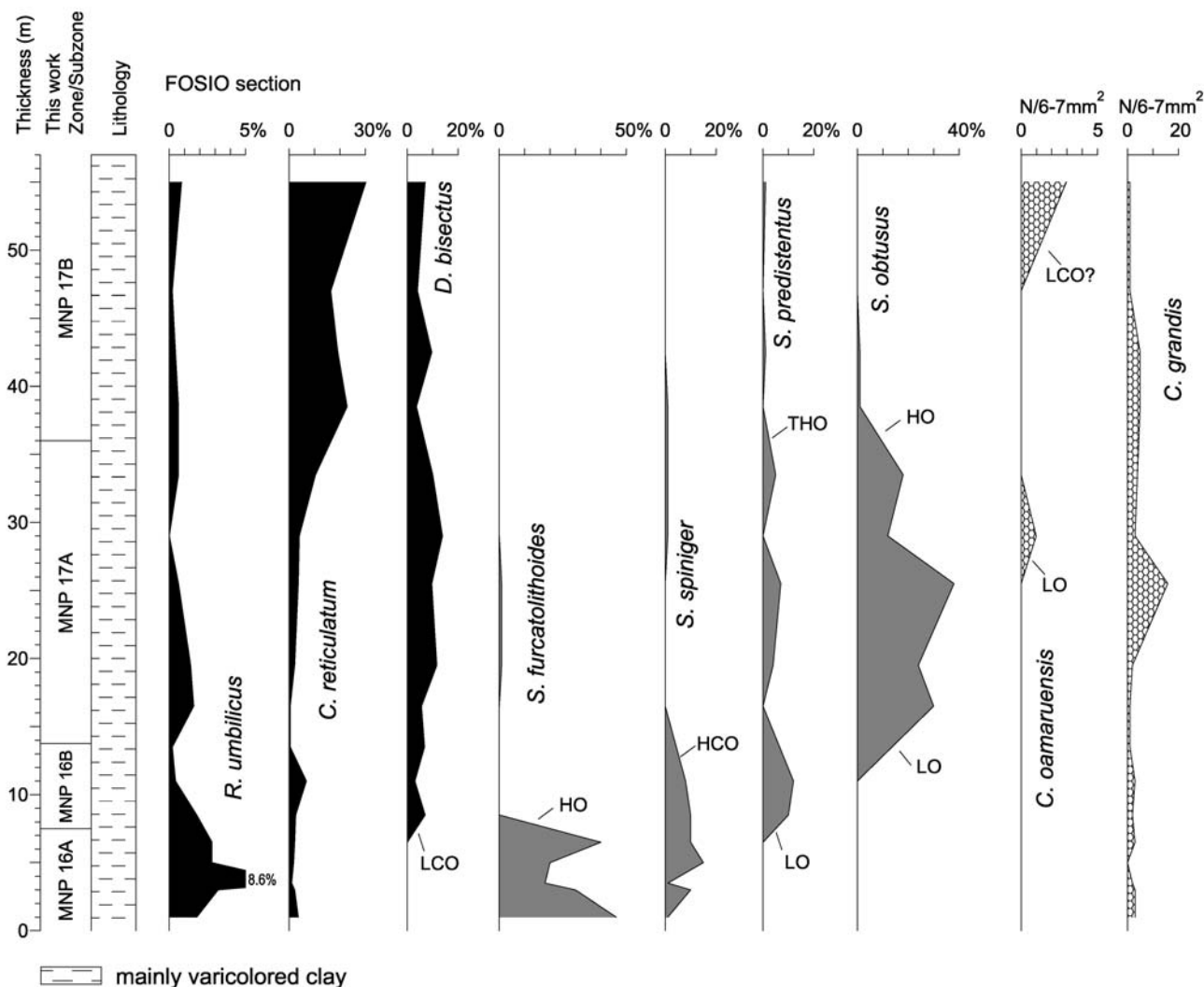


TEXT-FIGURE 8  
 Spettine section (Piacenza Province, Northern Apennines, N Italy). Abundance patterns of selected calcareous nanofossil species are plotted against the biostratigraphy. The lithologic column is also reported. The X-axis values represent the percentages relative to 500 specimens counted, except for sphenoliths (percentage relative to 50-100 sphenoliths) and when it is differently specified ( $N/6-7 \text{ mm}^2$ ).

considered the spike of *I. recurvus* as due to down hole contamination, but the data reported from Alano and ODP Site 1052 clearly demonstrate that the absolute first occurrence of *I. recurvus* is considerably older than generally assumed in the literature, where it is prevalently associated with Chron C16n.2n (Persico and Villa 2004; Marino and Flores 2002a; b; Berggren et al. 1995). The LCO of *I. recurvus*, that can be observed over a wide latitudinal range (see also Villa et al. 2008), is apparently a diachronous event and must be used with caution for long distance correlation. However, on a regional basis the LCO of the species provides a useful correlation tool as demonstrated by its distribution in other sections (text-fig. 15).

#### Additional calcareous nanofossil biohorizons

The data and observations presented above imply that virtually none of the biohorizons used in the standard zonations of Martini (1971) and Okada and Bukry (1980) work well in the middle-late Eocene interval. A possible exception may be the LO of *R. umbilicus*, which, however, have been monitored in single section suggesting that this biohorizon needs further scrutiny. Thus, in the approximately 6-8 Myr long time interval considered here, there is a strong need to employ alternative events in order to establish a meaningful biostratigraphic correlation and classification. Some authors (e.g., Perch-Nielsen 1985;



TEXT-FIGURE 9

Fosio section (Parma Province, Northern Apennines, N Italy). Abundance patterns of selected calcareous nannofossil species are plotted against the biostratigraphy. The lithologic column is also reported. The X-axis values represent the percentages relative to 500 specimens counted, except for sphenoliths (percentage relative to 50-100 sphenoliths) and when it is differently specified ( $N/6-7 \text{ mm}^2$ ). The lack of Subzones MNP16Ba and MNP16Bc may be due to a short hiatus or to the low-resolution sampling. THO= Temporary High Occurrence.

Backman 1987; Nocchi et al. 1988; Okada 1990) proposed alternative biohorizons based on taxa not considered in the standard zonations. In the following we will examine the distribution patterns of taxa within the following three genera: *Criboecentrum*, *Dictyococcites* and *Sphenolithus*. We will discuss their reliability and biochronology of biohorizons previously adopted in the literature as well as new bioevents.

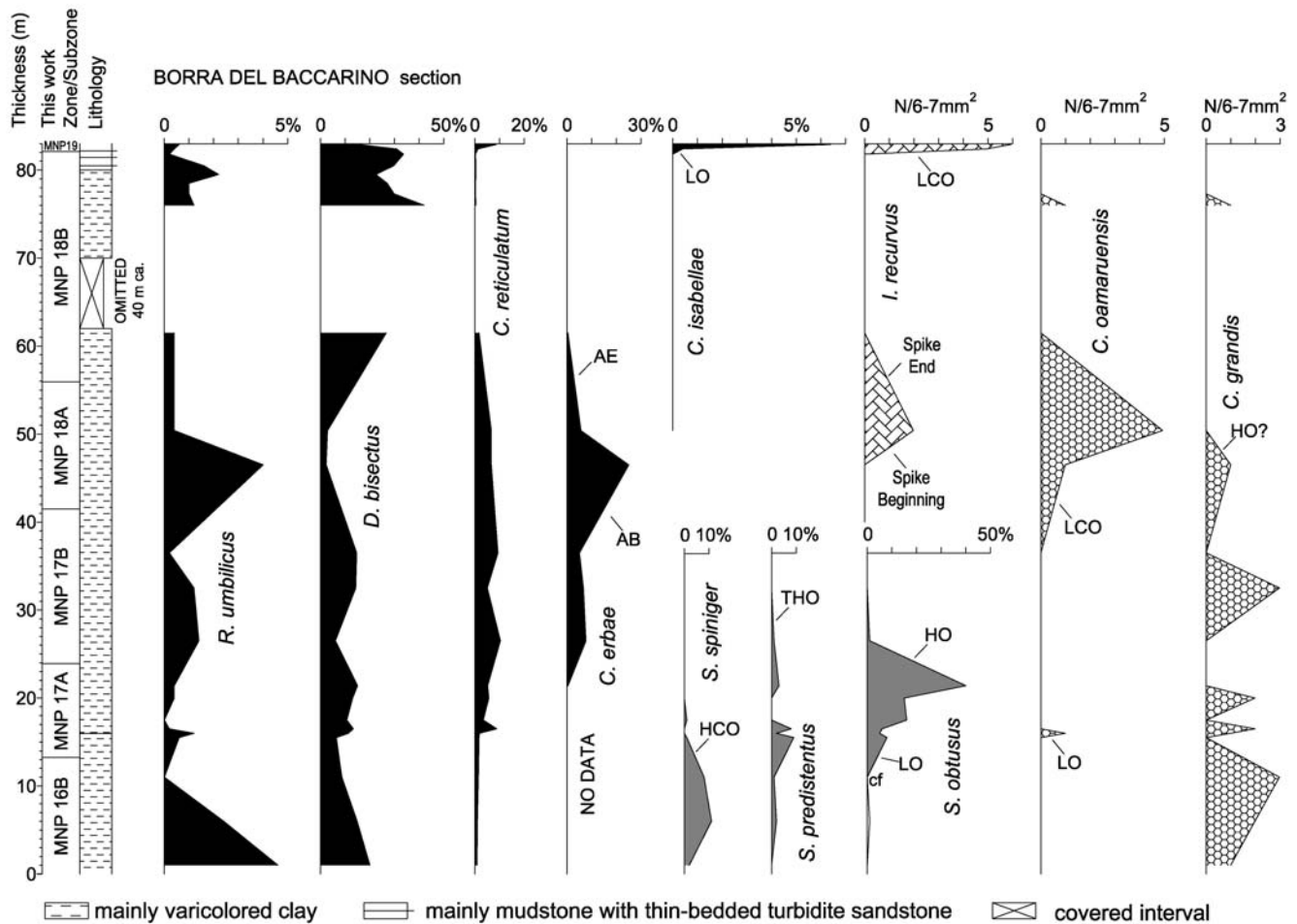
### *Criboecentrum*

Species belonging to *Criboecentrum* are common to dominant in most of our sections, except in South Atlantic ODP Site 1263, where this group is rare and/or missing for long intervals (text-fig. 14). *Criboecentrum reticulatum* is the only species within this genus that is commonly described from the middle-late Eocene interval. It has been reported as common from high (Müller 1976; Wise 1983) to low latitudes (Bukry 1977), in neritic (Siesser 1983) as well as pelagic environments (Gart-

ner 1974). Both the LO and HO of this species have been utilized in regional biostratigraphy of the middle-late Eocene interval (Backman 1987; Wei and Wise 1989; 1990; 1992; Wei and Thierstein 1991; Catanzariti et al. 1997; Marino and Flores 2002a; b; Villa et al. 2008). As discussed in the taxonomic remarks, we recognize two additional species within this genus, *C. erbae* and *C. isabellae*, which are easily distinguished from *C. reticulatum* s.s. in the light microscope. Within the framework of this revised taxonomy, several apparently reliable biohorizons are provided by *Criboecentrum* species.

### *The LO and LCO of Criboecentrum reticulatum*

The LO of *C. reticulatum* is a widely used biohorizon (Wei and Wise 1989; 1990; 1992; Wei and Thierstein 1991; Berggren et al. 1995; Marino and Flores 2002a; b), and it has been proposed as the guiding criterion for defining the base of the middle Eocene Bartonian Stage (Berggren et al. 1985; 1995, p. 197;



TEXT-FIGURE 10  
 Borra del Baccarino section (Parma Province, Northern Apennines, N Italy). Abundance patterns of selected calcareous nanofossil species are plotted against the biostratigraphy. The lithologic column is also reported. The X-axis values represent the percentages relative to 500 specimens counted, except for sphenoliths (percentage relative to 50-100 sphenoliths) and when it is differently specified ( $N/6-7 \text{ mm}^2$ ). The lack of Subzone MNP16B is probably due to the low-resolution sampling. THO= Temporary High Occurrence.

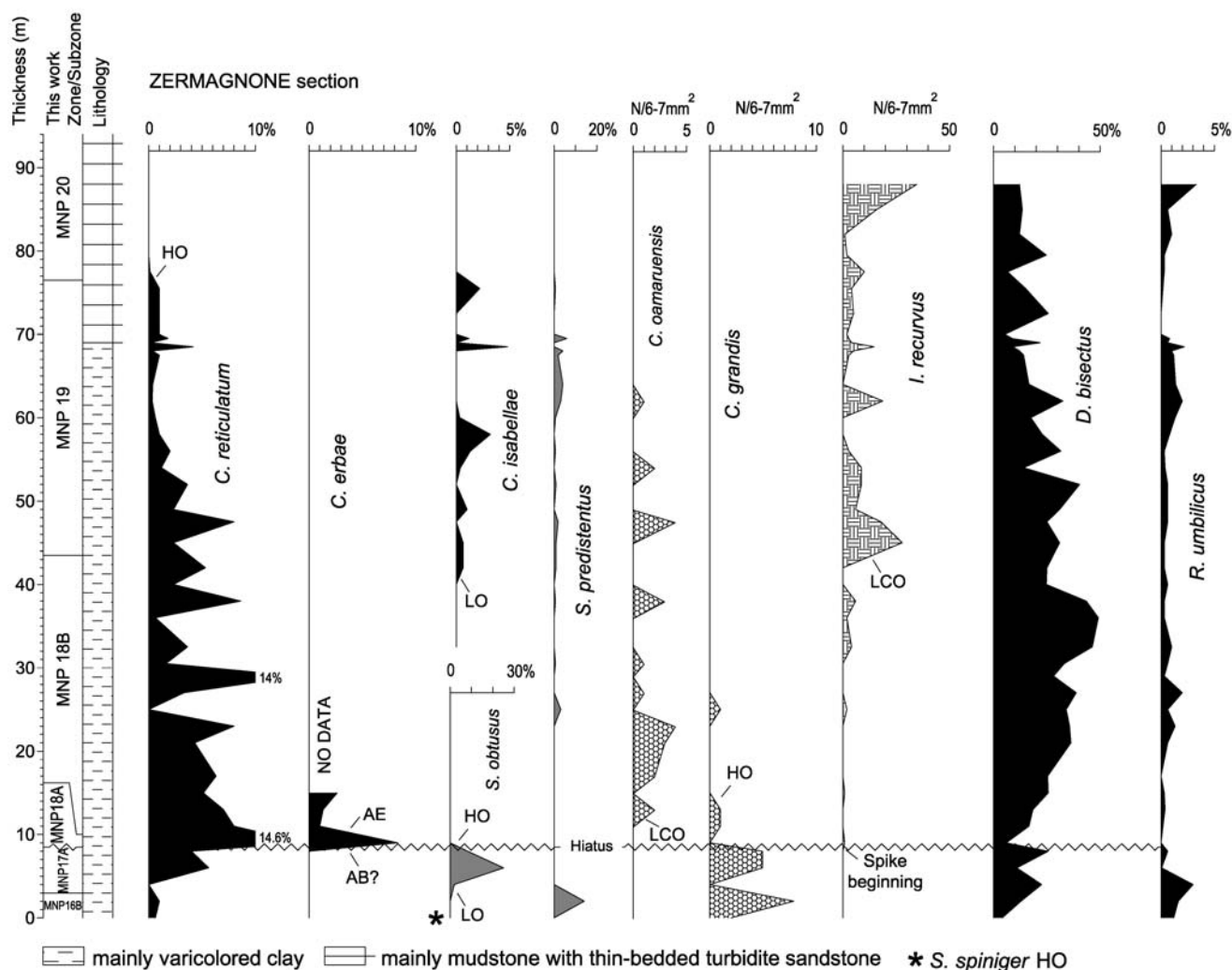
Fluegeman 2007), though its calibration to the GPTS (Table 3) is actually quite contradictory; For example, Berggren et al. (1995, p. 197) associated the event with Chron C19n, while Wei and Wise (1990) found the event in Chron C18n.2n. Rare and discontinuous specimens of *C. reticulatum* have been observed at the top of Chron C20n in Bottaccione section (text-fig. 6). Moreover, unpublished data on the Possagno section (NE Italy) indicate that this species is present at least in the lower part of Chron C20r. The reproducibility of these earliest occurrences is probably low and we retain that the absolute first occurrence datum of the species is to be considered a poor event. Data from ODP Site 1052 suggest that the LCO of *C. reticulatum* is located at the very base of Chron C18r (text-fig. 5), which is consistent with Berggren's et al. (1995) observations. At Alano (text-fig. 4), the LCO of the species occurs at the base of the section in an interval lacking magnetic polarity data, but having an extrapolated age of 41.1 Ma (Table 2). At Bottaccione, the LCO of *C. reticulatum* has been observed in an interval of negative polarity that is difficult to correlate to the

GPTS because of the presence of a fault (Cresta et al. 1989; text-fig. 6). This datum is not documented in the Northern Apennines sections, and, hence, a final assessment on the reliability of the event is premature. However, the LCO of *C. reticulatum* at ca. 41 Ma appears as a promising biohorizon for subdivision of the long interval between the LO of *R. umbilicus* at ca. 42.7 Ma (Table 2) and the HO of *S. furcatolithoides* at ca. 40.78 Ma.

#### The AB and AE of *Criboecentrum erbae*

The most striking feature observed in the calcareous nanofossil distribution patterns reported in the present study is represented by the short-lived prominent acme interval shown by a circular *Criboecentrum* having a very bright central area. This new species is here described as *Criboecentrum erbae* sp. nov. The species shows a distinct increase in abundance resulting in a short-lived acme at both ODP Site 1052 and Alano, reaching 20-50% of the total nanofossil assemblage. This short high abundance interval is followed by a more gradual decrease in





TEXT-FIGURE 11

Zermagnone section (Parma Province, Northern Apennines, N Italy). Abundance patterns of selected calcareous nannofossil species are plotted against the biostratigraphy. The lithologic column is also reported. The X-axis values represent the percentages relative to 500 specimens counted, except for sphenoliths (percentage relative to 50-100 sphenoliths) and when it is differently specified ( $N/6-7\text{ mm}^2$ ). The truncated spacing between the HO of *S. obtusus* and the AB of *C. erbae* suggests that a short hiatus may be present.

abundance (text-figs. 4 and 5). We define the Acme Beginning (AB) and the Acme End (AE) of *C. erbae* as follows: the initial distinct increase from 0.3-1% to 5-8% of the total assemblage, and the final decrease in abundance from 4-6% to 0-2% of the total assemblage, respectively (text-figs. 4 and 5).

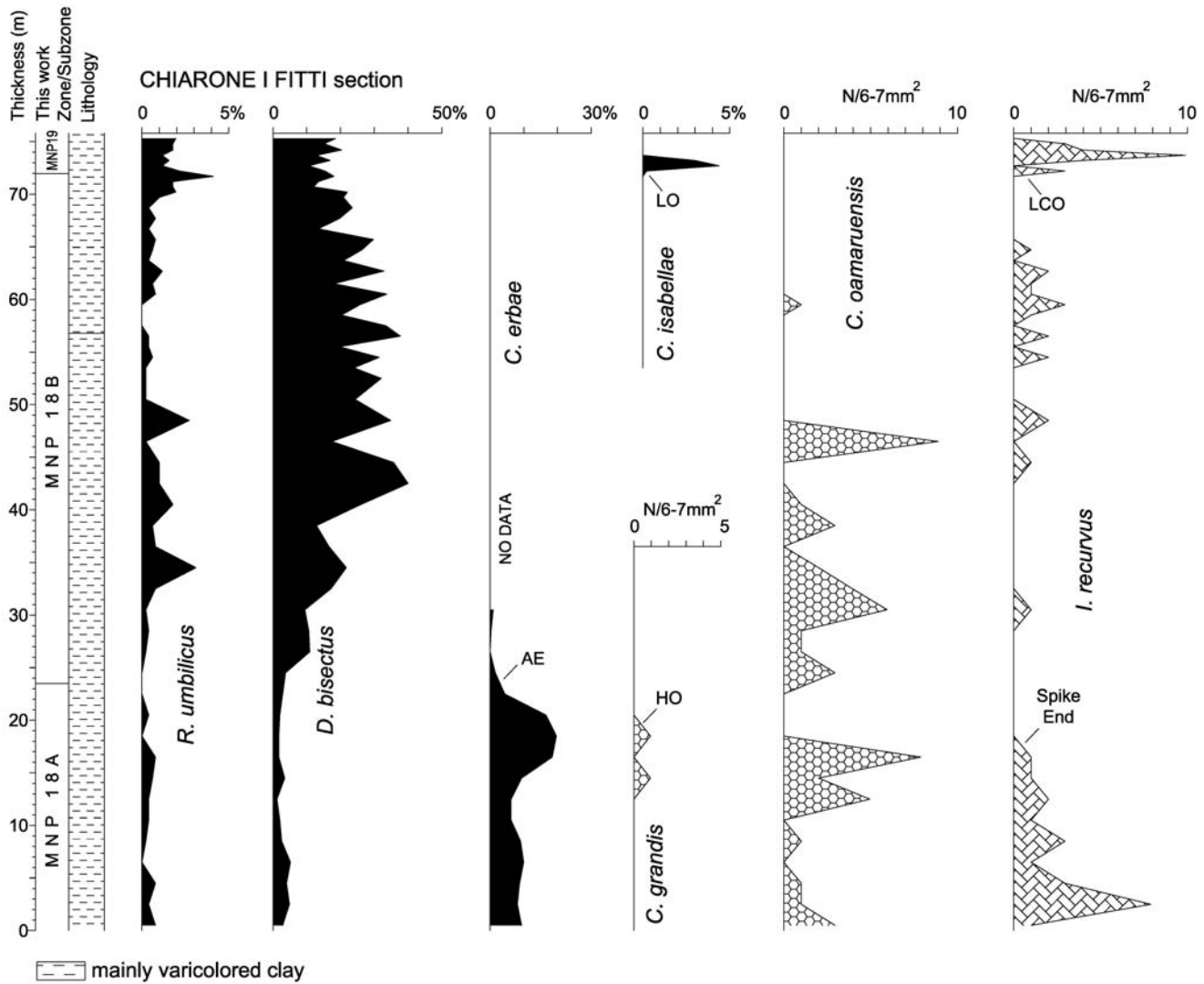
The AB and the AE events of *C. erbae* are recorded in the same magnetostratigraphic positions at both ODP Site 1052 and Alano: the AB occurs in the early part of Chron C17n.2n and the AE in the lower part of Chron C17n.1n (text-figs. 4 and 5). The estimated ages of the two biohorizons are thus consistent (Table 2) in the Atlantic and Mediterranean areas, suggesting synchrony for these biostratigraphic bioevents (text-fig. 1).

We have monitored the distribution of *C. erbae* also at the South Atlantic Ocean ODP Site 1263, where the genus *Criboecentrum* is poorly represented. *Criboecentrum erbae* is present, albeit rare, in this area. This species reaches significant abun-

dances in an interval that is probably affected by a hiatus, thus preventing the assessment of the reliability of the event in the area. However, the increase in abundance occurs in a stratigraphic position roughly comparable to that observed at Alano and ODP Site 1052 (text-figs. 4, 5 and 14). The same feature, the acme of *C. erbae*, is observed also in the Northern Apennines sections of Spettine (text-fig. 8) and Borra del Baccarino (text-fig. 10).

#### The LO of *Criboecentrum isabellae*

Catanzariti et al. (1997) observed the appearance of very large circular specimens of *Criboecentrum* in the late Eocene that they referred to as *Criboecentrum* aff. *reticulatum*, *C. isabellae* sp. nov. of this work. The initial distribution of this taxon is recorded at ODP Site 1052 and in the Massignano section. The LO of the species is distinct and occurs within the lower part of C16n.2n (text-fig. 5 and 7).



TEXT-FIGURE 12  
Chiarone i Fitti section (Piacenza Province, Northern Apennines, N Italy). Abundance patterns of selected calcareous nanofossil species are plotted against the biostratigraphy. The lithologic column is also reported. The X-axis values represent the percentages relative to 500 specimens counted except when it is differently specified (N/6-7 mm<sup>2</sup>).

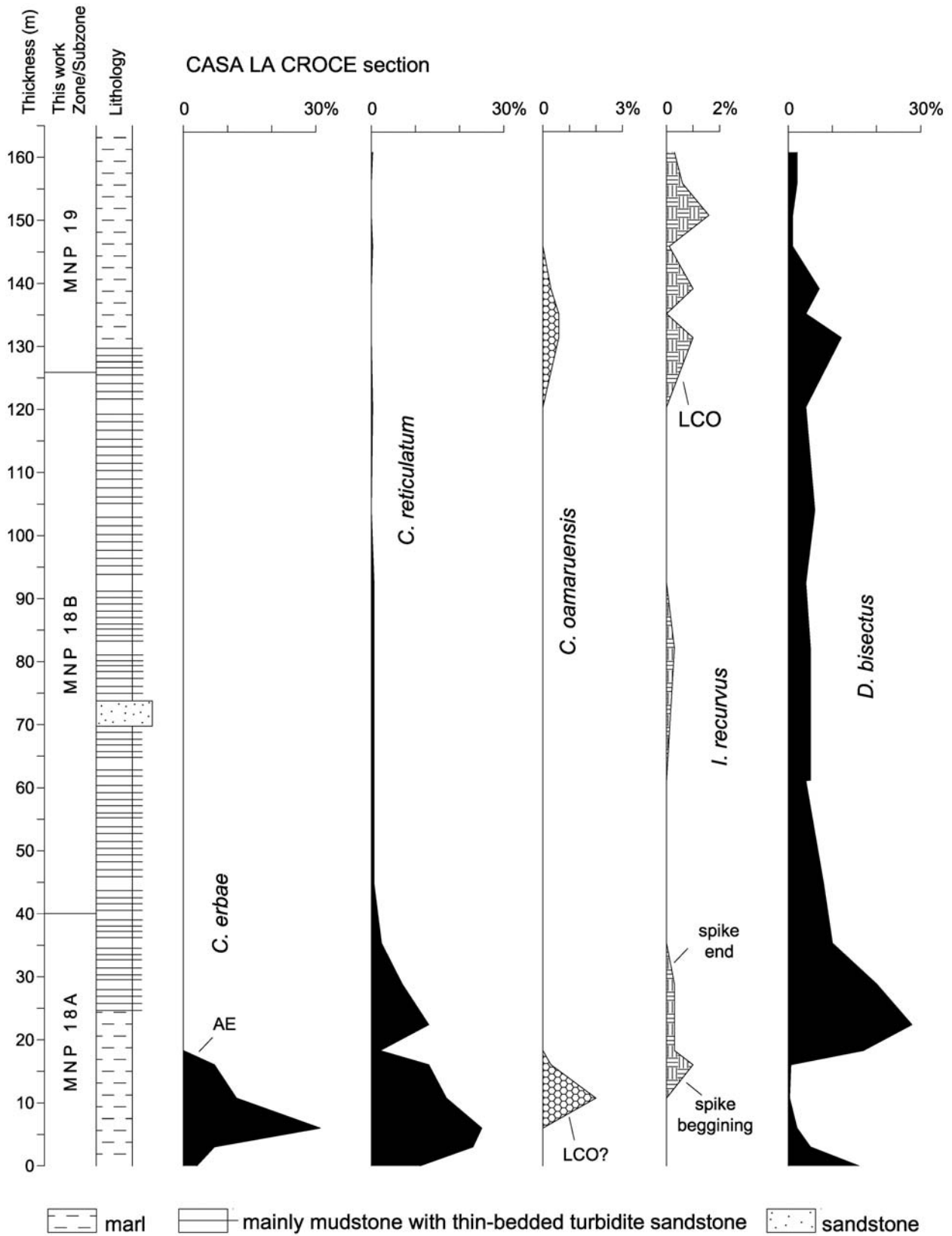
This biohorizon is recorded also in the Northern Apennines sections of Spettine, Chiarone i Fitti, Borra del Baccarino, and Zermagnone (text-figs. 8, 10, 11, 12), where it occurs virtually together with the LCO of *I. recurvus*. We thus consider the LO of *C. isabellae* as a reliable biohorizon that can be utilized in the Northern Apennines, also for the purpose of better assessing the LCO of *I. recurvus*.

*The LCO of Dictyococcites scrippsae and Dictyococcites bisectus*

The ambiguities in the taxonomy of the genus *Dictyococcites* limit its biostratigraphic usefulness (Wei and Wise 1989). However, by using the easily reproducible biometric definition of *D. bisectus*, as comprehending all specimens larger than 10 µm, both *D. bisectus* and *D. scrippsae* show biostratigraphically useful distribution patterns. In particular, *D. bisectus*, provides one of the strongest biostratigraphic signals observed both at Alano and ODP Site 1052 in the middle-late Eocene interval.

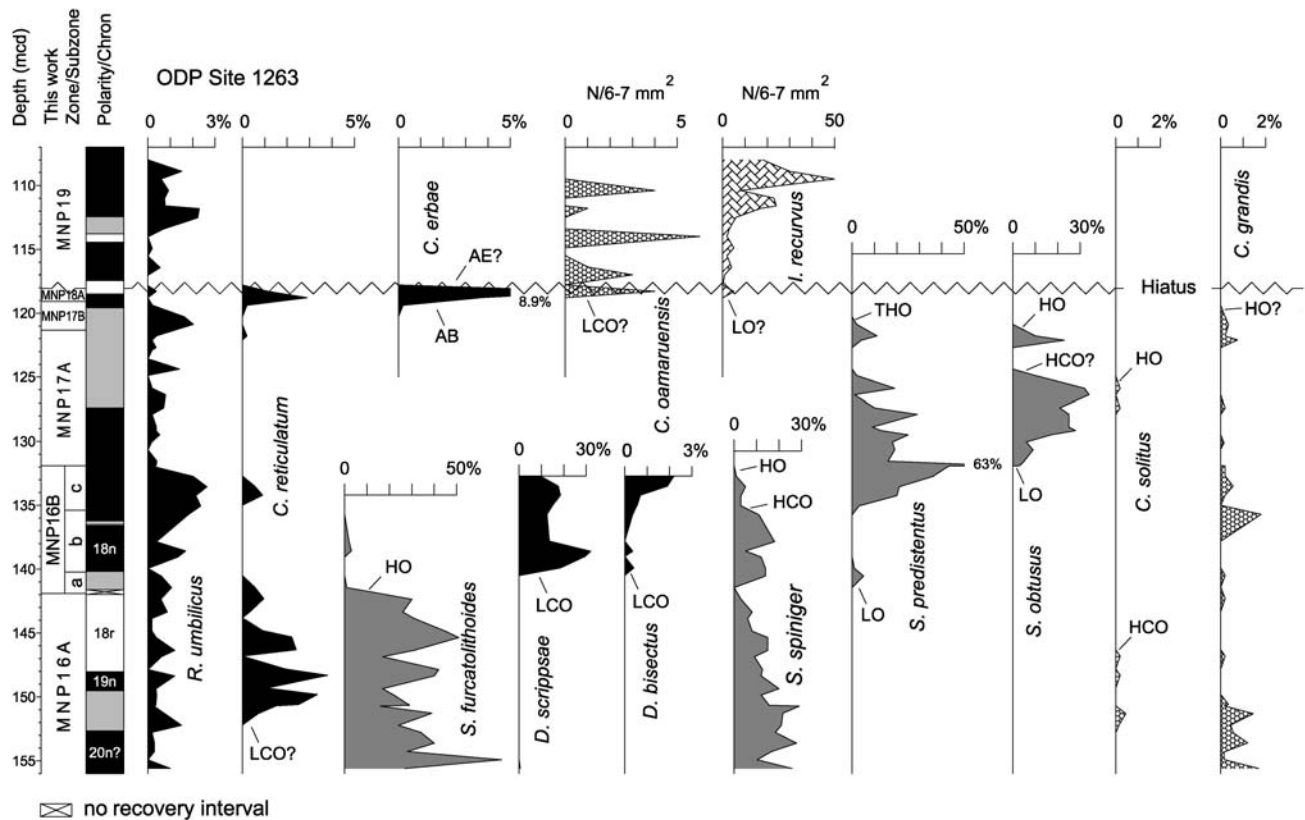
These morphotypes abruptly rise to abundances greater than 1-2 % of the total assemblage, based on counts of 500 specimens, and remain common to abundant in all examined samples (text-figs. 4 and 5). The appearance of larger forms defines the LCO of *D. bisectus*. *Dictyococcites scrippsae* increases in abundance virtually in coincidence with the LCO of *D. bisectus* and becomes a common and continuous component of the assemblages allowing a definition of its LCO (text-figs. 4 and 5). The same distribution pattern is observed in the poorly preserved material of the Bottaccione section (text-fig. 6), at ODP Site 1263 (text-fig. 14) and in the Northern Apennines Fosio section (text-fig. 9). Correlation shown in text-figure 15 suggests that the two biohorizons consistently occur in the same relative stratigraphic position.

Data from Alano and ODP Site 1052 indicate that the events occur within late Chron C18r, although at different stratigraphic



TEXT-FIGURE 13

Casa la Croce section (Alessandria Province, Northern Apennines, NW Italy). Abundance patterns of selected calcareous nannofossil species are plotted against the biostratigraphy. The lithostratigraphic column is also reported. The X-axis values represent the percentages relative to 500 specimens counted.



TEXT-FIGURE 14  
 ODP Site 1263 (Leg 208, Walvis Ridge, SE Atlantic Ocean) Abundance patterns of selected calcareous nannofossil species are plotted against the magnetostratigraphy and biostratigraphy. The X-axis values represent the percentages relative to 500 specimens counted, except for sphenoliths (percentage relative to 50-100 sphenoliths) and when it is differently specified ( $N/6-7 \text{ mm}^2$ ). Magnetostratigraphy after Zachos et al. (2004). THO= Temporary High Occurrence.

levels (Table 2). Data from ODP Site 1263, based on the magnetostratigraphic age model presented by Bohaty et al. (2009), seem to be consistent with the data produced in the North Atlantic and Italy. We have labeled the sharp increase of *D. bisectus* as a LCO, not LO, because the taxon has been reported from the middle latitude ODP Site 1051 and the Agost section at lower stratigraphic levels (Mita 2001; Larrasoña et al. 2008). The distribution of *D. bisectus* is biogeographically controlled (Perch-Nielsen 1985; Wei and Wise 1989; 1990) resulting in an apparently delayed appearance of *D. bisectus* within Chron C17n (Wei et al. 1992; Villa et al. 2008).

### Sphenolithus

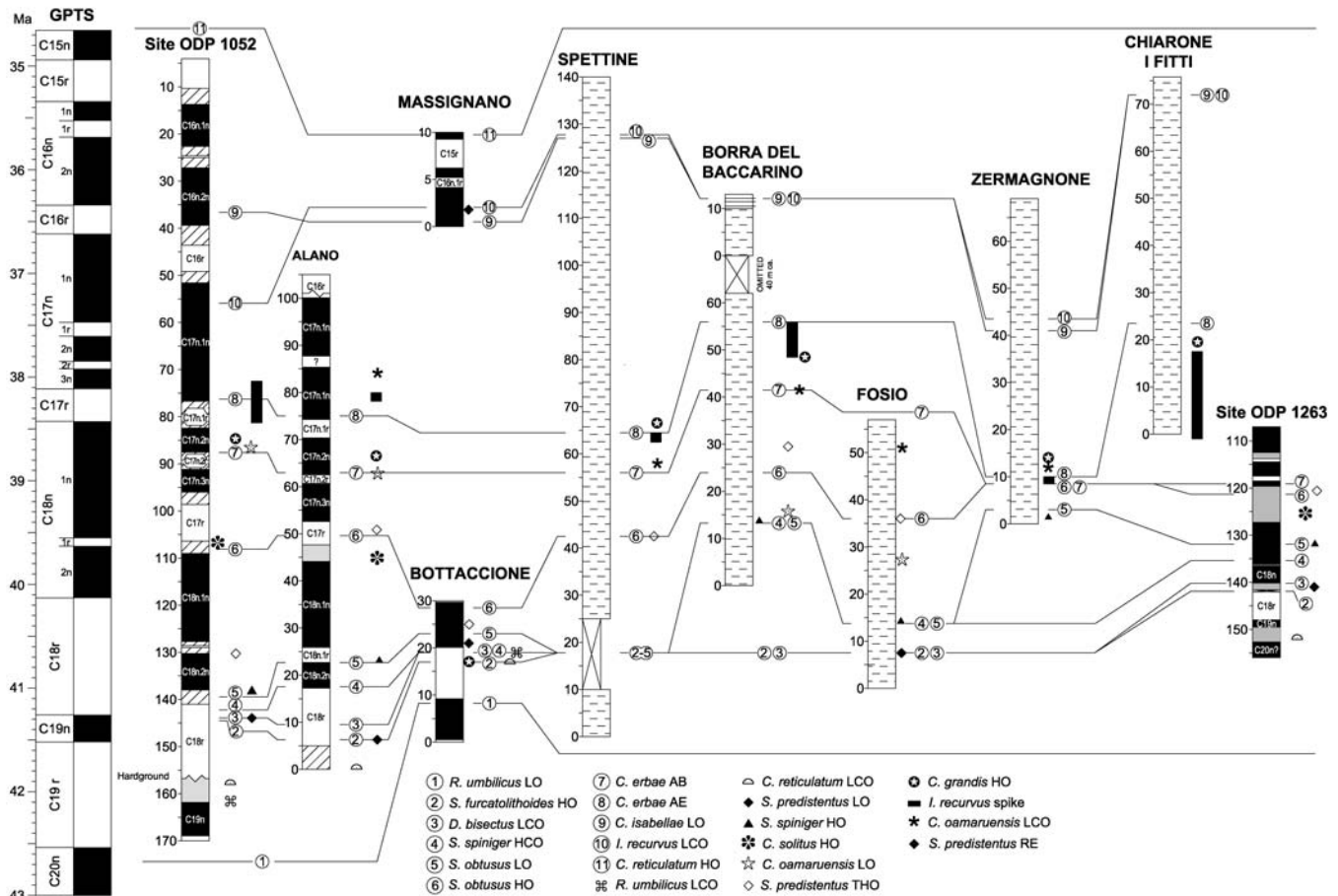
Sphenoliths are thought to be dissolution resistant taxa (Bukry 1973; Kahn and Aubry 2004), that generally show common to abundant abundances in low to middle latitudes. This biogeographic distribution suggests that sphenoliths are a warm-water indicator (Haq and Lohmann 1976; Wei and Wise 1990). However, this genus is also considered to be a K-mode specialist (Young 1994) adapted to oligotrophic conditions (Aubry 1998; Bralower 2002; Gibbs et al. 2004). Gibbs et al. (2006) and Agnini et al. (2007) further suggest that the paleofertility overrides the paleotemperature in driving the marked decrease of sphenoliths during the PETM (Paleocene Eocene Thermal Maximum) event.

This genus provides several biohorizons that are discussed below.

### The HO of *Sphenolithus furcatolithoides*

The distribution patterns of *S. furcatolithoides* reported in text-figures 4-6, 8, 9 and 14 indicate that its HO is one of the most distinct biohorizons. The HO of *S. furcatolithoides* has often been reported as occurring in the late part of the middle Eocene (Proto Decima et al. 1975; Perch-Nielsen 1977; Parisi et al. 1988; Nocchi et al. 1988; Firth 1989; Wei and Wise 1989; 1992; Okada 1990; Bralower and Mutterlose 1995; Mita 2001; Marino and Flores 2002a; b). Perch-Nielsen (1985) proposed that the extinction of this taxon approximately correlates with the base of Zones NP17 and CP14b of Martini (1971) and Okada and Bukry (1980), respectively.

In all the middle latitude sections having good magnetostratigraphic control (ODP Sites 1052 and 1263, Alano and Bottaccione sections), the abundance patterns of *S. furcatolithoides* show a distinct HO datum consistently occurring in the late part of Chron C18r, shortly below the LCOs of *D. bisectus* and *D. scrippsae* (text-figs. 4-6, 14). Some specimens of this species occurs above labeled HO in several sections (Alano, Fosio and ODP Sites 1052 and 1263) and this pattern can be attributable either to reworking or a final tail of distribution, that



TEXT-FIGURE 15

Biostratigraphic correlations for the middle and late Eocene between the ODP Sites 1052 and 1263 and several Mediterranean sections considered in this work. Geomagnetic polarity time scale is Cande and Kent (1995). Magnetostratigraphies after Ogg and Bardot (2001) and Pälike et al. (2001) for the ODP Site 1052; Agnini et al. (in press) for the Alano section; Napoleone et al. (1983) for the Bottaccione section; Lowrie and Lanci (1994) and Jovane et al. (2007b, 2009) for the Massignano section; Zachos et al. (2004) for ODP Site 1263.

is, however, biostratigraphically meaningless. The event has been observed also in the Spettine and Fosio sections (text-figs. 8 and 9) in approximately the same stratigraphic position (text-fig. 15). Taken together, these findings suggest a substantial synchrony. However, interpolated ages estimated from the investigated sections provide variable ages that spread over in an interval of up to 0.4 Myr (Table 2). Whether or not these age discrepancies reflect true diachrony, or depend upon vagaries of the stratigraphic record, or inadequate magnetostratigraphic control, cannot be properly assessed using available data.

#### *The LO of *Sphenolithus predistentus* and its range*

*Sphenolithus predistentus* is an easily recognizable species generally reported in upper Eocene and Oligocene sediments (Roth et al. 1971; Proto Decima et al. 1975; Verhallen and Romein 1983). Verhallen and Romein (1983) proposed the LO of *S. predistentus* as a zonal boundary within the late Eocene, above the LO of *I. recurvus*. However, several authors (Bukry 1973; Perch Nilesen 1977; Wei and Wise 1989; 1992) reported the LO

of *S. predistentus* at much lower stratigraphic levels, from middle Eocene sediments. Our data indicate that the LO of *S. predistentus* occurs consistently in the middle Eocene, in late Chron C18r at Alano and ODP Site 1052 (40.78 and 40.35 Ma respectively). Surprisingly, *S. predistentus* temporarily disappears (THO) in all sections we have examined, with highly variable decline patterns (text-figs. 4-6, 8-10 and 14) and apparently at different stratigraphic levels (text-fig. 15). This temporary disappearance begins in the top of Chron C18n.2n at ODP Site 1052 and in the base of Chron C17r at Alano (text-figs. 4, 5 and 15). The species re-appears in late Eocene time at Massignano (text-fig. 7), in lower Chron C16n.2n (36.09 Ma). According to these data, there is a variable but significant absence interval in the distribution of *S. predistentus* in middle latitude environments. We stress here that specimens ascribed to *S. predistentus* below and above the temporary absence interval cannot be differentiated from observations in the light microscope, and that the observed distribution pattern reflects some unknown ecological/biogeographical control on the distribution of the taxon.

### The HCO of *Sphenolithus spiniger*

*Sphenolithus spiniger* is reported as becoming extinct in middle Eocene sediments by several authors (Proto Decima et al. 1975; Nocchi et al. 1988, Wei and Wise 1989; Okada 1990; Mita 2001), although this biohorizon has not been previously employed in biostratigraphy. The final range of this taxon, well documented at both Alano and ODP Site 1052, indicates a clear drop in abundance (from 11-24% to 3-5%), that we define as HCO. This biohorizon occurs consistently in two sections (text-figs. 4 and 5; Table 2), at the transition between Chron C18r and Chron C18n. The HCO of *Sphenolithus spiniger* was observed at the Alano, Bottaccione, Fosio and Borra del Baccharino sections, and ODP Sites 1052 and 1263 maintaining the same ranking (text-figs, 4-6, 9, 10, 14 and 15).

### The LO and HO of *Sphenolithus obtusus*

*Sphenolithus obtusus* is reported in middle Eocene sediments by several authors (Bukry 1973; Nocchi et al. 1988; Wei and Wise 1989; 1992; Okada 1990). The range of this species is biostratigraphically useful, although not previously employed. The species is easily recognizable in the light microscope and shows a distinct LO datum at ODP Sites 1052 and 1263, and the Alano, Bottaccione, Fosio, Borra del Baccharino and Zermagnone sections (text-figs. 4-6, 9-11, 14). The correlation shown in text-figure 15 indicates that the event consistently occurs shortly above the *S. spiniger* HCO, thus providing a useful biostratigraphic correlation tool and sequence of events. However, the calibration of the event to the GPTS at Alano and ODP Site 1052 indicate a significant diachrony between the two areas (Table 2). Considering the distribution pattern, the spacing and ranking of the event in the central Tethyan sections, we suggest that the LO of *S. obtusus* is a biostratigraphically useful event. The final range of the species also provides a distinct and biostratigraphically useful event (text-figs. 4-6, 8-10, 14). Its HO appears to be synchronous between the central Tethys Alano section and the western Atlantic Site 1052, around basal Chron C17r and topmost of Chron 18n.1n (text-fig. 15; Table 2).

### A NEW CALCAREOUS NANNOFOSSIL BIOSTRATIGRAPHIC SCHEME

The results discussed above are summarized in text-figure 16 and Table 3. The classical zonal markers used for the middle-late Eocene nannofossil zonations are generally poor in terms of abundance patterns, geographic applicability and degree of synchrony. Distinct changes, however, occur among the calcareous nannofossil assemblages which are biostratigraphically and biochronologically useful in middle latitude regions. In these areas, the following twelve biohorizons provide reliable biostratigraphic correlation and classification tools: 1) LO of *R. umbilicus* 2) LCO of *C. reticulatum*, 3) HO of *S. furcatolithoides*, 4) LCO of *D. bisectus*, 5) LCO of *D. scrippsae*, 6) HCO of *S. spiniger*, 7) LO of *S. obtusus*, 8) HO of *S. obtusus*, 9) AB of *C. erbae*, 10) AE of *C. erbae*, 11) LO of *C. isabellae*, and 12) LCO of *I. recurvus*. On the basis of these events, we propose a revised calcareous nannofossil biostratigraphic scheme for the middle and late Eocene (Appendix B and text-fig. 2), that applies to the Tethyan region, and the NW and SE Atlantic. This biostratigraphic scheme encompasses six easily recognizable Zones and three Subzones, the latter usually detectable using high-resolution studies (text-fig. 2). This extends the biostratigraphic scheme proposed by Catanzariti et al. (1997) for the Oligocene and late Eocene. The new zonal

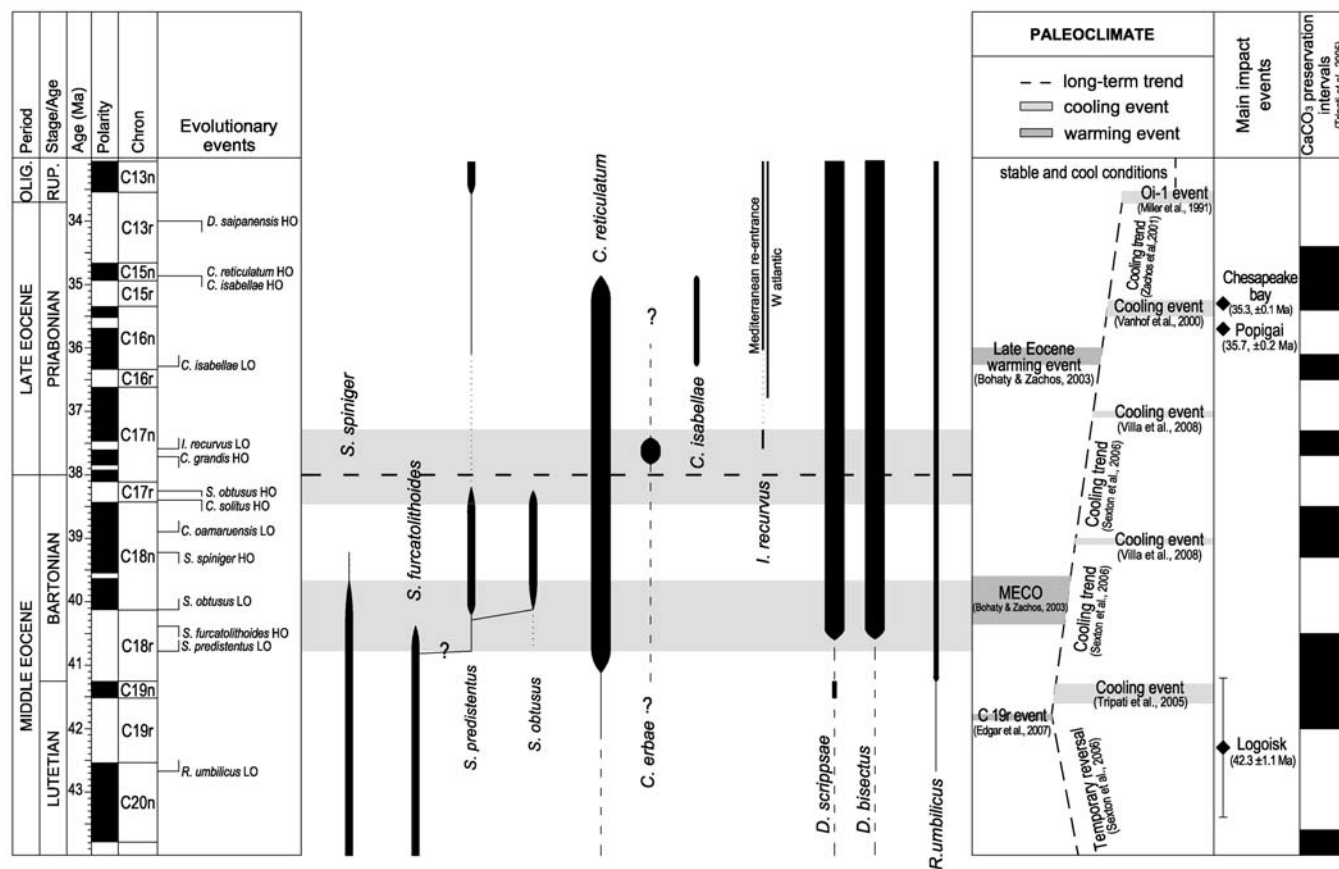
scheme is calibrated to the Cande and Kent (1995) time scale, and provides an average time resolution of ca. 840 kyr over the 6.7 Myr interval investigated. This represents a doubling of the time resolution provided by the standard zonations. The improved resolution is not uniform through time, varying significantly in the studied interval. The resolution decreases from the end of the MECO (ca. 39.6 Ma) to the beginning of middle/late Eocene transition (ca.38.5 Ma) (text-fig. 16). By contrast, the MECO event and the middle/late Eocene transition hold several biohorizons, with six biohorizons occurring close the MECO: the LOs of *S. predistentus*, *D. scrippsae*, *D. bisectus* and *S. obtusus*, HO of *S. furcatolithoides*, and HCO of *S. spiniger*. Six other biohorizons occur across the middle/late Eocene transition: the HOs of *S. obtusus*, *C. grandis*, AB and AE of *C. erbae*, and beginning and end of the *I. recurvus* spike. (text-fig. 16).

### A REVISED CALCAREOUS NANNOFOSSIL BIOCHRONOLOGY

The data discussed above and summarized in Table 3 greatly expand the existing poor database on calcareous nannofossil biochronology during the middle-late Eocene and indicate that the widely used synthesis of Berggren et al. (1995) needs to be revised. As already mentioned, an accurate absolute age evaluation of the biohorizons considered in this work is tricky in part because the chronology of the GPTS in the middle and late Eocene is in flux (Berggren and Pearson 2005). In fact, the timescales of Cande and Kent (1995), Pälike et al. (2001) and Luterbacher et al. (2004) are different from each other and the calcareous nannofossil biochronology varies as a consequence. In addition, based on data reported in Table 3, calculated adopting the chronology of CK95, we observe important discrepancies in the calibrations provided by different authors. Hence, most of the needed revision likely derives from the fact that many classical biohorizons used in the standard zonations are poor and it is not a surprise that their calibrations are contradictory. A major flaw in the age evaluation of Berggren et al. (1995), concerning also planktonic foraminifera, is derived from the fact that these authors relied heavily on the data collected in the Umbrian sections of Bottaccione and Contessa Highway. In these sections, the preservation of calcareous plankton is poor and, therefore, they are not ideally suited to establish detailed distribution patterns of calcareous nannofossil taxa. In addition, these two sections are affected by structural disturbances and the magnetostratigraphic interpretation above Chron C18r is ambiguous (see Jovane et al. 2007a).

### CONCLUSIONS

Calcareous nannofossil biostratigraphic investigations were carried out in 11 sections, nine located in the Mediterranean region and two in the Atlantic Ocean (ODP Sites 1052 and 1263). We have mapped 26 biohorizons in an 8 Myr long time interval from 42.7 Ma to 34.8 Ma. Most of these bioevents are used to provide a biostratigraphic partitioning that improves the biostratigraphic resolution of the investigated time interval. We demonstrate that index species used in the classical standard zonations are generally poor in terms of reliability and reproducibility, and that several additional biohorizons can be used to refine the biostratigraphic classification of this time interval. We thus propose a new biostratigraphic scheme for middle and early late Eocene times. The new zonation extends the biozonation presented by Catanzariti et al. (1997) beyond the upper part of late Eocene. Our new zonal scheme was developed from sediments deposited in the Tethyan region, but ap-



TEXT-FIGURE 16

Evolutionary events and biostratigraphic biohorizons are plotted against chronostratigraphy and GPTS of Cande and Kent (1995). The shaded bands highlight two episodes of time-concentrated calcareous nannoplankton bioevents. On the right, the main paleoclimatic events and/or long-term trends are presented together with enhanced preservation interval of  $\text{CaCO}_3$  (Lyle et al. 2005; Tripathi et al. 2005).

plies also to middle latitude regions in the North and South Atlantic. This scheme gives a mean resolution of ca. 840 kyr in a ca. 6.7 Myr time interval, thus doubling the biostratigraphic resolution compared to the classical standard zonation. Calcareous nannofossil biohorizons are calibrated to magnetostratigraphy providing an improved biochronologic framework of the investigated time interval (see Berggren et al. 1995, for comparison).

### SYSTEMATIC PALEONTOLOGY

The higher classification of calcareous nannofossils utilized is that of Young and Bown (1997a; b). The formal definition of this new species complies with the *International Code of Botanical Nomenclature* (ICBN; McNeill et al. 2007).

Order PRINSIALES Young and Bown 1997b

Family NOELAEHRABDACEAE (Jerkoviè 1970) Young and Bown 1997b

Genus *Cribrocentrum* Perch-Nielsen 1971

*Cribrocentrum erbae* Fornaciari, Agnini, Catanzariti and Rio **sp. nov.**

Plate 2, Figs. 1-2, 5-6, 9-10, 13-14

*Derivatio nominis*: In honor of Elisabetta Erba, Professor at the Department of Earth Sciences “Ardito Desio”, University of Milano (Italy), geologist and calcareous nannofossil paleontologist.

*Diagnosis*: Medium to large circular placolith with a closed central area, very bright in cross polarized light (XPL).

*Description*: This circular placolith consists of two shields. The rim of the larger distal shield consists of ca. 60-62 slightly overlapping ray-shaped elements that are rounded at the periphery. The sutures are straight and almost radially arranged. Numerous irregular elements, forming a blanket, are disposed on more cycles covering the whole central area that, therefore, is closed. The rim of the smaller proximal shield is composed of ca. 60-66 ray-shaped elements bending downward and directed toward the central area to roughly resemble a funnel-shaped body. The elements show a faintly laevogyre overlap. Numerous radial bars create a grill or a plate filling in the central area, that thus results to be characterized by a “plug”, strongly illuminated in XPL. The isogyres are bended and continuous from the center to the periphery, becoming broader toward the periphery. In XPL both the proximal and the distal shields are bright.

**Differentiation:** In the light microscope, *Criboecium erbae* can be differentiated from *Criboecium reticulatum* (Gartner and Smith 1967) Perch Nielsen 1971 (Plate 1, Fig. 5), by the latter's open central area and distinctive extinction pattern and, sometimes, by thick "collar" with high birefringence surrounding the central area. Furthermore, *C. erbae* differs from *C. isabellae* in having a smaller size, a brighter central area and a thinner small birefringent "collar".

**Size:** range approx 7-11µm (diameter). For details see Table B, Supplementary Data.

**Holotype:** Plate 2, Fig.1 (SEM); Sample ODP 171B-1052B-10H-4W, 70.

**Holotype size:** Proximal view. Distal shield: total diameter = 9.0µm. Proximal shield: total diameter= 7.3µm.

**Paratype:** Plate 2, Fig. 5.

**Paratype size:** Plate 2, Fig. 5 (SEM); Distal view. Distal shield: total diameter = 10µm; diameter of central area= 5.8µm.

**Type locality:** Blake Nose, NW Atlantic Ocean, ODP Leg171B, Site 1052.

**Type level:** Zone MNP18A (this work; Catanzariti et al. 1997). Upper Eocene; Sample ODP 171B-1052B-10H-4W, 70 cm

**Range:** MNP16Bb-MNP19 (this work; Catanzariti et al. 1997), late middle Eocene-late Eocene.

**Remarks:** At Site ODP 1052, the presence of specimens with intermediate morphological features between *Criboecium erbae* and *Criboecium reticulatum* suggests that a phylogenetic relationship between the two species probably exists.

Strong overgrowth or dissolution can blur these distinguishing. In previous work, this species has probably been included in *C. reticulatum*.

**Occurrence:** The species occurs with high frequencies (acme) in the interval between the base of Chron C17n.2n and the base of Chron C17n.1n. Rare and scattered specimens of *C. erbae* have also been observed below and above the acme interval in the upper middle Eocene (upper part of Chron C18r) and in the late Eocene (middle part of Chron C15r), respectively.

**Repository:** Holotype and paratypes are deposited in the permanent collection of the Museo di Geologia e Paleontologia dell'Università di Padova (MGPD), Padova, Italy (protocol #MGPD31020).

***Criboecium isabellae*** Catanzariti, Rio and Fornaciari **sp. nov.** Plate 2, Figs. 3-4, 7-8, 11-12, 15-16, 20

*Criboecium* aff. *reticulatum* Catanzariti et al. 1997 p. 244, pl.1, figs 4-6.

**Derivatio nominis:** In honor of Isabella Raffi, Professor at the Dipartimento di Geotecnologie per l'Ambiente ed il Territorio, University "G. d'Annunzio" of Chieti - Pescara (Italy), geologist and calcareous nannofossil palaeontologist.

**Diagnosis:** very large (=12 µm) circular placolith with a central area partially closed and bright in cross polarized light (XPL).

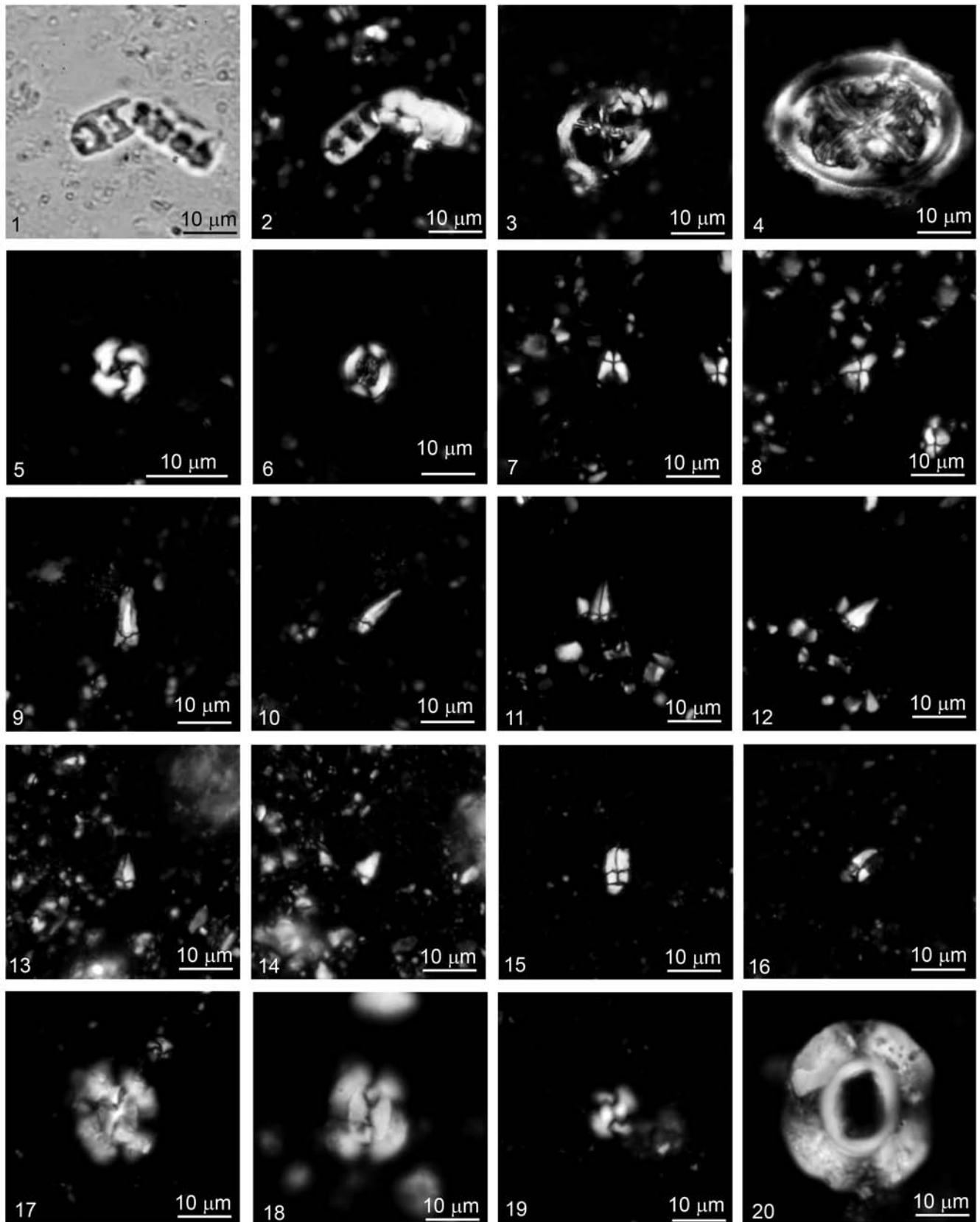
**Description:** The rim of the larger distal shield of this circular placolith consist of ca. 72 to 110 ray-shaped elements rounded at the periphery, radially arranged and very slightly overlapping. The sutures are straight. In distal view, the central area shows a cycle consisting of numerous irregular lath-shaped elements strongly overlapping and with a slight dextral obliquity.

## PLATE 1

Microphotographs of selected calcareous nannofossil taxa from the Middle-Late Eocene Alano section (Northern Italy). LM photographs are in XPL unless otherwise noted.

- |      |   |       |  |
|------|---|-------|--|
| 1,2  | <i>Isthmolithus recurvus</i> . Sample COL 4645c. 1. Parallel light. | 11,12 | <i>Sphenolithus predistentus</i> - <i>Sphenolithus distentus</i> intergrade. Sample COL 730b. 11. 0°. 12. 45°. |
| 3    | <i>Chiasmolithus oamaruensis</i> . Sample COL 5225c.                | 13,14 | <i>Sphenolithus predistentus</i> . Sample COL 1285b. 13. 0°. 14. 45°.  |
| 4    | <i>Chiasmolithus grandis</i> . Sample COL 40a.                      | 15,16 | <i>Sphenolithus</i> cf. <i>S. furcatolithoides</i> . Sample COL 0. 15. 0°. 16. 45°.                            |
| 5    | <i>Criboecium reticulatum</i> . Sample COL 3521c.                   | 17,18 | <i>Dictyococcites bisectus</i> . Sample COL 40a.   |
| 6    | <i>Chiasmolithus solitus</i> . Sample COL 40a.                      | 19    | <i>Dictyococcites scrippsae</i> . Sample COL 40a.  |
| 7,8  | <i>Sphenolithus spiniger</i> . Sample COL 40a. 7. 0°. 8. 45°.       | 20    | <i>Reticulofenestra umbilicus</i> . Sample 730b.   |
| 9,10 | <i>Sphenolithus obtusus</i> . Sample COL 1285b. 9. 0°. 10. 45°.     |       |  |





The rim of the smaller proximal shield is comprised of ca. 70-108 ray-shaped elements curved and slightly laevogyre. In proximal view, the central area is covered by a grill of radially disposed elements continuous with the element of the proximal shield. In crossed-polarized light both the proximal and the distal shields are bright. The central area is open or partially open with a distinctive extinction pattern, but occasionally, the central area can be completely filled. A thick "collar" showing high birefringence occasionally surrounds the central area (Pl. 2, fig. 7).

*Differentiation:* In the light microscope at XPL, *Criboecentrum isabellae* differs from *Criboecentrum reticulatum* (Gartner and Smith 1967) Perch Nielsen 1971 (Plate1, Fig. 5), in having a larger size (=12 µm) and more closed central area with a robust grill-like structure. *Criboecentrum isabellae* differs from *C. erbae* in having a larger size (=12 µm) and a brighter central area.

*Size:* range approx 12-16µm (diameter). For details see Table B, Supplementary Data.

*Holotype:* Plate 2, Fig. 4 (SEM); Sample ODP 171B-1052C-1H-6W, 20.

*Holotype size:* Proximal view. Distal shield: total diameter = 12.1µm. Proximal shield: total diameter= 9.6µm.

*Paratype:* Plate 2, Fig. 8.

*Paratype size:* Plate 2, Fig. 8, (SEM); Distal view. Distal shield: total diameter = 13.3µm; diameter of central area= 8.0µm.

*Type locality:* Blake Nose, NW Atlantic Ocean, ODP Leg171B, Site 1052.

*Type level:* Zone MNP19 (this work; Catanzariti et al. 1997). Upper Eocene; Sample ODP 171B-1052C-1H-6W, 20 cm.

*Range:* MNN18B-MNP19 (top) (this work; Catanzariti et al. 1997), late Eocene.

*Remarks:* The Highest Occurrence (HO) of *Criboecentrum isabellae* virtually coincides with the HO of *Criboecentrum reticulatum*, which is the marker species of the base of Zone MNP20 of Catanzariti et al. (1997).

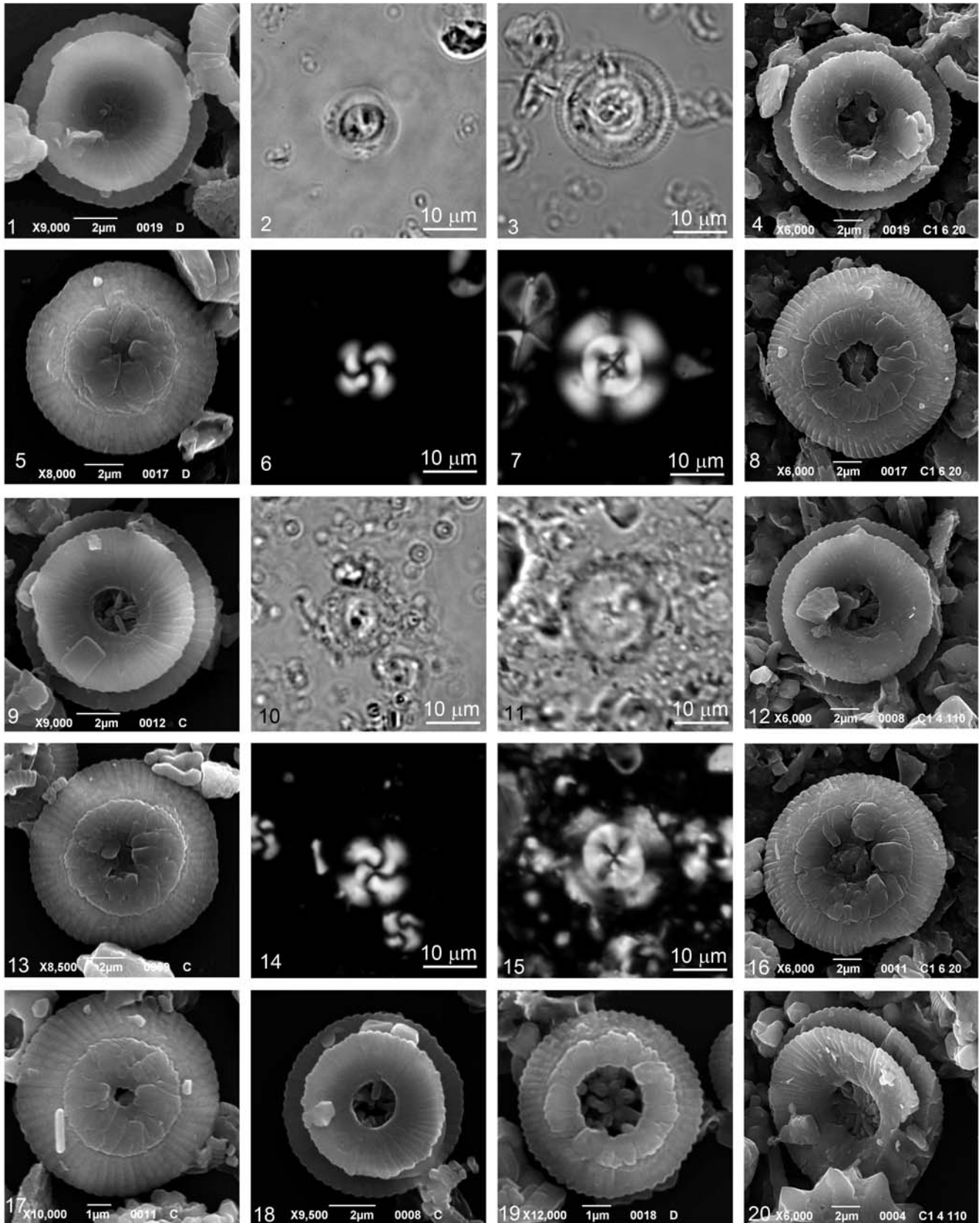
*Occurrence:* The species consistently occurs, albeit with low frequencies, between the lower part of Chron C16n.2n and the lower part of Chron C15n.

*Repository:* Holotype and paratypes are deposited in the permanent collection of the Museo di Geologia e Paleontologia dell'Università di Padova (MGPD), Padova, Italy (protocol #MGPD31021).

## PLATE 2

Microphotographs of *Criboecentrum erbae* sp. nov and *Criboecentrum isabellae* sp. nov. from the Middle-Late Eocene ODP Site 1052, Alano (NE Italy).and Massignano (central Italy) sections. LM photographs are in XPL unless otherwise noted

- |        |   |        |   |
|--------|---|--------|---|
| 1      | <i>Criboecentrum erbae</i> . Holotype. Sample ODP 171B-1052B-10H-4W, 70. SEM, proximal view.    | 11, 15 | <i>Criboecentrum isabellae</i> . Massignano section. Sample MAS 5.11. Parallel light.                           |
| 2,6    | <i>Criboecentrum erbae</i> . Sample ODP 171B-1052B-10H-4W, 70.                                  | 12     | <i>Criboecentrum isabellae</i> . Sample ODP 171B-1052C-1H-4W, 110. SEM, proximal view.                          |
| 3,7    | <i>Criboecentrum isabellae</i> . Sample ODP 171B-1052C-1H-6W, 20. 11. Parallel light.           | 13     | <i>Criboecentrum erbae</i> . Sample ODP 1052B-10-2W, 130. SEM, distal view.                                     |
| 4      | <i>Criboecentrum isabellae</i> . Holotype. Sample ODP 171B-1052C-1H-6W, 20. SEM, proximal view. | 16     | <i>Criboecentrum isabellae</i> . Sample ODP 171B-1052C-1H-6W, 20. SEM, distal view.                             |
| 5      | <i>Criboecentrum erbae</i> . Paratype. Sample ODP 171B-1052B-10H-4W, 70. SEM, distal view.      | 17     | <i>Criboecentrum reticulatum-Criboecentrum erbae</i> intergrade. Sample ODP 1052B-10-2W, 130. SEM, distal view. |
| 8      | <i>Criboecentrum isabellae</i> . Paratype. Sample ODP 171B-1052C-1H-6W, 20. SEM, distal view.   | 18     | <i>Criboecentrum reticulatum</i> . Sample ODP 1052B-10-2W, 130. SEM, proximal view.                             |
| 9      | <i>Criboecentrum erbae</i> . Sample ODP 1052B-10-2W, 130. SEM, proximal view.                   | 19     | <i>Criboecentrum reticulatum</i> . Sample ODP 171B-1052B-10H-4W, 70. SEM, distal view.                          |
| 10, 14 | <i>Criboecentrum erbae</i> . Alano section. Sample COL 3521c. 10. Parallel light.               | 20     | <i>Criboecentrum isabellae</i> . Sample ODP 171B-1052C-1H-4W, 110. SEM, side view.                              |



**Criboecentrum reticulatum** (Gartner and Smith) Perch-Nielsen  
*Cyclococcolithus reticulatus* GARTNER and SMITH 1967, p. 4, pl. 5,  
figs. 1-4.

*Criboecentrum reticulatum* (Gartner and Smith) – PERCH-NIELSEN  
1971, p. 28, pl. 25, figs. 4-9. – COCCIONI et al. 1988, pl. 4, figs. 7,10.  
– MONECHI, BUCCIANTI and GARDIN 2000, pl. 1, figs. 9,10. –  
KIRCI-ELMAS et al. 2008, pl. 1, fig. 23.

*Reticulofenestra reticulata* (Gartner and Smith) – ROTH, in ROTH and  
THIERSTEIN 1972, p. 436. – PROTODECIMA et al. 1975, pl. 2, fig.  
22 a, b. – AUBRY 1986, pl. 7, figs. 25-26. – WEI and WISE 1989, pl.  
4, fig. 11. – WEI and WISE 1990, pl. 6, figs. 2-3, 6-7. – WEI and  
THIERSTEIN 1991, pl. 5, figs. 2-4. – SISSIER and BRALOWER  
1992, pl. 4 fig. 19. – WEI 1998, pl. 2, fig. 12. – MARINO and  
FLORES 2002, pl. 1, fig. 5. – BOWN 2005, pl. 2, figs. 31-33; non fig.  
34.

## ACKNOWLEDGMENTS

This research partly used samples and data provided by the Ocean Drilling Program (ODP). ODP is sponsored by the U.S. National Science Foundation (NSF) and participating countries under management of Joint Oceanographic Institution (JOI) Inc. CA, EF, and DR were supported by MIUR/PRIN COFIN 2007 (# 2007W9B2WE\_004) coordinated by I. Premoli Silva (national) and DR (Padova). Istituto di Geoscienze e Georisorse, CNR-Pisa provided financial support to RC. We would like to thank Stefano Castelli for producing plates of calcareous nannofossil microphotographs and Lorenzo Franceschin for processing samples for micropaleontological analyses. We would warmly thank Jan Backman and Enrico Di Stefano for their fruitful comments on a previous version of this manuscript and two anonymous reviewers for their constructive suggestions.

## REFERENCES

AGNINI, C., FORNACIARI, E., GIUSBERTI, L., GRANDESSO, P., LANCI, L., LUCIANI, V., MUTTONI, G., RIO, D., STEFANI, C., PÄLIKE, H. and SPOFFORTH, D.J.A., in press. Integrated bio-magnetostratigraphy of the Alano section (NE Italy): a proposal for defining the middle-late Eocene boundary, *Geological Society of America Bulletin*.

AGNINI, C., FORNACIARI, E., RIO, D., TATEO, F., BACKMAN, J. and GIUSBERTI, L., 2007. Responses of calcareous nannofossil assemblages, mineralogy and geochemistry to the environmental perturbations across the Paleocene/Eocene boundary in the Venetian Pre-Alps. *Marine Micropaleontology*, 63:19–38.

AUBRY, M.-P., 1984. *Handbook of Cenozoic Calcareous Nannoplankton, book 1, Ortholithae (Discoaster)*. New York: Micropaleontology Press. American Museum of Natural History, 263 pp.

———, 1988. *Handbook of Cenozoic Calcareous Nannoplankton, book 2, Ortholithae (Holococcoliths, Ceratoliths, Ortholiths and Other)*. New York: Micropaleontology Press. American Museum of Natural History, 279 pp.

———, 1989. *Handbook of Cenozoic Calcareous Nannoplankton, book 3, Ortholithae (Pentaliths and Other), Heliolithae (Fasciculiths, Sphenoliths and Others)*. New York: Micropaleontology Press. American Museum of Natural History, 279pp.

———, 1990. *Handbook of Cenozoic Calcareous Nannoplankton, book 4, Heliolithae (Helicoliths, Cribroliths, Lopadoliths and Other)*. New York: Micropaleontology Press. American Museum of Natural History, 381 pp.

———, 1992. Late Paleogene calcareous nannoplankton evolution: a tale of climatic deterioration, in Eocene–Oligocene climatic and bi-

otic evolution. In: Prothero, D.R. and Berggren, W.A., Eds., *Eocene–Oligocene Climatic and Biotic Evolution*, 272–309. Princeton: Princeton University Press.

———, 1998. Early Paleogene Calcareous nannoplankton evolution: a tale of climatic amelioration. In: Aubry, M.-P., et al., Eds., *Late Paleocene–early Eocene Biotic and Climatic Events in the Marine and Terrestrial Records*, 158–201. New York: Columbia University Press.

———, 1999. *Handbook of Cenozoic Calcareous Nannoplankton. Book 5: Heliolithae (Zygoliths and Rhabdoliths)*. New York: Micropaleontology Press. American Museum of Natural History, 368 pp.

AUBRY, M.-P. and BORD, D., 2009. Reshuffling the cards in the photic zone at the Eocene/Oligocene boundary. In: Koeberl, C. and Montanari, A., Eds., *The late Eocene Earth - hothouse, icehouse, and impacts*, 279–301. Boulder: Geological Society of America Special Paper, no. 452.

BACKMAN, J., 1987. Quantitative calcareous nannofossil biochronology of middle Eocene through early Oligocene sediments from DSDP Sites 522 and 523. *Abhandlungen Der Geologischen Bundesanstalt*, 39:21-31.

BACKMAN, J. and HERMELIN, J.O.R., 1986. Morphometry of the Eocene nannofossil *Reticulofenestra umbilicus* lineage and its biochronological consequences. *Palaeogeography, Palaeoclimatology, Palaeoecology*, 57:103-116.

BACKMAN, J. and RAFFI, I., 1997. Calibration of Miocene nannofossil events to orbitally tuned cyclostratigraphies from Ceara Rise. In: Curry, W.B., Shackleton, N.J., Richter, C., et al., Eds., *Proceedings of the Ocean Drilling Program, Scientific Results*, 154: 83-99. College Station, TX: Ocean Drilling Program.

BACKMAN, J. and SHACKLETON, N.J., 1983. Quantitative biochronology of Pliocene and early Pleistocene calcareous nannoplankton from the Atlantic, Indian and Pacific Oceans. *Marine Micropaleontology*, 8:141-170.

BARNABA, P.F., 1958. Geologia dei monti di Gubbio. *Bollettino della Società Geologica Italiana*, 77:39-70.

BECKMANN, J.P., BOLLI, H.M., PERCH-NIELSEN, K., PROTODECIMA, F., SAUNDERS, J.B. and TOUMARKINE, M., 1981. Major calcareous nannofossil and foraminiferal events between the middle Eocene and early Miocene. *Palaeogeography, Palaeoclimatology, Palaeoecology*, 36:155-190.

BERGGREN, W.A. and PEARSON, P.N., 2005. A revised tropical to subtropical Paleogene planktonic foraminiferal zonation. *Journal of Foraminiferal Research*, 35:279-298.

BERGGREN, W.A., KENT, D.V., FLYNN, J.J. and VAN COUVERING, J.A., 1985. Cenozoic Geochronology. *Geological Society of America Bulletin*, 96:1407-1418.

BERGGREN, W.A., KENT, D.V., SWISHER III, C.C. and AUBRY, M.-P., 1995. A revised Cenozoic geochronology and chronostratigraphy. In: Berggren, W.A., et al., Eds., *Geochronology, Time Scales and Global Stratigraphic Correlation*, 129–212. Tulsa: Society for Sedimentary Geology Special Publication, no. 54.

BICE, D.M. and MONTANARI, A., 1988. Magnetic stratigraphy of the Massignano section across the Eocene–Oligocene boundary. In: Premoli Silva, I., Coccioni, R., Montanari, A., Eds., *The Eocene–Oligocene boundary in the Marche-Umbria Basin (Italy)*, 11-117. Ancona: Fratelli Anniballi. International Union of Geological Sciences International Subcommittee on Paleogene Stratigraphy. Special Publication.

- BOHATY, S.M. and ZACHOS, J.C., 2003. A Significant Southern Ocean warming event in the late middle Eocene. *Geology*, 31:1017-1020.
- BOHATY, S. M., ZACHOS, J. C., FLORINDO, F. and DELANEY, M. L., 2009., Coupled greenhouse warming and deep-sea acidification in the middle Eocene. *Paleoceanography*, 24:PA2207, doi:10.1029/2008PA001676.
- BRALOWER, T.J., 2002. Evidence of surface water oligotrophy during the Paleocene–Eocene thermal maximum: nannofossil assemblage data from Ocean Drilling Program Site 690, Maud Rise, Weddel Sea. *Paleoceanography*, 17 (2):1029–1042.
- BRALOWER, T.J. and MUTTERLOSE, J., 1995. Calcareous nannofossil biostratigraphy of Site 865, Allison Guyot, central Pacific Ocean: a tropical paleogene reference section. In: Winterer, E.L., Sager, W.W., Firth, J.V., and Sinton, J.M., Eds., *Proceedings of the Ocean Drilling Program, Scientific Results*, 143: 31-74. College Station, TX: Ocean Drilling Program.
- BRALOWER, T.J., MONECHI, S. and THIERSTEIN, H.R., 1989. Calcareous nannofossil zonation of the Jurassic-Cretaceous boundary interval and correlation with the geomagnetic polarity timescale. *Marine Micropaleontology*, 14:153-235.
- BRAMLETTE, M.N. and WILCOXON, J.A., 1967. Middle Tertiary calcareous nannoplankton of the Ciperio Section, Trinidad. *W.I. Tulane Studies in Geology and Paleontology*, 5:93-131.
- BUKRY, D., 1971. Cenozoic calcareous nannofossils from the Pacific Ocean. *Transactions of the San Diego Society of Natural History*, 16:303–328.
- , 1973. Low-latitude coccolith biostratigraphic zonation. In: Edgar, N.T., Saunders, J.B., et al., Eds., *Proceedings of the Deep Sea Drilling Project, Initial Reports*, 15: 685-703. Washington, DC: US Government Printing Office.
- , 1975. Silicoflagellate and coccolith stratigraphy, Leg 29. In: Kennett, J.P., Houtz, R.E., et al., Eds., *Proceedings of the Deep Sea Drilling Project, Initial Reports*, 29: 845-872. Washington, DC: US Government Printing Office.
- , 1977. Cenozoic coccolith and silicoflagellate stratigraphy, offshore northwest Africa. In: Lancelot, Y., Seibold, E., et al., Eds., *Proceedings of the Deep Sea Drilling Project, Initial Reports*, 41: 689-719. Washington, DC: US Government Printing Office.
- , 1978. Biostratigraphy of Cenozoic marine sediments by calcareous nannofossils. *Micropaleontology*, 24:44–60.
- BUKRY, D., DOUGLAS, R.G., KLING, S.A. and KRASHENINNIKOV, V., 1971. Planktonic microfossil biostratigraphy of the northwestern Pacific Ocean. In: Fischer, A.G., Heezen, B.C. et al., Eds., *Proceedings of the Deep Sea Drilling Project, Initial Reports*, 6: 1253-1300. Washington, DC: US Government Printing Office.
- CANDE, S.C. and KENT, D.V., 1992. A new geomagnetic polarity timescale for the Late Cretaceous and Cenozoic. *Journal of Geophysical Research*, 97:13917–13951.
- , 1995. Revised calibration of the geomagnetic polarity time scale for the Late Cretaceous and Cenozoic. *Journal of Geophysical Research*, 100 (B4):6093–6096.
- CASCELLA, A. and DINARÈS-TURELL, J., 2009. Integrated calcareous nannofossil biostratigraphy and magnetostratigraphy from the uppermost marine Eocene deposits of the southeastern Pyrenean foreland basin: evidences for marine Priabonian deposition. *Geologica Acta*, 7(1-2):281-296.
- CATANZARITI, R., RIO, D. and MARTELLI, L., 1997. Late Eocene to Oligocene calcareous nannofossil biostratigraphy in the northern Apennines: the Ranzano sandstone. *Memorie di Scienze Geologiche*, 49:207-253.
- CERRINA FERONI, A., OTTRIA, G. and VESCOVI, P., 2002. *Note Illustrative della Carta geologica d'Italia alla scala 1:50.000 Foglio 217 – Neviano degli Arduini*. Firenze: SELCA, 112 pp., 1 sheet.
- COCCIONI, R., MONACO, P., MONECHI, S., NOCCHI, M. and PARISI, G., 1986. The Eocene/Oligocene boundary at Massignano (Ancona), Italy: Biostratigraphy based on calcareous nannofossils and planktonic foraminifera. *Bulletin de Liaison et Informations, IGCP Project*, 196(6):37-44.
- COCCIONI, R., MONACO, P., MONECHI, S., NOCCHI, M. and PARISI, G., 1988. Biostratigraphy of the Eocene–Oligocene boundary at Massignano (Ancona, Italy). In: Premoli Silva, I., Cocconeri, R., Montanari, A., Eds., *The Eocene-Oligocene boundary in the Marche-Umbria Basin (Italy)*, 59-80. Ancona: Fratelli Anniballi. International Union of Geological Sciences International Subcommittee on Paleogene Stratigraphy. Special Publication.
- CRESTA, S., MONECHI, S. and PARISI, G., 1989. Stratigrafia del Mesozoico e Cenozoico nell'area umbro-marchigiana. Itinerari geologici sull'Appennino umbro-marchigiano (Italia). *Memorie Descrittive della Carta Geologica d'Italia*, 39:1-185.
- DI DIO, G., LASAGNA, S., MARTINI, A. and ZANZUCCHI, G., 2005b. *Note illustrative della Carta geologica d'Italia alla scala 1:50.000 Foglio 199 – Parma Sud*. Firenze: SELCA, 177 pp., 1 sheet
- DI DIO, G., PICCIN, A. and VERCESI, P.L., 2005a. *Note Illustrative della Carta Geologica d'Italia alla scala 1:50.000 foglio 179 Ponte dell'Olio*. Firenze: SELCA, 108 pp., 1 sheet.
- DOGLIONI, C., GUEGUEN, E., SABAT, F. and FERNANDEZ, M., 1997. The western Mediterranean extensional basins and the Alpine orogen. *Terra Nova*, 9(3):109-112.
- EDGAR, K.M., WILSON, P.A., SEXTON, P.F. and SUGANUMA, Y., 2007. No extreme bipolar glaciation during the main Eocene calcite compensation shift. *Nature*, 448:908-911.
- ERBA, E., 2006. The first 150 million years history of calcareous nannoplankton: biosphere-geosphere interactions. *Palaeogeography, Palaeoclimatology, Palaeoecology*, 232: 237-250.
- FIRTH, J.V., 1989. *Biometric analysis of Eocene and Oligocene calcareous nannofossil*. PhD dissertation, Florida State University, Tallahassee.
- FLUEGEMAN, R. H., 2007. Unresolved issues in Cenozoic chronostratigraphy. *Stratigraphy*, 4:109-116.
- FORNACIARI, E. and RIO, D., 1996. Latest Oligocene to Early Miocene Quantitative Calcareous Nannofossil Biostratigraphy in the Mediterranean Region. *Micropaleontology*, 42:1-36.
- GALLAGHER, L., 1989. *Reticulofenestra*: a critical review of taxonomy, structure and evolution. In: Crux, J.A., van Heck, S.E., Eds., *Nannofossils and Their Applications*, 41–75. Chichester: Ellis Horwood LIMITED.
- GARTNER Jr., S., 1974. Nannofossil biostratigraphy. In: von der Borch, C.C., Sclater, J.G., et al., Eds., *Proceedings of the Deep Sea Drilling Project, Initial Reports*, 22: 577-599. Washington, DC: US Government Printing Office.
- GIBBS, S.J., BRALOWER, T.J., BOWN, P.R., ZACHOS, J.C. and BYBELL, L.M., 2006. Shelf and open-ocean calcareous phyto-

- plankton assemblages across the Paleocene–Eocene thermal maximum: implications for global productivity gradients. *Geology*, 34 (4):233–236.
- GIBBS, S.J., SHACKLETON, N.J. and YOUNG, J.R., 2004. Orbitally forced climate signals in mid-Pliocene nannofossil assemblages. *Marine Micropaleontology* 51:39–56.
- GRADSTEIN, F. M., AGTERBERG, F. P., BROWER, J.C. and SCHWARZACHER, W., 1985. *Quantitative Stratigraphy*. Dordrecht, Holland: Unesco and Reidel Publishing Co., 598 pp.
- HALLAM, A., HANCOCK, J.M., LABREQUE, J.L., LOWRIE, W. and CHANNELL, J.E.T., 1985. Jurassic to Palaeogene magnetostratigraphy. In: Snelling, N.J., Ed., *The Chronology of the Geological Record*, 118–140. Oxford: Blackwell Scientific. Geological Society of London Memoir, no. 10.
- HAQ, B.U. and LOHMANN, G.P., 1976. Early Cenozoic Calcareous nannoplankton biogeography of the Atlantic Ocean. *Marine Micropaleontology*, 1: 120-197.
- HAQ, B.U., HARDENBOL, J. and VAIL, P.R., 1987. Chronology of Fluctuating Sea Levels Since the Triassic. *Science*, 235:1156-1167.
- HAY, W.W., MOHLER, H.P., ROTH, P.H., SCHMIDT, R.R. and BOUDREAUX, J.R., 1967. Calcareous nannoplankton zonation of the Cenozoic of the Gulf Coast and Caribbean-Antillean area, and transoceanic correlation. *Transactions of the Gulf Coast Association of geological Societies*, 17:428-480.
- HEDBERG, H.D., 1976, *International stratigraphic guide*. New York, NY: John Wiley and Sons, 200 pp.
- HILGEN, F.J., 2008. Recent progress in the standardization and calibration of the Cenozoic Time Scale: *Newsletters on Stratigraphy*, 43(1):15-22.
- HILLS, S.J. and THIERSTEIN, H.R., 1989. Plio-Pleistocene calcareous plankton biochronology. *Marine Micropaleontology*, 14:67–69.
- HUANG, T.C., 1977. Calcareous nannoplankton stratigraphy of the upper Wulai Group (Oligocene) in northern Taiwan. *Petroleum Geology of Taiwan*, 14:147-179.
- JOVANE, L., COCCIONI, R., MARSILI, A. and ACTON, G., 2009. The late Eocene greenhouse-icehouse transition: Observations from the Massignano global stratotype section and point (GSSP). In: Koeberl, C., Montanari, A., Eds., *The Late Eocene Earth—Hot-house, Icehouse, and Impacts*, 149–168. Boulder: Geological Society of America Special Paper, no. 452.
- JOVANE, L., FLORINDO, F., COCCIONI, R., DINARÈS-TURELL, J., MARSILI, A., MONECHI, S., ROBERTS, A.P. and SPROVIERI, M., 2007a. The middle Eocene climatic optimum event in the Contessa Highway section, Umbrian Apennines, Italy. *Geological Society of America Bulletin*, 119:413-427.
- JOVANE, L., FLORINDO, F., DINARÈS-TURELL, J. and TURRELL, S., 2004. Environmental magnetic record of paleoclimate change from the Eocene-Oligocene stratotype section, Massignano, Italy. *Geophysical Research Letters*, 31(15):L15601.
- JOVANE, L., FLORINDO, F., SPROVIERI, M. and PÄLIKE, H., 2006. Astronomic calibration of the late Eocene/early Oligocene Massignano section (central Italy). *Geochemistry, Geophysics and Geosystems*, 7 (7):Q07012.
- JOVANE, L., SPROVIERI, M., FLORINDO, F., ACTON, G., COCCIONI, R., DALL'ANTONIA, B. and DINARÈS-TURRELL, J., 2007b. Eocene-Oligocene paleoceanographic changes in the stratotype section, Massignano, Italy: Clues from rock magnetism and stable isotopes. *Journal of Geophysical Research*; 112:B11101.
- KAHN, A. and AUBRY, M.-P., 2004. Provincialism associated with the Paleocene/Eocene thermal maximum: temporal constraint. *Marine Micropaleontology*, 52:117-131.
- LANCI, L., LOWRIE, W. and MONTANARI, A., 1996. Magnetostratigraphy of the Eocene/Oligocene boundary in a short drill-core. *Earth and Planetary Science Letters*, 143: 37-48.
- LARRASOÑA, J.C., GONZALVO, C., MOLINA, E., MONECHI, S., ORTIZ, S., TORI, F. and TOSQUELLA, J., 2008. Integrated magnetobiochronology of the Early/Middle Eocene transition at Agost (Spain): Implications for defining the Ypresian/Lutetian boundary stratotype. *Lethaia*, 41(4):395-415.
- LOWRIE, W. and LANCI, L., 1994. Magnetostratigraphy of Eocene-Oligocene boundary sections in Italy - no evidence for short subchrons within chrons 12r and 13r. *Earth and Planetary Science Letters*, 126:247-258.
- LUCIANI, V., NEGRI, A. and BASSI, D., 2002. The Bartonian-Priabonian transition in the Mossano section (Colli Berici, north-eastern Italy): a tentative correlation between calcareous plankton and shallow-water benthic zonations. *Geobios*, 35(1):140–149.
- LUTHERBACHER, H.P., ALI, J.R., BRINKUIS, H., GRADSTEIN, F.M., HOOKER, J.J., MONECHI, S., OGG, J.G., POWELL, J., RÖHL, U., SANFILIPPO, A. and SCHIMITZ, B., 2004. The Paleogene period. In: Gradstein, F.M., Ogg, J.G., Smith, A.G., Eds., *A Geologic Time Scale 2004*, 384-408. Cambridge: Cambridge University Press.
- LYLE, M., OLIVAREZ LYLE, A., BACKMAN, J. and TRIPATI, A., 2005. Biogenic sedimentation in the Eocene equatorial Pacific—the stuttering greenhouse and Eocene carbonate compensation depth. In: Wilson, P.A., Lyle, M., and Firth, J.V., Eds., *Proceedings of the Ocean Drilling Program, Scientific Results*, 199: 1–35. College Station, TX: Ocean Drilling Program.
- MANCIN, N. and COBIANCHI, M., 2000. Le Marne di Montepiano della Val di Nizza (Appennino Settentrionale): biostratigrafia integrata e considerazioni paleoambientali. *Atti Ticinesi di Scienze della Terra* 41:145-162.
- MANCIN, N. and PIRINI, C., 2001. Middle Eocene to Early Miocene foraminiferal biostratigraphy in the Epiligurian Succession (Northern Apennines, Italy). *Rivista Italiana di Paleontologia e Stratigrafia*, 107: 371-393
- MARRONI, M. and FLORES, J.A., 2002a. Middle Eocene to Early Oligocene calcareous nannofossil stratigraphy at Leg 177 Site 1090. *Marine Micropaleontology* 45:383–398.
- , 2002b. Data report: calcareous nannofossil data from the Eocene to Oligocene, Leg 177, Hole 1090B. In: Gersonde, R., Hodell, D.A., Blum, P., Eds., *Proceedings of the Ocean Drilling Program, Scientific Results*, 177: 1–9. College Station, TX: Ocean Drilling Program.
- MARRONI, M., OTTRIA, G. and PANDOLFI, L., in press. *Note illustrative della Carta geologica d'Italia alla scala 1:50.000 Foglio 196 – Cabella Ligure*. Firenze: SELCA.
- MARTINI, E., 1971, Standard Tertiary and Quaternary calcareous nannoplankton zonation. In: Farinacci, A., Ed., *Proceedings of the 2<sup>nd</sup> Planktonic Conference*, 739–785. Roma: Edizioni Tecnoscienza, vol. 2.

- MARTINI, E. and MÜLLER, C., 1986. Current Tertiary and Quaternary calcareous nannoplankton stratigraphy and correlations. *Newsletters on Stratigraphy*, 16: 99-112.
- MCNEILL, J., BARRIE, F. R., BURDET, H. M., DEMOULIN, V., HAWKSWORTH, D. L., MARHOLD, K., NICOLSON, D. H., PRADO, J., SILVA, P. C., SKOG, J. E., WIERSEMA, J. H. and TURLAND, N. J., 2007. International Code of Botanical Nomenclature (Vienna Code). Regnum Vegetabile. Gantner, Ruggell, 568 pp.
- MILLER, K. G., WRIGHT, J. D. and FAIRBANKS, R. G., 1991. Unlocking the ice house: Oligocene-Miocene oxygen isotopes, eustasy, and margin erosion. *Journal of Foraminiferal Research*, 96:6829-6848.
- MITA, I., 2001. Data Report: Early to Late Eocene calcareous nannofossil assemblages of the Sites 1051 and 1052, Blake Nose, northwestern Atlantic Ocean. In: Kroon, D., Norris, R.D., Klaus, A., Eds., *Proceedings of the Ocean Drilling Program, Scientific Results, 171B*: 1-28. College Station, TX: Ocean Drilling Program.
- MONECHI, S. and THIERSTEIN, H.R., 1985. Late Cretaceous-Eocene nannofossil and magnetostratigraphic correlations near Gubbio, Italy. *Marine Micropaleontology*, 9:419-440.
- MONTANARI, A., DRAKE, R., BICE, M.D., ALVAREZ, W., CURTIS, G.H., TURRIN, B.D. and DEPAOLO, D.J., 1985. Radiometric time scale for the upper Eocene and Oligocene based on K/Ar and Rb/Sr dating of volcanic biotites from the pelagic sequence of Gubbio, Italy. *Geology*, 13:596-599.
- MÜLLER, C., 1976. Tertiary and Quaternary calcareous nannoplankton in the Norwegian-Greenland Sea, DSDP, Leg 38. In: Talwani, M., Udintsev, G., et al., Eds., *Proceedings of the Deep Sea Drilling Project, Initial Reports*, 38: 823-841. Washington, DC: US Government Printing Office.
- NAPOLEONE, G., PREMOLI SILVA, I., HELLER, F., CHELI, P., COREZZI, S. and FISCHER, A.G., 1983. Eocene magnetic stratigraphy at Gubbio, Italy, and its implications for Paleogene geochronology. *Geological Society of America Bulletin*, 94: 181-191.
- NOCCHI, M., PARISI, G., MONACO, P., MONECHI, S., MADILE, M., NAPOLEONE, G., RIPEPE, M., ORLANDO, M., PREMOLI SILVA, I. and BICE, D.M., 1986. The Eocene-Oligocene boundary in the umbrian pelagic sequences, Italy. In: Pomerol, Ch., Premoli Silva, I., Eds., *Terminal Eocene Events*, 25-40. Amsterdam: Elsevier. *Developments in Palaeontology and Stratigraphy*, vol. 9.
- NOCCHI, M., PARISI, G., MONACO, P., MONECHI, S. and MADILE, M., 1988. Eocene and Early Oligocene micropaleontology and paleoenvironments in SE Umbria, Italy. *Palaeogeography, Palaeoclimatology, Palaeoecology*, 67:181-124.
- NORRIS, R.D., KROON, D., KLAUS, A. et al., 1998. *Blake Nose Paleooceanographic Transect Sites 1049-1053. Proceedings of the Ocean Drilling Program, Initial Report, Volume 171B*. College Station, TX: Ocean Drilling Program, 360pp.
- OGG, J.G. and BARDOT, L., 2001. Aptian through Eocene magnetostratigraphic correlation of the Blake Nose Transect (Leg 171B), Florida continental margin. In: Kroon, D., Norris, R.D., Klaus, A., Eds., *Proceedings of the Ocean Drilling Program, Scientific Results, 171B*: 1-58. College Station, TX: Ocean Drilling Program.
- OKADA, H., 1990. Quaternary and Paleogene calcareous nannofossils, Leg 115. In: Duncan, R.A., Backman, J., Peterson, L.C., et al., Eds., *Proceedings of the Ocean Drilling Program, Scientific Results*, 115: 129-174. College Station, TX: Ocean Drilling Program.
- OKADA H. and BUKRY D., 1980. Supplementary modification and introduction of code numbers to the low-latitude coccolith biostratigraphic zonation (Bukry, 1973;1975). *Marine Micropaleontology*, 5:321-325.
- PÄLIKE, H., SHACKLETON, N.J. and RÖHL, U., 2001. Astronomical forcing in late Eocene marine sediments. *Earth and Planetary Science Letters*, 193:589-602.
- PARISI, G., GUERRERA, F., MADILE, M., MAGNONI, G., MONACO, P., MONECHI, S. and NOCCHI, M., 1988. Middle Eocene to early Oligocene calcareous nannofossil and foraminiferal Biostratigraphy in the Monte Cagnero section, Piobbico (Italy). In: Premoli Silva, I., Coccioni, R., Montanari, A., Eds., *The Eocene-Oligocene boundary in the Marche-Umbria Basin (Italy)*, 119-235. Ancona: Fratelli Anniballi. International Union of Geological Sciences International Subcommittee on Paleogene Stratigraphy. Special Publication.
- PERCH-NIELSEN, K., 1977. Albian to Pleistocene calcareous nannofossils from the western South Atlantic, DSDP Leg 39. In: Supko, P.R., Perch-Nielsen, K., et al., Eds *Proceedings of the Deep Sea Drilling Project, Initial Reports*, 39: 699-823. Washington, DC: US Government Printing Office.
- , 1985. Cenozoic Calcareous Nannofossils: In: Bolli, H.M., Saunders, J.B., Perch-Nielsen, K., Eds., *Plankton Stratigraphy*, 427-554. Cambridge: Cambridge University Press.
- PERCIVAL JR, S.F., 1984. Late Cretaceous to Pleistocene calcareous nannofossils from the South Atlantic, Deep Sea Drilling Project Leg 73. In: Hsü, K.J., LaBrecque, J., et al., Eds., *Proceedings of the Deep Sea Drilling Project, Initial Reports*, 73: 391-424. Washington, DC: US Government Printing Office.
- PERSICO, D. and VILLA, G., 2004. Eocene-Oligocene calcareous nannofossils from Maud Rise and Kerguelen Plateau (Antarctica): paleoecological and paleoceanographic implications. *Marine Micropaleontology*, 52:153-179.
- POORE, R.Z., TAUXE, L., PERCIVAL JR., S.F., LABREQUE, J.L., WRIGHT, R., PETERSON, N.P., SMITH, C.C., TUCKER, P. and HSÜ, K.J., 1984. Late Cretaceous-Cenozoic magnetostratigraphy and biostratigraphic correlation of the South Atlantic Ocean. In: Hsü, K.J., Montadert, L. et al., Eds., *Proceedings of the Deep Sea Drilling Project, Initial Reports*, 73: 645-656. Washington, DC: US Government Printing Office.
- PREMOLI SILVA, I. and JENKINS, D.G., 1993. Decision on the Eocene-Oligocene boundary stratotype: *Episodes*, 16(3):379-382.
- PREMOLI SILVA, I., COCCIONI, R. and MONTANARI, A., 1988. *The Eocene-Oligocene Boundary in the Marche-Umbria Basin (Italy)*. Ancona: Fratelli Anniballi. International Union of Geological Sciences International Subcommittee on Paleogene Stratigraphy. Special Publication, 268 pp.
- PREMOLI SILVA, I., NAPOLEONE, G. and FISCHER, A.G., 1974. Risultati preliminari sulla stratigrafia paleomagnetica della Scaglia cretaceo-paleocenica della sezione di Gubbio (Appennino centrale). *Bollettino della Società Geologica Italiana*, 93(03):647-659.
- PROTO DECIMA, F., MEDIZZA, F. and TODESCO, L., 1978. South-eastern Atlantic Leg 40 calcareous nannofossils. In: Bolli, H.M., Ryan, W.B.F, et al., Eds., *Proceedings of the Deep Sea Drilling Project, Initial Reports*, 40: 571-634. Washington, DC: US Government Printing Office.
- PROTO DECIMA, F., ROTH, P.H. and TODESCO, L., 1975. Nannoplankton calcareo del Paleocene e dell'Eocene della Sezione di Possagno. In: Bolli, H.M., Ed., *Monografia Micropaleontologica*

- , *sul Paleocene e l'Eocene di Possagno, Provincia di Treviso, Italia*, 35-55. Basel: Kommission für die Paläontologischen Abhandlungen. *Schweizerische Palaeontologische Abhandlungen*, vol. 97.
- RAFFI, I., 1999. Precision and accuracy of nannofossil biostratigraphic correlation. *Philosophical Transactions of the Royal Society of London*, A 357(1757):1975-1993.
- RAFFI, I., BACKMAN, J., RIO, D. and SHACKLETON, N.J., 1993. Plio-Pleistocene nannofossil biostratigraphy and calibration to oxygen isotope stratigraphies from Deep Sea Drilling Project Site 607 and Ocean Drilling Program Site 677. *Paleoceanography*, 8:387-408.
- RAFFI, I., BACKMAN, J., FORNACIARI, E., PÄLIKE, H., RIO, D., LOURENS, L.J. and HILGEN, F.J., 2006. A review of calcareous nannofossil astrobiochronology encompassing the past 25 Million years. *Quaternary Science Reviews*, 25: 3113-3137.
- RENZ, O., 1936. Stratigraphische und mikropalaeontologische Untersuchung der Scaglia (Obrere Kreide-Tertiar) im zentralen Apennin. *Eclogae Geologicae Helvetiae*, 29:1-149.
- , 1951. Ricerche stratigrafiche e micropalaeontologiche sulla Scaglia (Cretaceo Superiore-Terziario) dell'Appennino centrale. *Memorie Descrittive della Carta Geologica d'Italia*, 29:1-173.
- RIO, D., RAFFI, I. and VILLA, G., 1990. Pliocene-Pleistocene calcareous nannofossil distribution, patterns in the western Mediterranean. In: Kasten, K., Mascle, J., et al., Eds., *Proceedings of the Ocean Drilling Program, Scientific Results*, 107: 513-533. College Station, TX: Ocean Drilling Program.
- ROTH, P.H., 1970. Oligocene calcareous nannoplankton biostratigraphy. *Eclogae Geologicae Helvetiae*, 63:799-881.
- , 1973. Calcareous nannofossils. Leg 17, Deep Sea Drilling Project. In: Winterer, E.L., Ewing, J.I., et al., Eds., *Proceedings of the Deep Sea Drilling Project, Initial Reports*, 17: 695-795. Washington, DC: US Government Printing Office 17: Washington D.C. (U.S. Govt. Printing Office), pp..
- ROTH, P.H., BAUMANN, P. and BERTOLINO, V., 1971. Late Eocene-Oligocene calcareous nannoplankton from central and northern Italy. In: Farinacci, A., Ed., *Proceedings of the 2<sup>nd</sup> Planktonic Conference*, 1069-1097. Roma: Edizioni Tecnoscienza, vol. 2.
- SALVADOR, A., 1994. *International stratigraphic guide: a guide to stratigraphic classification, terminology, and procedure, second edition*: Boulder: Geological Society of America, International Union of Geological Sciences, 214 pp.
- SEXTON, P.F., WILSON, P.A. and NORRIS, R.D., 2006. Testing the Cenozoic multisite composite  $\delta^{18}\text{O}$  and  $\delta^{13}\text{C}$  curves: new monospecific Eocene records from a single locality, Demerara Rise (Ocean Drilling Program Leg 207). *Paleoceanography*, 21(2):PA2019.
- SIESSER, W.G. 1983. Paleogene calcareous nannoplankton biostratigraphy: Mississippi, Alabama, and Tennessee. *Mississippi Bureau of Geology Bulletin*, 125:1-61.
- THIERSTEIN, H., GEITZENAUER, K.R., MOLFINO, B. and SHACKLETON, N.J., 1977. Global synchronicity of late Quaternary coccolith datum levels: validation by oxygen isotopes. *Geology*, 5:400-404.
- TRIPATI, A., BACKMAN, J., ELDERFIELD, H. and FERRETTI, P., 2005. Eocene bipolar glaciation associated with global carbon cycle changes. *Nature*, 436:341-346.
- VAROL, O., 1998. Palaeogene. In: Bown, P.R., Ed., *Calcareous nannofossil biostratigraphy*, 200-224. Cambridge: British Micropalaeontological Society Publication Series, Chapman and Hall (Kluwer Academic Publishers).
- VERHALLEN, P.J.J.M and ROMEIN, A.J.T., 1983. Calcareous nannofossils from Priabonian stratotype and correlation with the parastratotype. In: Setiawan, J.R., Ed., *Foraminifers and Microfacies of the Type-Priabonian*, 163-173. Utrecht: Utrecht Micropaleontological Bulletin, vol. 29.
- VESCOVI, P., 2002. *Note Illustrative della Carta Geologica d'Italia alla scala 1:50.000 foglio 216 Borgo Val di Taro*. Firenze: SELCA, 115 pp., 1 sheet.
- VILLA, G., FIORONI, C., PEA, L., BOHATY, S.M. and PERSICO, D., 2008. Middle Eocene-late Oligocene climate variability: Calcareous nannofossil response at Kerguelen Plateau, Site 748: *Marine Micropaleontology*, 69(2):173-192.
- VONHOF, H.B., SMIT, J., BRINKHUIS, H., MONTANARI, A. and NEDERBRAGT, A.J., 2000. Global cooling accelerated by early late Eocene impacts?. *Geology*, 28:687-690.
- WADE, B.S., 2004. Planktonic foraminiferal biostratigraphy and mechanisms in the extinction of Morozovella in the late Middle Eocene. *Marine Micropaleontology*, 51:23-38.
- WEI, W. and THIERSTEIN, H.R., 1991. Upper Cretaceous and Cenozoic calcareous nannofossils of the Kerguelen Plateau (southern Indian Ocean) and Prydz Bay (East Antarctica). In: Barron, J.A., Larsen, B., et al., Eds., *Proceedings of the Ocean Drilling Program, Scientific Results*, 119: 467-493. College Station, TX: Ocean Drilling Program.
- WEI, W. and WISE JR., S.W., 1989. Paleogene calcareous nannofossil magnetobiostratigraphy: results from South Atlantic DSDP 516. *Marine Micropaleontology*, 14:119-152.
- , 1990. Biogeographic gradients of middle Eocene-Oligocene calcareous nannoplankton in the South Atlantic Ocean. *Palaeogeography, Palaeoclimatology, Palaeoecology*, 79:29-61.
- , 1992. Eocene-Oligocene calcareous nannofossil magneto-biochronology of the Southern Ocean. *Newsletters on Stratigraphy*, 26:119-132.
- WEI, W., VILLA, G. and WISE JR., S.W., 1992. Paleocyanographic implications of Eocene-Oligocene calcareous nannofossils from Sites 711 and 748 in the Indian Ocean. In: Wise Jr., S.W., Schlich, R., et al., Eds *Proceedings of the Ocean Drilling Program, Scientific Results*, 120: 979-999. College Station, TX: Ocean Drilling Program.
- WISE, S. W., 1983. Mesozoic and Cenozoic calcareous nannofossil recovered by Deep Sea Drilling Project Leg 71 in the Falkland Plateau region, southwest Atlantic Ocean. In: Ludwig, W. J., Krasheninnikov, V. A., et al., Eds., *Proceedings of the Deep Sea Drilling Project, Initial Reports*, 71: 481-550. Washington, DC: US Government Printing Office
- YOUNG, J.R., 1990. Size variation of Neogene Reticulofenestra coccoliths from Indian Ocean DSDP cores. *Journal of Micropalaeontology*, 9:71-85.
- , 1994. Functions of coccoliths. In: Winter, A., Siesser, W.G., Eds., *Coccolithophores*, 63-82. Cambridge: Cambridge University Press.
- YOUNG, J.R. and BOWN, P.R., 1997a. Higher classification of calcareous nannofossils. *Journal of Nannoplankton Research*; 19:15-20.



———, 1997b. Cenozoic calcareous nannofossil classification. *Journal of Nannoplankton Research*, 19:36-47.

ZACHOS, J.C., KROON, D., BLUM, P. et al., 2004. *Early Cenozoic Extreme Climates: The Walvis Ridge Transect. Proceedings of the Ocean Drilling Program, Initial Report, Volume 208*: College Station TX: Ocean Drilling Program, 112 pp.

ZACHOS, J.C., PAGANI, M., SLOAN, L., THOMAS, E. and BILLUPS, K., 2001. Trends, rhythms, and aberrations in global climate 65 Ma to Present. *Science*, 292:686-693.

Received June 27, 2010

Accepted October 4, 2010

Published December 29, 2010

#### APPENDIX A Taxonomic List

*Blackites* Hay and Towe (1962)  
*Blackites gladius* (Locker 1967) Varol 1989  
*Chiasmolithus* Hay, Mohler and Wade (1966)  
*Chiasmolithus grandis* (Bramlette and Riedel 1954) Radomski (1968)  
*Chiasmolithus oamaruensis* (Deflandre 1954) Hay, Mohler and Wade (1966)  
*Chiasmolithus solitus* (Bramlette and Sullivan 1961) Locker (1968)  
*Criboocentrum* Perch-Nielsen (1971)  
*Criboocentrum erbae* sp. nov.  
*Criboocentrum isabellae* sp. nov.  
*Criboocentrum reticulatum* (Gartner and Smith 1967) Perch-Nielsen (1971)  
*Dictyococcites* Black (1967)  
*Dictyococcites bisectus* (Hay, Mohler and Wade 1966) Bukry and Percival (1971)  
*Dictyococcites scrippsae* Bukry and Percival (1971)  
*Discoaster* Tan Sin Hok (1927)  
*Discoaster bifax* (Bukry 1973)  
*Discoaster saipanensis* Bramlette and Riedel (1954)  
*Isthmolithus* Deflandre (1954)  
*Isthmolithus recurvus* Deflandre (1954)  
*Reticulofenestra* Hay et al. (1966)  
*Reticulofenestra umbilicus* (Levin 1965) Martini and Ritzkowski (1968)  
*Sphenolithus* Deflandre in Grassé (1952)  
*Sphenolithus furcatolithoides* Locker (1967)  
*Sphenolithus moriformis* (Bronnimann and Stradner 1960) Bramlette and Wilcoxon (1967)  
*Sphenolithus obtusus* Bukry (1971)  
*Sphenolithus predistentus* Bramlette and Wilcoxon (1967)  
*Sphenolithus spiniger* Bukry (1971)

#### APPENDIX B

Middle to Late Eocene calcareous nannofossil zonal system.

The biostratigraphic zonal concept and terminology here adopted are identical to that of Catanzariti et al. (1997), following the International Stratigraphic Guide (ISG, Hedberg 1976; Salvador 1994) and as discussed by Fornaciari and Rio (1996). The middle-late Eocene biozones, which will be described in the following section from the oldest to the youngest, have been

given alphanumeric notation (“MNP” = Mediterranean Nannofossil Paleogene plus a number) for easy communication and similar to the notation used by Catanzariti et al. (1997). Correlations to previous zonations are shown in text-figure 2.

The correlation of the zonal scheme to the Global Chronostratigraphic Scale follows the recent proposal of Coccioni et al. (in prep.) and Agnini et al. (in press) for defining the Bartonian and the Priabonian Stages, respectively.

#### *Sphenolithus furcatolithoides* Partial-range Zone (MNP16A)

*Authors*: this paper.

*Definition*: Interval of common presence of *S. furcatolithoides* above the LO of *R. umbilicus*

*Age*: Bartonian (Middle Eocene).

*Reference sections*: Bottaccione section, Alano section and ODP Site 1052 (text-figs. 4-6). The zonal interval is poorly represented because most of investigated sections do not cover entirely this interval. The biozone is clearly recognizable only in the Bottaccione section.

*Characteristics*: A normal assemblage in this zone contains: *Blackites* spp. (R), *Calcidiscus protoannulus* (R), *Campylosphaera dela* (R), *Chiasmolithus grandis*, *C. solitus* (R), *Chiasmolithus* spp. (R/F), *Clausicoccus fenestratus* (R), *C. subdistichus/obrutus* (R), *Coccolithus pelagicus* (C/A), *Criboocentrum reticulatum* (R), *Cyclicargolithus floridanus* (A), *Dictyococcites scrippsae* (F), *Dictyococcites* spp. (F), *Discoaster barbadiensis*, *D. deflandrei*, *D. nodifer*, *D. saipanensis*, *D. tani*, *Ericsonia cava/subpertusa* (C), *E. formosa* (C), *Helicosphaera compacta* (R), *H. euphratis* (RR), *H. heezenii* (R), *H. lophota* (RR), *H. reticulata* (RR), *H. seminulum* (RR), *Lanternithus minutus* (C), *Lanternithus* spp. (C), *Pontosphaera* spp. (RR), *Reticulofenestra umbilicus*, *R. daviesii* (R), *Reticulofenestra* spp. (C), *Sphenolithus anarrhopus* (R), *S. conspicuus* (R), *S. furcatolithoides*, *S. moriformis* (C), *S. radians* (F), *S. spiniger* (C), *Tetralithoides* spp. (F), *Zygrhablithus bijugatus* (C).

*Remarks*: The zone corresponds to the upper part of the NP15 Zone and the lower part of the NP16 Zone of Martini (1971); and to the lower part of the CP14 Zone of Okada and Bukry (1980). The zonal marker *R. umbilicus* is very rare and discontinuously present in its initial range but it shows a sharp increase in abundance (LCO) within this zone roughly in correspondence to Chron C19n/C18r boundary (text-fig. 5). Also *C. reticulatum* exhibits a similar pattern and its abrupt LCO apparently occurs in the lower part of Chron C18r (text-fig. 5). The genus *Dictyococcites* is very rare or virtually missing for most part of this interval except in a short interval between upper Chron C19n and lower Chron C18r (text-fig. 5).

#### *Sphenolithus furcatolithoides-obtusus* Interval Zone (MNP16B)

*Authors*: this paper.

*Definition*: interval from the HO of *Sphenolithus furcatolithoides* to the LO of *Sphenolithus obtusus*.

*Age*: Bartonian (Middle Eocene)

**Reference sections:** Alano section, Fosio and Bottaccione sections; with reduced thicknesses in ODP Sites 1263 and 1052. (text-figs. 4-6, 9 and 14).

**Characteristics:** A normal assemblage in this zone contains: *Blackites* spp. (R), *Calcidiscus protoannulus* (R), *Campylosphaera dela* (R), *Chiasmolithus grandis*, *C. solitus* (R), *Chiasmolithus* spp. (R/F), *Clausicoccus fenestratus* (R), *C. subdistichus/obrutus* (R), *Coccolithus pelagicus* (C/A), *Criboecentrum reticulatum* (R), *Cyclicargolithus floridanus* (A), *Dictyococcites scrippsae* (F), *Dictyococcites* spp. (F), *Discoaster barbadiensis*, *D. deflandrei*, *D. nodifer*, *D. saipanensis*, *D. tanii*, *Ericsonia cava/subpertusa* (C), *E. formosa* (C), *Helicosphaera compacta* (R), *H. euphratis* (RR), *H. heezenii* (R), *H. lophota* (RR), *H. reticulata* (RR), *H. seminulum* (RR), *Lanternithus minutus* (C), *Lanternithus* spp. (C), *Pontosphaera* spp. (RR), *Reticulofenestra umbilicus*, *R. daviesii* (R), *Reticulofenestra* spp. (C), *Sphenolithus anarrhopus* (R), *S. conspicuus* (R), *S. moriformis* (C), *S. radians* (F), *S. spiniger* (C), *Tetralithoides* spp. (F), *Zygrhablithus bijugatus* (C).

**Remarks:** The zone corresponds to the upper part of the NP16 Zone and the lower part of the NP17 Zone of Martini (1971); and to the middle part of the CP14 Zone of Okada and Bukry (1980). In this Zone, *S. spiniger* is mostly represented with high frequencies, which is followed by a sharp decrease in abundance and its extinction at the top of the Zone. *Sphenolithus predistentus* first occurs when *S. furcatolithoides* has its highest occurrence, and becomes abundant in the upper part of the Zone. *Chiasmolithus grandis* and *Chiasmolithus solitus* are scarce and scattered. *Dictyococcites bisectus* and *Dictyococcites scrippsae* become common in the lower part of the Zone. This interval can be subdivided into three subzones.

#### ***Sphenolithus spiniger* Partial-range Subzone (MNP16Ba)**

**Authors:** this paper.

**Definition:** interval of common and continuous presence of *S. spiniger* between the HO of *S. furcatolithoides* and the LCO of *D. bisectus*.

**Age:** Bartonian (Middle Eocene).

**Reference sections:** Alano section, Bottaccione section, and ODP Site 1263 (text-figs. 4, 5 and 14).

**Characteristic:** a normal assemblage in this Subzone contains: *Blackites* spp. (R), *Calcidiscus protoannulus* (R), *Campylosphaera dela* (R), *Chiasmolithus grandis*, *C. solitus* (R), *Chiasmolithus* spp. (R/F), *Clausicoccus fenestratus* (R), *C. subdistichus/obrutus* (R), *Coccolithus pelagicus* (C/A), *Criboecentrum reticulatum* (C), *C. erbae* (R), *Cyclicargolithus floridanus* (A), *Dictyococcites bisectus* (occasional), *Dictyococcites scrippsae* (R/F), *Dictyococcites* spp. (F), *Discoaster barbadiensis*, *D. deflandrei*, *D. nodifer*, *D. saipanensis*, *D. tanii*, *Ericsonia cava/subpertusa* (C), *E. formosa* (C), *Helicosphaera compacta* (R), *H. euphratis* (RR), *H. heezenii* (R), *H. lophota* (RR), *H. reticulata* (RR), *H. seminulum* (RR), *Lanternithus minutus* (C), *Lanternithus* spp. (C), *Pontosphaera* spp. (RR), *Reticulofenestra umbilicus*, *R. daviesii* (R), *Reticulofenestra* spp. (C), *Sphenolithus moriformis* (C), *S. predistentus*, *S. radians* (F), *S. spiniger* (C), *Tetralithoides* spp. (F), *Zygrhablithus bijugatus* (C).

**Remarks:** The estimated ages indicate a short duration of ca. 0.19 Myr for this subzone. Nevertheless, it has been considered useful to define the interval, because it is easily recognizable in sections with high sedimentation rate and/or high-resolution sampling. The Lowest Common Occurrence of *D. scrippsae* characterizes the assemblage in this subzone in the uppermost part of the interval.

#### ***Dictyococcites bisectus-Sphenolithus spiniger* concurrent-range Subzone (MNP16Bb)**

**Authors:** this paper.

**Definition:** interval of concomitant range of common and continuous *D. bisectus* and *S. spiniger* above the LCO of *D. bisectus*.

**Age:** Bartonian (Middle Eocene).

**Reference sections:** Alano section, Fosio section, ODP Site 1263. (text-figs. 4, 9 and 14).

**Characteristic:** a normal assemblage in this Subzone contains: *Blackites* spp. (F), *Calcidiscus protoannulus* (R), *Campylosphaera dela* (R), *Chiasmolithus grandis*, *C. solitus* (R), *Chiasmolithus* spp. (R/F), *Clausicoccus fenestratus* (R), *C. subdistichus/obrutus* (R), *Coccolithus pelagicus* (C/A), *Criboecentrum reticulatum* (C), *C. erbae* (R), *Cyclicargolithus floridanus* (A/D), *Dictyococcites bisectus* (C), *Dictyococcites scrippsae* (C), *Dictyococcites* spp. (C), *Discoaster barbadiensis*, *Discoaster deflandrei*, *D. nodifer*, *D. saipanensis*, *D. tanii*, *Ericsonia cava/subpertusa* (F), *E. formosa* (F), *Helicosphaera compacta* (R), *H. euphratis* (RR), *H. heezenii* (R), *H. lophota* (RR), *H. reticulata* (RR), *H. seminulum* (RR), *Lanternithus minutus* (R), *Lanternithus* spp. (R), *Pontosphaera* spp. (RR), *Reticulofenestra umbilicus*, *R. daviesii* (R), *Reticulofenestra* spp. (C), *Sphenolithus moriformis* (C), *S. predistentus*, *S. radians* (F), *S. spiniger* (C), *Tetralithoides* spp. (R), *Zygrhablithus bijugatus* (R).

**Remarks:** The drop in abundance of *S. spiniger* below 10% of the sphenoliths defines the top of the subzone. *Sphenolithus predistentus* becomes common in the uppermost part of the subzonal interval. The genus *Lanternithus* and *Z. bijugatus* become rare and *Blackites* spp. are few in the middle/upper part of the subzonal interval.

#### ***Dictyococcites scrippsae* Partial-range Subzone (MNP16Bc)**

**Authors:** this paper.

**Definition:** interval of common and continuous presence of *D. scrippsae* between the HCO of *S. spiniger* and the LO of *S. obtusus*.

**Age:** Bartonian (Middle Eocene).

**Reference sections:** Alano section, partially Borra del Baccarino and Zermagnone sections, ODP Sites 1052 and 1263. (text-figs. 4, 5, 10, 11 and 14).

**Characteristic:** a normal assemblage in this Subzone contains: *Blackites* spp. (F), *Calcidiscus protoannulus* (R), *Campylosphaera dela* (R), *Chiasmolithus grandis*, *C. solitus* (R), *Chiasmolithus* spp. (R/F), *Clausicoccus fenestratus* (R), *C. subdistichus/obrutus* (R), *Coccolithus pelagicus* (C/A), *Criboecentrum reticulatum* (C), *C. erbae* (R), *Cyclicargolithus*

*floridanus* (A), *Dictyococcites bisectus* (C), *Dictyococcites scrippsae* (C), *Dictyococcites* spp. (A), *Discoaster barbadiensis*, *D. deflandrei*, *D. nodifer*, *D. saipanensis*, *D. tanii*, *Ericsonia cava/subpertusa* (F), *E. formosa* (F), *Helicosphaera compacta* (R), *H. euphratis* (RR), *H. heezenii* (R), *H. lophota* (RR), *H. reticulata* (RR), *H. seminulum* (RR), *Lanternithus minutus* (R/F), *Lanternithus* spp. (R/F), *Pontosphaera* spp. (RR), *Reticulofenestra umbilicus* (R), *R. daviesii* (RR), *Reticulofenestra* spp. (C), *Sphenolithus moriformis* (C), *S. predistentus* (C), *S. radians* (R), *S. spiniger* (F/R), *Tetralithoides* spp. (R), *Zygrhablithus bijugatus* (R/F).

**Remarks:** Generally, the HO of *S. spiniger* has been observed in correspondence of the top of the Zone.

#### ***Sphenolithus obtusus* Total-range Zone (MNP17A)**

**Authors:** this paper.

**Definition:** interval corresponding to the total range of *S. obtusus*.

**Age:** Bartonian (Middle Eocene).

**Reference sections:** Alano section, Bottaccione section, Spettine section, Fosio section, ODP Sites 1052 and 1263 (text-figs. 4-6, 9, 10 and 14).

**Characteristic:** a normal assemblage in this Zone contains: *Blackites* spp. (R), *Calcidiscus protoannulus* (F/C), *Campylosphaera dela* (R), *Chiasmolithus grandis* (RR), *C. oamaruensis* (RR), *C. solitus* (RR), *Chiasmolithus* spp. (R), *Clausicoccus fenestratus* (R), *C. subdistichus/obrutus* (R), *Coccolithus pelagicus* (C/A), *Criboecentrum reticulatum* (C/A), *C. erbae* (R/F), *Cyclicargolithus floridanus* (A), *Dictyococcites bisectus* (C), *Dictyococcites scrippsae* (C), *Dictyococcites* spp. (A), *Discoaster barbadiensis*, *D. deflandrei*, *D. nodifer*, *D. saipanensis*, *D. tanii*, *Ericsonia cava/subpertusa* (F), *E. formosa* (F), *Helicosphaera bramlettei* (RR), *H. compacta* (R), *H. euphratis* (RR), *H. heezenii* (R), *H. lophota* (RR), *H. reticulata* (RR), *H. seminulum* (RR), *Lanternithus minutus* (F/C), *Lanternithus* spp. (C), *Pontosphaera* spp. (RR), *Reticulofenestra umbilicus* (R), *R. daviesii* (RR), *Reticulofenestra* spp. (C), *Sphenolithus moriformis* (C), *S. obtusus* (C), *S. predistentus* (C), *S. radians* (R), *Tetralithoides* spp. (R), *Zygrhablithus bijugatus* (F/C).

**Remarks:** The Zone roughly corresponds to the middle part of the NP17 Zone of Martini (1971) and to the middle part of the CP14b Zone of Okada and Bukry (1980). *Sphenolithus predistentus* has a temporary disappearance in the uppermost part of the Zone. *Calcidiscus protoannulus* and *C. reticulatum* increase gradually in abundance, while *C. solitus* disappears and *C. grandis* is virtually missing in the upper part of the zonal interval. The abundance of *Lanternithus* and *Z. bijugatus* rise again in this zone, whilst those of *Blackites* decrease. The occurrence of sporadic but typical *C. oamaruensis* in a short interval is noteworthy.

#### ***Sphenolithus obtusus*-*Criboecentrum erbae* Interval Zone (MNP17B)**

**Authors:** this paper.

**Definition:** interval from the HO of *S. obtusus* to the AB of *C. erbae*.

**Age:** Bartonian-Priabonian (Middle-Late Eocene).

**Reference sections:** Alano section, Spettine section, Borra del Baccarino section, Fosio section, ODP Sites 1263 and 1052. (text-figs. 4, 5, 8-10 and 14).

**Characteristic:** a normal assemblage in this Zone contains: *Blackites* spp. (R), *Calcidiscus protoannulus* (F/R), *Campylosphaera dela* (R), *Chiasmolithus grandis* (RR), *Chiasmolithus* spp. (RR), *Clausicoccus fenestratus* (R), *C. subdistichus/obrutus* (R), *Coccolithus pelagicus* (A), *Criboecentrum reticulatum* (C/A), *C. erbae* (R), *Cyclicargolithus floridanus* (C), *Dictyococcites bisectus* (C), *Dictyococcites scrippsae* (C), *Dictyococcites* spp. (A), *Discoaster barbadiensis*, *D. deflandrei*, *D. nodifer*, *D. saipanensis*, *D. tanii*, *Ericsonia cava/subpertusa* (F), *E. formosa* (F/C), *Helicosphaera bramlettei* (RR), *H. compacta* (R), *H. euphratis* (RR), *H. heezenii* (R), *H. reticulata* (RR), *H. seminulum* (RR), *Lanternithus minutus* (F/C), *Lanternithus* spp. (C), *Pontosphaera* spp. (RR), *Reticulofenestra umbilicus* (R), *R. daviesii* (RR), *Reticulofenestra* spp. (C), *Sphenolithus moriformis* (C), *S. radians* (R), *Tetralithoides* spp. (R), *Zygrhablithus bijugatus* (F/C).

**Remarks:** The Zone roughly corresponds to the upper part of the NP17 Zone of Martini (1971) and to the upper part of the CP14b Zone of Okada and Bukry (1980). This zone is short and is difficult to observe in condensed sections and/or with low-resolution sampling. Apparently, *C. grandis* re-enters in the upper part of the zonal interval.

#### ***Criboecentrum erbae* Acme Zone (MNP18A)**

**Authors:** this paper.

**Definition:** interval of strong increase in abundance (acme) of *C. erbae*.

**Age:** Priabonian (Late Eocene).

**Reference sections:** Alano section, Spettine section, Borra del Baccarino section, Zermagnone section, Chiarone I Fitti section (upper part), ODP Sites 1052 and 1263. (text-figs. 4, 5, 8, 10-12 and 14).

**Characteristic:** a normal assemblage in this Zone contains: *Blackites* spp. (R), *Calcidiscus protoannulus* (R), *Campylosphaera dela* (R), *Chiasmolithus grandis* (RR), *C. oamaruensis* (scattered), *Chiasmolithus* spp. (RR), *Clausicoccus fenestratus* (R), *C. subdistichus/obrutus* (R), *Coccolithus pelagicus* (C/A), *Criboecentrum reticulatum* (C/A), *C. erbae* (D), *Cyclicargolithus floridanus* (C), *Dictyococcites bisectus* (F), *Dictyococcites scrippsae* (F/R), *Dictyococcites* spp. (A), *Discoaster barbadiensis*, *D. deflandrei*, *D. nodifer*, *D. saipanensis*, *D. tanii*, *Ericsonia cava/subpertusa* (R), *E. formosa* (F/R), *Helicosphaera bramlettei* (RR), *H. compacta* (R), *H. euphratis* (RR), *H. heezenii* (R), *H. reticulata* (RR), *Isthmolithus recurvus* (spike), *Lanternithus minutus* (F/C), *Lanternithus* spp. (C), *Pontosphaera* spp. (RR), *Reticulofenestra umbilicus* (R), *R. daviesii* (RR), *Reticulofenestra* spp. (C), *Sphenolithus moriformis* (C), *S. radians* (R), *Tetralithoides* spp. (R), *Zygrhablithus bijugatus* (F/C).

**Remarks:** The Zone roughly corresponds to the NP18 Zone of Martini (1971) and to the CP15a Subzone of Okada and Bukry (1980). The interval is short but very distinctive, because of the dominance of *C. erbae*. The Acme Beginning (AB) corresponds to the increase in abundance above the 5-8% while the Acme End (AE) corresponds to the decrease in abundance below the

4-6%. In this Zone, *C. grandis* has its HO, *C. oamaruensis* has its LO at the bottom, and *Isthmolithus recurvus* presents a peak in abundance (the spike).

***Criboecium erbae*- *Isthmolithus recurvus* Interval Zone (MNP18B)**

Authors: this paper.

Definition: interval between the AE of *C. erbae* and the LCO of *I. recurvus* or the LO of *C. isabellae*.

Age: Priabonian (Late Eocene).

Reference sections: Alano section (lower part), Spettine section, Borra del Baccarino section, Zermagnone section, Chiarone i Fitti, ODP Site 1263. (text-figs. 4, 8, 10-12 and 14).

Characteristic: a normal assemblage in this Zone contains: *Blackites* spp. (R), *Calcidiscus protoannulus* (R), *Campylosphaera dela* (R), *Chiasmolithus oamaruensis* (rare and scattered), *Chiasmolithus* spp. (RR), *Clausicoccus fenestratus* (R),

*C. subdistichus/obrutus* (R), *Coccolithus pelagicus* (C/A), *Criboecium reticulatum* (F), *C. erbae* (R), *Cyclicargolithus floridanus* (C), *Dictyococcites bisectus* (C), *Dictyococcites scrippsae* (C), *Dictyococcites* spp. (A), *Discoaster barbadiensis*, *D. deflandrei*, *D. nodifer*, *D. saipanensis*, *D. tanii*, *Ericsonia cava/subpertusa* (R), *E. formosa* (F/C), *Helicosphaera compacta* (R), *H. euphratis* (RR), *H. heezenii* (R), *H. reticulata* (RR), *Isthmolithus recurvus* (rare and scattered), *Lanternithus minutus* (F), *Pontosphaera* spp. (RR), *Reticulofenestra umbilicus* (R), *R. daviesii* (RR), *Reticulofenestra* spp. (C), *Sphenolithus moriformis* (C), *S. radians* (R), *Tetralithoides* spp. (R), *Zygrhablithus bijugatus* (F/C).

Remarks: This Zone correlates with the lower part of the NP19 Zone of Martini (1971) and of the CP15b Subzone of Okada and Bukry (1980). In most of the sections, the appearance of large forms (= 12µm) referred to as *C. isabellae* is virtually concomitant with the LCO of *I. recurvus*. Hence, the LO of *C. isabellae* is used as secondary criterion to define the top of this Zone. From lower to the uppermost part of the zonal interval the abundance of *C. reticulatum* is low.